OPIOID-SENSITIVE BRAINSTEM NEURONS SEPARATELY MODULATE PAIN AND RESPIRATION

By

Daniel R. Cleary

A DISSERTATION

Presented to the Neuroscience Graduate Program

and the Oregon Health & Science University

School of Medicine

in partial fulfillment of

the requirements for the degree of

Doctor of Philosophy

June, 2012

School of Medicine

Oregon Health & Science University

CERTIFICATE OF APPROVAL

_____

This is to certify that the PhD dissertation of

Daniel R. Cleary

has been approved

_____
Mentor : Mary M. Heinricher, PhD

_____
Committee Chair: Michael C. Andresen, PhD

_____
Member: Nabil J. Alkayed, MD, PhD

_____
Member: Michael M. Morgan, PhD

_____
Member: Shaun F. Morrison, PhD

_____
Member: Susan L. Ingram, PhD

TABLE OF CONTENTS

LIST OF FIGURES AND TABLES

LIST OF ABBREVIATIONS

β-FNA	β-funaltrexamine
ACC	Accelerometry-based inductive plethysmography
aCSF	Artificial cerebrospinal fluid
BAT	Brown adipose tissue
BDNF	Brain-derived neurotrophic factor
CCK	Cholecystokinin
CFA	Complete Freund's adjuvant
DAMGO	d-Ala^2, n-MePhe^4, Gly-ol]-enkephalin
DMH	Dorsal medial nucleus of the hypothalamus
EMG	Electromyograph
ERK	Extracellular signal-related kinase
GABA	γ-aminobutyric acid
ICV	Intracerebroventricular
IML	Intermediolateral region
MAPK	Mitogen-activated protein kinase
MPE	Maximum possible effect
MPO	Medial preoptic area
NGCα	Nucleus gigantocellularis pars alpha
NMDA	N-Methyl-D-Aspartic acid
NPY	Neuropeptide Y
PAG	Periaqueductal grey
pERK	Phosphorylated extracellular signal-related kinase
PGE_2	Prostaglandin E_2
RM	Raphe magnus
RMg	Raphe magnus
ROb	Raphe obscurus
RPa	Raphe pallidus
RVM	Rostral ventromedial medulla

SNL	Spinal nerve ligation
TF	Tail flick
TPH	Tryptophan hydroxylase
VPT	Ventilatory pressure transduction
WBP	Whole-body plethysmography

ACKNOWLEDGEMENTS

This work could not have been completed without the assistance from a great many people. First and foremost among them is my mentor, Mary Heinricher, who took a chance by taking me on as a student, and has since then patiently guided me on the path to becoming a scientist. The past four years have been an amazing learning experience, and I will continue to draw inspiration from her teaching throughout my career. Thank you.

A special thanks is also owed to my committee members, many of whom also acted as mentors at one point or another: Nabil Alkayed, Mike Andresen, Susie Ingram, Mike Morgan, and Shaun Morrison.

Jonathan Carlson and Justin Cetas provided me with advice about research, career, and life.

Many members of the lab contributed to this work, both directly and indirectly. A special thanks to Melissa Martenson, Ryan Phillips, Zach Roeder, and Kate Wagner.

My family and loved ones deserve a very special thanks, for so much patience and assistance. Karen Tonsfeldt has listened to all my talks, twice, read all my manuscripts, twice, and continues to be there for me. My family continually amazes me and inspires me, too numerous to all be named here.

Funding for this work came from NIH (NINDS NS070374, NINDS NS065406, NIDA DA022492), OHSU Brain Institute Neurobiology of Disease Fellowship, and the Tartar Trust Foundation.

To my parents, who never pressured me, but always inspired me.

ABSTRACT

The brainstem regulates core functions of the body, both at rest and in response to threat. The mechanism of this regulation is still under study, although core regulatory areas have been identified. The rostral ventromedial medulla (RVM) is a brainstem region that has been extensively studied in the context of somatosensory responsiveness and pain. Under different behavioral settings, neurons in the RVM can facilitate or inhibit the detection of tissue damage (nociception). The nociceptive modulation from the RVM is governed by two populations of neurons, the ON-cells and the OFF-cells. Firing of ON-cells increases sensitivity to stimuli and facilitates spinal reflexes, whereas OFF-cell activity decreases sensitivity and produces analgesia. The responses of ON- and OFF-cells to acute injury have been well studied, but the role of these RVM neurons in other behavioral contexts is less well understood. The first aim of this thesis is to contrast the contributions of ON- and OFF-cells during acute injury versus chronic pain. The second aim is to examine other modulatory roles of RVM neurons and how core regulatory functions overlap with pain modulation in the RVM.

The RVM plays an important role in chronic pain, although the underlying neuronal contributions remain unclear. In acute pain, increased ON-cell activity drives hyperalgesia, and from that observation it has been hypothesized that ON-cells also maintain chronic pain. In a model of chronic inflammatory pain, an initial subcutaneous injection of an irritant into the hindpaw produced immediate increased responsiveness to stimulation (hyperalgesia). This acute hyperalgesia was blocked by inhibiting the ON-cells. Animals with irritant injections that were allowed to recover continued to display hyperalgesia in the days after the injection, and ON- and OFF-cells similarly showed increased sensitivity to stimulation. However, in a model of chronic inflammation, inhibition of ON-cells did not reverse the hyperalgesia, but actually exacerbated it. Thus ON-cells drive hyperalgesia in acute but not chronic injury. This finding reinforces the idea that chronic pain is not simply an extension of an acute injury.

As ON- and OFF-cells can separately modulate acute and chronic pain, and their activity may also separately modulate other core regulatory functions associated with the RVM, such as respiration and heart rate. To examine how RVM neuronal activity intersected with respiration, I built a device for monitoring respiration during RVM manipulations. From this device, we find that RVM neurons concurrently modulate respiration and analgesia, such that opioid injection locally in the RVM depresses respiration and produces analgesia. However, these modulatory functions are separable, such that analgesia is possible without respiratory depression. Manipulations of ON-cell activity modulate respiration, whereas changes in OFF-cell activity were only associated with analgesia. The separate roles of ON- and OFF-cells in modulating pain and respiration open the possibility of developing potent, opioid-like painkillers that don't depress respiration.

Collectively, these results show a separation of function between ON- and OFF-cells. ON-cells modulation core functions related to acute injury or threat, including somatosensory, respiratory, and cardiovascular responsiveness. Conversely, OFF-cell activity was specifically related to the inhibition of pain, such that decreased OFF-cell activity can be a mechanism of pain facilitation. A greater understanding of RVM physiology will aid in improved treatment of chronic pain states and the development of analgesic drugs with fewer side effects.

CHAPTER 1

INTRODUCTION

1.1 Overview

Pain is an unpleasant yet vitally important sensory experience that draws attention to potential or actual injury. Nociception, the process by which the nervous system detects damage, is actively regulated, and both behavioral priorities and extrinsic factors can inhibit or enhance nociception. In extreme stress, the pain and nociception are inhibited (analgesia), which removes distractions from minor injury to allow immediate prioritization of survival. Alternatively, pain and nociception can be enhanced (hyperalgesia), as occurs with illness or prolonged mild stress. In such cases even non-injuring touch is perceived as acutely painful, and movement is kept to a minimum, which promotes rest and recovery. This bidirectional pain modulation is controlled by a complex network of neural circuits, involving input from many levels of the nervous system. These neural circuits converge on an area within the brainstem, the rostral ventromedial medulla (RVM), which modulates pain and nociception through descending projections onto sensory areas of the spinal cord.

The RVM and surrounding brainstem areas also control other physiological responses which are often altered during stress and injury, including respiration, cardiac output, and core temperature. Whether the RVM modulates these functions in conjunction with nociceptive modulation is not known. The overlap between pain modulation and the physiological stress response has not been studied extensively, and whether these RVM-mediated responses share a common neuronal basis has not been explored. This thesis examines the neuronal basis of bidirectional pain modulation and how inhibition or facilitation of nociception may overlap with other physiological responses. By examining this relationship, I found that the RVM neurons effecting descending nociceptive facilitation share common characteristics with those modulating respiration and core temperature, whereas the activity of neurons controlling descending inhibition of nociception did not correlate with other physiological effects. From these results, I conclude that the separate populations of neurons modulating facilitation and inhibition of pain can independently control nociception, an idea that is confirmed in studies of acute and chronic inflammatory pain. This

work furthers our understanding of the fundamentals of brainstem nociceptive modulation and will contribute to the development of novel analgesics with fewer side effects.

1.2 Rostral ventromedial medulla and the maintenance of homeostasis

1.2.1 Convergence of pain modulation and homeostasis

Pain relief has always been beset by side effects, which become more noticeable with the increased efficacy of the pain reliever. Over-the-counter pain relievers like acetylsalicylic acid (Aspirin) and acetaminophen (Tylenol) function well in the treatment of mild, non-urgent pain, and their side effects are similarly moderate. Opioids, on the other hand, provide powerful pain control for even the worst acute pain, but respiratory depression from opioid overdose can be lethal. Endogenous pain modulation, as demonstrated by Reynolds, is no exception. Electrical stimulation in the midbrain periaqueductal grey (PAG), an area that sends extensive projections to the RVM, produced potent analgesia in the rat (Abols and Basbaum 1981; Reynolds 1969). Within a few years of this initial report, the first generators had been implanted in humans (Adams 1976; Hosobuchi et al. 1977; Mayer and Liebeskind 1974). While the implants provided reliable pain control, use of the stimulators was often accompanied by unpleasant side effects, such as “a feeling of impending doom” (Richardson and Akil 1977). Subsequent work in rats showed that pain relief from stimulation of the PAG was likely part of a larger behavioral response, such as an escape reaction. During stimulation of the PAG, animals showed freezing behaviors and escape responses, and rats would actively work to shut off a mid-brain stimulator (Di Scala et al. 1987). These trials show the complexity of the neuronal circuits that control nociception and other core functions.

The RVM and PAG are key sites in a neural circuit that controls the perception of pain and the detection of noxious stimulation, but the diffuse, extensive connections of these regions to the rest of the brain also hints at a greater physiological role (Basbaum and Fields 1984; Cameron et al. 1995a; Cameron et al. 1995b; Sandkuhler 1996). In addition to analgesia, the RVM is associated with modulation of core homeostatic functions, including cardiovascular, respiratory, and thermoregulatory pathways (Lovick 1997). These functions are all regulated through distinct neural circuits that each have a relay in the RVM,

although how these connections are organized within the RVM is still unclear. Anatomical separation of function, although appealing, has not been proven. Below I discuss how nociceptive, cardiovascular, thermogenic, and respiratory functions are modulated in the RVM, as well as the degree of physiological overlap and anatomical divergence.

1.2.2 Anatomy of brainstem modulation

For each functional field of brainstem regulation, investigators focus on different areas of the anatomy related to the behavior of interest. Because different anatomical nomenclature is used often interchangeably, it is worth briefly discussing and distinguishing the anatomical foci for each function of interest. The areas under consideration include the RVM, raphe magnus, raphe pallidus, raphe obscurus, and nucleus gigantocellularis pars alpha (NGCα) (see Figure 1A and 1B). Among these areas, NGCα is least distinguished and often simply referred to as the reticular area surrounding raphe magnus, although it may have some function separate from or complementary to that of raphe magnus (Beitz et al. 1983; Gebhart et al. 1983; Sandkühler and Gebhart 1984b). The midline raphe nuclei (magnus, pallidus, and obscurus) each have distinguishing features, but all contain serotonin and are anatomically and developmentally related. The boundaries of RVM are not defined by anatomy but instead by the regions in which electrical stimulation produces analgesia (Fields and Basbaum 1978; Sandkühler and Gebhart 1984a). The RVM includes the majority of raphe magnus, as well as a significant portion of NGCα, raphe pallidus, and raphe obscurus.

The traditional, albeit oversimplified, division is that raphe magnus controls pain, raphe pallidus controls heart rate and thermogenesis, and raphe obscurus controls respiration. This functional segregation is difficult to validate, in part due to extensive connections among the raphe nuclei (Figure 1C). The heterogeneity of cells and interconnectedness of these regions, the imprecision with which we can manipulate cells in such small areas, and the presence of diffuse fiber tracts among the neurons all make distinguishing sub-region function a challenge. Acknowledging potential overlaps between sites, the

anatomical terms used in the following sections will be based on the target under consideration and apparent intentions of the authors.

1.2.2.1 RVM in the modulation of nociception

The RVM, composed primarily of the raphe magnus and surrounding reticular region, has long been established as a site involved in descending modulation of nociception. The anatomy and physiology is discussed in greater detail in later sections, but a few key points should be mentioned here. The RVM was defined as the area within this brainstem region where electrical stimulation was sufficient to produce analgesia (Zorman et al. 1981). The RVM sends projections along the entire length of the spinal cord, and a single fiber can have extensive descending collateral branches (Light 1985; Light and Kavookjian 1985). RVM neurons synapse at superficial areas of the spinal dorsal horn that receive input from the dorsal root ganglia, predominantly lamina I, II, and V (Basbaum et al. 1978; Basbaum and Fields 1978). These projections modulate nociception by inhibiting or facilitating the activity of dorsal horn neurons, many of which also concurrently receive direct projections from dorsal root neurons (Waters and Lumb 2008; Waters and Lumb 1997).

Three classes of RVM neurons, all of which project to the spinal cord (Fields et al. 1995; Vanegas et al. 1984), have been differentiated within the pain modulation field by their reflex-related responses to a noxious stimulus. As the animal withdraws from the noxious stimulus, ON-cells increase firing, OFF-cells stop firing, and NEUTRAL cells do not change their firing. Increased firing of ON-cells facilitates nociception, whereas increased firing of OFF-cells is analgesic (Fields and Heinricher 1985). NEUTRAL cells are reportedly the only RVM cell class that contains serotonin, which ties NEUTRAL cells to both pain modulation and respiration (Feldman et al. 2003; Mason et al. 2007; Potrebic et al. 1994; Sorkin et al. 1993). How ON- and OFF-cell firing relate to other modulatory functions of the RVM has not been well established.

1.2.2.2 Respiratory modulation by raphe nuclei

The focus of respiratory modulation in this area of the brainstem has largely been on serotonergic neurons of the raphe obscurus (Corcoran et al. 2009; Depuy et al. 2011; Dreshaj et al. 1998; Guyenet et al. 2010), although raphe magnus and non-serotonergic raphe neurons are also important for respiratory modulation (Dias et al. 2008; Dias et al. 2007; Hellman et al. 2009). The raphe nuclei are the source of most of the serotonin in the central nervous system, and the actions of serotonin in other regions of the brainstem is important for modulation of breathing and in response to hypercapnia (Hodges and Richerson 2008; Manzke et al. 2003; Veasey et al. 1995). The serotonergic raphe cells respond directly to pH changes in both slice and culture, and acidification of the raphe nuclei *in vivo* increases breathing (Hodges et al. 2004; Nattie and Li 2001). Although the serotonergic status of ON- and OFF-cells remains indeterminate, the activity of both serotonergic and non-serotonergic RVM neurons can reliably predict changes in respiratory rate and is correlated with respiratory motor activity (Hellman et al. 2007; Jacobs et al. 2002; Mason et al. 2007) (Figure 2).

Although neurons in raphe magnus have not been shown to project directly to respiratory motorneurons , many neurons in the raphe nuclei have afferent and efferent connections to others areas involved in respiratory function, such as the nucleus of the solitary tract and the rostral ventrolateral medulla (Bago et al. 2002; Basbaum et al. 1978; Holtman et al. 1984). Stimulation of the dorsal medial nucleus of the hypothalamus (DMH), which initiates raphe-mediated hyperalgesia, thermogenesis, tachycardia, and increases in respiratory rate (Madden and Morrison 2004; Martenson et al. 2009; McDowall et al. 2007). Whether this increase in respiration is an effect mediated by direct neuronal projections or whether it is secondary to changes in metabolism from tachycardia and thermogenesis is unresolved (Morrison 2004). Although it has also been proposed that the CO_2-insensitive areas of raphe magnus and RVM coincide with regions that control thermogenesis, this anatomical division has not been verified in detail (Guyenet et al. 2010). Whether nociception and respiration are modulated by separate areas has also not been thoroughly evaluated, but morphine injected directly into raphe magnus does affect respiration in the waking animal. However, whether these changes in respiration coincided with changes in nociception was not reported (Hellman et al. 2009).

1.2.2.3 Thermoregulation via raphe nuclei

Studies of thermoregulation arising from the reticular brainstem have found that the raphe nuclei, especially raphe pallidus and magnus, contain cells that drive sympathetic premotor neurons in the intermediolateral region (IML) of the spinal cord (Morrison 1993). Either direct activation of these or the injection of prostaglandin E_2 (PGE_2) into the medial preoptic area (MPO) increases thermogenesis and core temperature (Morrison 2004; 2003; Zaretsky et al. 2003). Likewise, inactivation of raphe pallidus/magnus lowers core temperature and prevents the system from correctly responding to a decrease in core or skin temperature (Nakamura and Morrison 2007; Ootsuka and Blessing 2005). Although MPO-driven activation of raphe neurons may uniformly increase core temperature, as many as four distinct thermoregulatory systems synapse in the raphe nuclei. Raphe magnus/pallidus modulates changes in brown adipose tissue (BAT) activation, back skin vasomotor, tail vasomotor, and fusimotor responses. Each of these outputs can be activated by injection of PGE_2 into the MPO and likewise can be blocked by non-selective inhibition of neurons in the raphe nuclei (McAllen et al. 2010; Morrison 2011).

These four different thermoregulatory systems are distinguished by the areas of functional output, but connections prior to synapsing in the raphe nuclei provide further separation. For instance, fusiform activity is only responsive to changes in skin temperature, whereas the other three systems respond primarily to changes in core temperature (McAllen et al. 2010). Also, while blockade of the DMH suppresses BAT responses in the face of MPO activation, DMH inactivation does not change tail vasomotor responses (Madden and Morrison 2004; Rathner et al. 2008). In addition to driving BAT activity, DMH stimulation in the anesthetized animal also increases ON-cell activity in the RVM and produces hyperalgesia (Martenson et al. 2009). Similar effects can also be brought about with behavioral paradigms in the awake animal, and are similarly linked to the RVM. Social defeat stress induces hyperalgesia, hyperthermia, tachycardia, and hypertension, as well as a persistent increase in c-*fos* staining in the raphe nuclei (Beig et al. 2009; Hayashida et al. 2010; Marcinkiewcz et al. 2009). Thus, while a separation of the four thermoregulatory systems has not been identified at the level of the individual

neurons of the raphe nuclei, a clear overlap exists between neural circuits of thermoregulation and nociceptive modulation.

1.2.2.4 Cardiovascular regulation

Cardiovascular modulation via the RVM has significant ties and overlap with thermoregulatory modulation. Stimulation of the raphe nuclei increases heart rate in many of the same sites as with thermogenesis, especially ventral and midline at the caudal edge of the facial nucleus (Morrison 2004). These effects are also mediated by monosynaptic connections to sympathetic preganglionic neurons in the IML (Bacon et al. 1990; Morrison 1993). However, with electrical stimulation sympatholytic or bradycardic responses can also sometimes be elicited, depending on the nature and location of the stimulus (Dampney 1994). This observation led to the suggestion that the cardiac function of the raphe nuclei is one of modulation rather than direct control (Lovick 1997).

Stimulation at sites in the DMH sufficient to produce hyperalgesia and hyperthermia also increase heart rate, which can be blocked by inhibition of the RVM (Martenson et al. 2009). The DiMicco lab has performed detailed mapping showing that a functional connection between DMH and RVM is key for tachycardia from low level, persistent stress (DiMicco et al. 2002; Samuels et al. 2004; 2002; Zaretskaia et al. 2003). In my experiments with awake animals, the same stress that they used to produce tachycardia also produces hyperalgesia, which is abolished by inhibition of either the DMH or the RVM (unpublished data).

Raphe nuclei modulation of cardiovascular parameters also occurs through actions at the μ-opioid receptor (Fields et al. 1988). Opioid injection into the RVM decreases heart rate and dampens the tachycardic response in states of arousal (Hellman et al. 2009). Unpublished work from our collaborators shows that opioid actions in the RVM exacerbate decreased cerebral blood flow following a subarachnoid hemorrhage, whereas blockade of μ-opioid receptors improves cerebral blood flow. These results follow directly from another study showing similar results with non-selective RVM blockade, which collectively implicates ON-cells in the RVM-mediated maintenance of cardiac output to the brain (Cetas et al. 2009).

1.2.3 Specificity of function of RVM neurons

The RVM must contain single neurons or groups of neurons that control these functions, although only three cell classes have been described *in vivo*. This raises the question of whether the various inputs driving these responses are integrated by a single group of functionally homogenous neurons, or if several independent neural circuits all relay in the RVM. The long, extensive dendritic arborizations of RVM neurons point to a highly interconnected system but do not rule out the possibility the RVM is composed of intertwined but functionally distinct neurons. The question of specificity of reticular neurons and whether the RVM uses labeled lines, patterned outputs, or multimodal connections is a complicated problem (Brazier and Hobson 1980). By comparing behavioral and neuronal patterns, this thesis explores an element of the overlap and separation of function in this region.

1.3 Modulation of pain in the maintenance of homeostasis

1.3.1 Anatomy of descending nociceptive modulation

The mechanism by which the nervous system modulates pain is not through suppression at higher levels, where the signals that convey damage are already widespread, but at the spinal cord, where the signal first enters the central nervous system. Since the first demonstrations of stimulation-produced analgesia, extensive work has gone into characterizing the anatomy and physiology behind descending nociceptive modulation (Reynolds 1969). Stimulation in the PAG inhibits dorsal horn neurons, but not through direct connections (Basbaum et al. 1976; Basbaum and Fields 1979). Rather, the PAG projects to the rostral ventromedial medulla (RVM), a brainstem area composed of the nucleus raphe magnus and surrounding reticular areas (Basbaum and Fields 1984). Direct electrical stimulation or application of excitatory neurotransmitters in the RVM also is sufficient to produce analgesia (Fields and Heinricher 1985; Oliveras et al. 1979; Zorman et al. 1981). The RVM sends direct projections to dorsal horn neurons, although an individual axon may have collateral connections at multiple levels (Light 1985; Light and Kavookjian 1985; Mokha et al. 1986; Sandkuhler et al. 1987; Watkins et al. 1980).

One of the most important recent discoveries in the field of descending pain modulation has been the recognition of bidirectional pain modulation by the RVM (Fields 1992; Heinricher et al. 2009; Porreca et al. 2002; Saadé and Jabbur 2008; Zhuo and Gebhart 1992). Much of the early work characterizing descending pain modulation focused on analgesia and responses to stimulation, but more recently overwhelming evidence shows that the RVM can also facilitate nociception (Kincaid et al. 2006; Neubert et al. 2004; Sanoja et al. 2008). This facilitatory influence appears to parallel the analgesic aspect in many ways, where projections from RVM to the spinal cord alter nociception and the ascending relay of information by changing the responsiveness of dorsal horn neurons (Fields et al. 1977; Light et al. 1986; Zhuo and Gebhart 1997).

1.3.2 Physiology of the rostral ventromedial medulla

1.3.2.1 ON- and OFF-cells modulate nociception

The neurophysiological basis of bidirectional descending modulation from the RVM is through the actions of two classes of neurons, the ON-cells and the OFF-cells (Heinricher and Ingram 2008). These two classes of neurons were so named because of their responses during a withdrawal from noxious stimuli: ON-cells fire a burst of action potentials and OFF-cells go silent. Extensive work has since gone into characterizing the anatomy, physiology, and pharmacology of these two cell classes, as well as that of the remaining non-responsive cells of the RVM, collectively referred to as the NEUTRAL cells (Fields et al. 1983). Although the role of NEUTRAL cells is undetermined, ON- and OFF-cells respectively facilitate and inhibit nociception through descending projections onto superficial dorsal horn neurons (Fields et al. 1995; Vanegas et al. 1984). The defining properties that separate ON-, OFF-, and NEUTRAL cells are discussed in detail below and summarized in Table 1.

The OFF-cells are the RVM neurons responsible for descending inhibition of nociception. OFF-cell activity pauses during a withdrawal from noxious stimulus, and either systemic or local μ-opioid administration abolishes the pause in conjunction with analgesia (Fields et al. 1988). These observations led investigators to propose that OFF-cell firing mediates the inhibitory influence of the RVM through

descending projections to the dorsal horn (Fields et al. 1977; Fields et al. 1995). Indeed, subsequent investigation has confirmed that increases in OFF-cell activity at the withdrawal are matched by behavioral effects, and any perturbation that eliminates the OFF-cell pause will produce analgesia (Fields et al. 1988; Heinricher et al. 2010a; Heinricher et al. 2010b).

Conversely, ON-cells increase firing at the withdrawal, and administration of morphine suppresses ON-cell activity (Barbaro et al. 1986; Fields et al. 1988). When research on descending modulation was predominantly focused on the analgesic influence of the RVM, ON-cells were thought to function as inhibitory interneurons, possibly to aid in synchronization of OFF-cell activity. However, subsequent investigation has shown that ON-cells are unlikely to be local inhibitory interneurons (Cleary et al. 2008; Fields 1992; Fields et al. 1995). Further work has found that perturbations of ON-cell firing had effects on nociception independent of changes in OFF-cell firing (Kincaid et al. 2006; Neubert et al. 2004).

NEUTRAL cells, the third class of RVM neurons, are notable in their physiological and pharmacological differences from ON- and OFF-cells. NEUTRAL cells do not modulate their firing in response to the onset of noxious stimuli nor increase or decrease firing at the withdrawal response. Also distinct from ON- and OFF-cells, NEUTRAL cells do not respond to μ-opioid or δ-opioid agonists, although they do express the κ-opioid receptor (Harasawa et al. 2000; Winkler et al. 2006). Some NEUTRAL cells do express tryptophan hydroxylase (TPH), the precursor enzyme for serotonin, and some NEUTRAL cells do send projections to the spinal cord, although the convergence of these two properties is unknown (Mason 1997; Vanegas et al. 1984). Since the RVM is the predominant source of descending serotonin and serotonin at the spinal cord influences nociception, NEUTRAL cells may have a yet unknown role in nociception (Alhaider et al. 1991; Hammond et al. 1985; Jacobs and Fornal 1991; LeBars 1988; Potrebic et al. 1994; Wei et al. 2010).

1.3.2.2 Parallels between ON-cells and OFF-cells

ON- and OFF-cells show several physiological and pharmacological similarities, raising the possibility that they represent two sides of a single modulatory mechanism. In anesthetized animals, cells of the same class fire in relative synchrony, such that all ON-cells share the same alternating periods of high and

low activity. OFF-cells likewise have highly correlated activity between cells of the same class, although the periods of activity of OFF-cells are opposed to those of ON-cells (Figure 3). That is, during periods of high ON-cell activity, OFF-cells collectively fire few action potentials, whereas the period of low ON-cell activity is when OFF-cells are the most active (Barbaro et al. 1989; Heinricher et al. 1989). A second parallel is in the ON- and OFF-cell responses to μ-opioids. When administered either systemically or directly into the RVM, μ-opioids agonists produce opposing responses of ON- and OFF-cells. OFF-cells become continuously active and no longer exhibit the characteristic pause, while ON-cells decrease firing, grow silent, and no longer burst (Heinricher et al. 1994). However, a major difference in the responses of ON- and OFF-cells to μ-opioids is in where the drugs act to produce their effects. Iontophorectically applied opioids directly inhibit ON-cells, whereas OFF-cells do not respond to the direct application of opioids (Heinricher et al. 1992). This observation led to the hypothesis that ON-cells have post-synaptic μ-opioid receptors on the cell body or nearby processes, whereas opioid modulation of OFF-cells occurs through presynaptic disinhibition (Heinricher et al. 1994). A corollary of this observation is the reinforcement of the idea that ON- and OFF-cells are distinct groups of neurons, both pharmacologically and by firing patterns.

1.3.3 Descending modulation in acute and chronic pain states

Much of our understanding of RVM physiology and the descending modulatory system has come from the study ON- and OFF-cells during various pain states. The ON- and OFF-cells are defined by their responses to acute noxious stimulation, but their activity is also important in chronic pain conditions. Much of the work to date classifying changes in firing of RVM neurons has focused on two aspects: the spontaneous activity of the cells, and the evoked activity. The evoked activity is the characteristic ON- or OFF-cell response at the withdrawal, although which characteristics of the responses are physiologically relevant is not known. ON-cells fire a of burst action potentials at the withdrawal, which can be described in terms of total number of spikes, peak firing rate, duration of burst, and time to return to baseline. OFF-cells slow or pause firing at the withdrawal, which can be quantified by the duration of pause, the

absolute change in firing rate at the withdrawal, or the percent inhibition relative to pre-stimulation firing rates. The spontaneous firing is more simply measured as the average firing rate in a period without recent noxious stimulation. Since spontaneous activity is the neuronal firing rate at the onset of stimulation, it is proposed to set the behavioral threshold to withdraw. This effect is seen in experiments in which increased ON-cell spontaneous activity manifests as hyperalgesia (increased responsiveness or sensitivity to noxious and non-noxious stimulation) (Heinricher and Neubert 2004; Kincaid et al. 2006; Neubert et al. 2004).

1.3.3.1 Models of acute pain

Many models of acute pain focus on the facilitatory role of ON-cells, where a clear relationship exists between increased ON-cell spontaneous activity and hyperalgesia. Injections into the RVM that increase ON-cell firing without changing that of OFF-cells decreases the threshold to withdrawal from thermal stimulation (Heinricher and Neubert 2004; Neubert et al. 2004). Mustard oil (allyl isothiocyanate) applied to the shaved surface of a limb increases the spontaneous activity of ON-cells, decreases the activity of OFF-cells, and similarly decreases the withdrawal threshold for thermal stimulation. The application of lidocaine to the RVM silences neurons and blocks the hyperalgesia, implicating the increased activity of ON-cells in thermal hyperalgesia (Kincaid et al. 2006). A similar situation occurs during acute inflammation from visceral application of capsaicin, a potent chemical irritant. After colorectal application of capsaicin, increased spontaneous activity of ON-cells drives generalized decreases in thermal withdrawal threshold at the hindpaw (Sanoja et al. 2010). In naloxone precipitated opioid withdrawal, a model of acute hyperalgesia not involving peripheral irritants, ON-cells also display increased spontaneous activity in conjunction with decreased withdrawal thresholds, and RVM block similarly reversed the hyperalgesia (Bederson et al. 1990; Kaplan and Fields 1991). Interestingly, while RVM lidocaine injection reduces hypersensitivity during opioid-withdrawal, in opioid-naïve rats RVM inhibition is frequently reported to increase sensitivity to noxious stimulation and produces hyperalgesia (Martenson et al. 2009; Proudfit 1980a; Proudfit and Anderson 1975; Sandkühler and Gebhart 1984a). In the early stages of nerve injury,

blocking increased ON-cell activity delayed the development of mechanical hyperalgesia (Sanoja et al. 2008). These results show a clear influence of ON-cells and descending facilitation in acute pain.

1.3.3.2 Models of neuropathic pain

The modulatory influence of the RVM in chronic pain is less well understood. Certainly some of the ambiguity in understanding the RVM's influence is due to normal physiological variance in development of any pathology, but also significant differences exist between animal models, methods of nociceptive testing, and the state of the animal at the time of testing (Luukko et al. 1994; Luukko and Pertovaara 1993). Here I will briefly summarize current understanding as well as gaps in knowledge on the influence of the RVM in chronic pain, with a focus on models of persistent inflammation and of nerve injury.

Although several animal models of nerve injury are in common use, most involve damage to a peripheral nerve, usually along the distribution of the L5/L6 roots, followed several weeks later by behavioral testing within the distribution of the damaged nerve. Following nerve injury, many but not all animals display increased sensitivity to stimulation ipsilateral but not contralateral to the injury. The influence of both facilitatory and inhibitory descending modulation is a factor in whether an animal exhibits hypersensitivity after nerve injury. During the first days after nerve injury, blocking increased ON-cell activity inhibits the development of hyperalgesia, although as the injury progresses the same treatment no longer blocks the increased mechanical sensitivity (Sanoja et al. 2008). In later stages, descending inhibition is an important factor in the expression of hyperalgesia, and greater spontaneous OFF-cell activity is associated with decreased expression of hyperalgesia after nerve injury (De Felice et al. 2011). Although these results suggest that ON- and OFF-cells may respectively mediate early and late stages of nerve injury hyperalgesia, other groups argue that ON-cells have a more active role in maintenance of chronic nerve injury hyperalgesia. Increased mechanical sensitivity in awake animals with nerve injury can be blocked by injections of lidocaine into the RVM or lesions of descending fiber tracts (Burgess et al. 2002; Pertovaara et al. 1996; Urban et al. 1999a). RVM lesions targeted towards ON-cells also block the later expression of hyperalgesia from nerve injury (Porreca et al. 2001), and in recordings,

both ON- and OFF-cells show novel and exaggerated responses to stimulation in conjunction with behavioral hypersensitivity (Carlson et al. 2007). From these results, we can conclude that descending facilitation from the RVM is a driving influence in hypersensitivity from nerve injury, although the underlying neuronal mechanisms are still not well understood.

1.3.3.3 Models of chronic inflammatory pain

As a model of chronic inflammatory pain, persistent inflammation can be induced through the subcutaneous injection of Complete Freund's Adjuvant (CFA). Over the days and weeks following CFA injection into a hindpaw, the hindpaw becomes edematous and red, animals eat less and gain less weight, and they protect the paw when waking and sleeping (Stein et al. 1988). As the inflammation progresses, many changes occur in the RVM that maintain or reinforce the chronic pain condition. μ-Opioids injected into the RVM reverse CFA hyperalgesia, and as the inflammation progresses the efficacy of RVM opioids increases (Hurley and Hammond 2000). NMDA receptors in the RVM are upregulated after CFA injection, and intrathecal administration of NMDA antagonists reverses CFA hyperalgesia (Guan et al. 2004; Miki et al. 2002; Ren and Dubner 1993; Ren et al. 1992; Terayama et al. 2000). ERK phosphylation, a marker for changes in cell activity, is increased in the day after CFA injection, and blocking ERK phosphylation blocks the development of hyperalgesia (Imbe et al. 2008; Imbe et al. 2005). However, in contrast to nerve injury, blocking the RVM in chronic inflammation does not relieve the increased sensitivity. Lesions or blockade of the RVM prior to inflammation induction actually worsens the hyperalgesia (Urban et al. 1999b; Vanegas and Schaible 2004; Wei et al. 1999). Likewise, in animals with prior CFA injection, removing the influence of the RVM on dorsal horn neurons increases their sensitivity and receptive fields (Ren and Dubner 1996). These results suggest that the dominant influence from the RVM during chronic inflammation is not one of descending facilitation, but rather descending inhibition.

1.4 Summary

At the level of the RVM, a correlation exists between modulation of nociception, respiration, thermoregulation, and cardiovascular function. Through neurons in the RVM and surrounding regions,

overlapping neural pathways drive facilitation and inhibition of nociception along with other responses to challenges to homeostasis. The intertwined relationship of these circuits is seen through behavioral and cell manipulations, although dissociating whether these are parallel intertwined pathways or multiple outputs of a single system is a difficult task. For the purpose of this work, the independence and overlap of inhibitory and facilitatory nociceptive modulation, thermogenesis, respiration, and cardiac control are considered in the context of ON- and OFF-cells. Since all RVM neurons fall into the grouping of ON-, OFF-, and NEUTRAL cells, then matching the physiological and behavioral changes with neuronal patterns will aid in understanding how multiple effectors are regulated through the RVM and raphe nuclei.

1.4.1 Aim 1: ON- and OFF-cell responses to acute and chronic inflammatory pain

RVM function has been well studied during *acute* challenges to homeostasis, which drive an immediate, adaptive response to injury or threat. Less well understood are the changes that occur in the RVM with *chronic* injury, and how the neurons adapt their responses to a continuous insult or challenge. The focus of the first aim of this thesis is on the comparison of RVM neuronal responses during the acute onset of inflammation against those at a later time point, after the nervous system has adapted to the prolonged inflammatory insult.

The responses of RVM neurons to acute application of irritants are generally consistent. Application or injection of an irritant increases spontaneous activity of ON-cells, decreases activity of OFF-cells, and decreases withdrawal threshold from thermal stimulation. Inhibiting ON-cells blocks the decreases in withdrawal threshold. Although the neuronal effects of CFA injection have not been previously documented, they will likely resemble other acute conditions. However, whether the increased spontaneous ON-cell activity would continue in the case of prolonged irritation has not been studied.

The neuronal changes of within the RVM during prolonged inflammation and other models of chronic pain are not well understood. Chronic pain is a pathological condition resulting from dysfunction of nociception, such that perceptions of pain no longer represent actual tissue injury. While the RVM is clearly tied to the initiation and maintenance of chronic pain, the neuronal basis is less clear. In chronic

pain from nerve injury, RVM neurons displayed sensitization of evoked responses to non-noxious stimuli (Carlson et al. 2007). If chronic inflammation is a prolongation of acute inflammation, then the spontaneous activity of ON-cells would be expected to increase. However, with changes that occur in the RVM, chronic inflammation may more resemble that of chronic nerve injury, such that spontaneous activity is unchanged but evoked responses are potentiated.

The manifestation of chronic inflammatory pain in firing of RVM neurons addresses an important question about RVM physiology. If ON-cell spontaneous activity is increased in chronic inflammation, in a manner similar to that of acute inflammation, then the nature of the acute insult determines the manifestations of the chronic condition. Whereas if in chronic inflammation the ON- and OFF-cell evoked activity resembles that seen with chronic nerve injury, then the time course and chronicity of the insult determines the RVM response. A comparison of RVM neuronal manifestations of acute and chronic inflammation will elucidate the adaptive responses that occur with chronic pain, and will further our understanding of how changes occur in descending modulation of nociception. **My hypotheses are that RVM ON- and OFF-cell firing in acute inflammation will be distinct from that of chronic inflammation, and that changes in RVM neuronal firing during chronic inflammatory pain is part of a time-dependent, maladaptive response.**

1.4.2 Aim 2: ON- and OFF-cell modulation of nociception and respiration

As outlined above, RVM neurons are functionally linked to nociceptive, respiratory, cardiovascular, and thermogenic modulation, although whether these functions are modulated by overlapping sets of neurons or even modulated in conjunction is not clear. This observation of potentially overlapping somatosensory and physiological modulation led to the unsubstantiated hypothesis that separating analgesia from side effects will never be possible (Mason 2011). In Aim 2, I developed methods to study the overlap between respiratory and nociceptive modulation at the level of the RVM, with the goal of elucidating whether opioid analgesia is possible without respiratory depression.

Addressing this question first required a system for monitoring respiration in conjunction with nociceptive testing. Many methods exist for monitoring respiration in small animals, but only a few are compatible with stereotaxy, and of those, none were acceptable solutions for lightly anesthetized animals. In these experiments, the number and severity of invasive procedures changes the nociceptive responsiveness of the animal, so non-invasive methods are ideal for minimal impact on the experiment. With no acceptable alternatives, I developed a non-invasive method for monitoring respiratory rate and tidal volume suitable for use with stereotaxy and nociceptive testing (see Chapter 3). Results from this method were compared to measurements from whole body plethysmography, which is an accurate and validated non-invasive method, but blocks access to the hindpaws. The novel method was also compared to accelerometry based inductance plethysmography, which is also non-invasive and has minimal space requirements, but was found to be less reliable. The construction, testing, and validation of the device are outlined in Chapter 3. This novel method, termed here ventilatory pressure transduction (VPT), provides reliable, unobtrusive, and accurate recordings of respiration without interfering with nociceptive testing and stereotaxic manipulations. VPT provided a practical method to examine the interplay between respiration and nociception at the level of the RVM.

While some suggestion has been made that respiration is anatomically segregated from other functions of the midline raphe, few studies have looked at the possibility of overlapping function (Guyenet et al. 2010). The RVM and surrounding regions have been separately established as important for respiratory modulation and analgesia. Functioning RVM neurons are necessary for responsiveness to challenges such as hypoxia or hypercapnia, and pharmacological manipulations of the RVM will change respiratory rate and tidal volume in the absence of a external challenge (Dias et al. 2007; Hellman et al. 2009; Madden and Morrison 2005). Similarly, RVM lesions attenuate analgesia from systemic morphine, showing that the RVM is necessary for descending antinociception (Proudfit 1980b; Proudfit and Anderson 1975). In these experiments, injection of a μ-opioid agonist into the RVM simultaneously changes nociception and respiration, and blocking μ-opioid receptors in the RVM reverses both analgesia and respiratory depression from systemic injection of morphine.

While these data show that the RVM contains neurons that may modulate both respiration and analgesia, further work from our lab with the compound improgan showed that these two effects are separable. Intracerebroventricular (ICV) injection of improgan, a non-opioid analgesic compound, produces a potent analgesia in conjunction with increased OFF-cell activity (Heinricher et al. 2010b). Muscimol inhibition of RVM neurons prevented analgesia from ICV improgan, showing that improgan produces analgesia through the descending modulatory system (Heinricher et al. 2010a; Nalwalk et al. 2004). Although improgan produces analgesia through the same neural circuits as morphine, the question of respiratory depression accompanying analgesia had not yet been addressed. We found that direct injection of improgan into the RVM produces a potent analgesia and, increased rather than depressed respiration. This aim compares behavioral responses, including heart rate and core temperature, with neural responses to identify the basis by which improgan produces analgesia without respiratory depression. **I hypothesize that ON-cells modulate descending facilitation of nociception, thermogenesis, respiration, and cardiac output, whereas OFF-cells independently modulate descending inhibition of nociception.**

	Net effect on nociception	Response at withdrawal from pain	Response to morphine	Location of opioid receptor
ON-cells	Facilitation (hyperalgesia)	Increased (burst)	Decreased (silent)	Post-synaptic (direct inhibtion)
OFF-cells	Inhibition (analgesia)	Decreased (pause)	Increased (continuous)	Pre-synaptic (disinhibition)
NEUTRAL-cells	Unknown	No change	No change	No receptor

Table 1: Physiological and pharmacological distinctions of ON-, OFF-, and NEUTRAL cells.

A

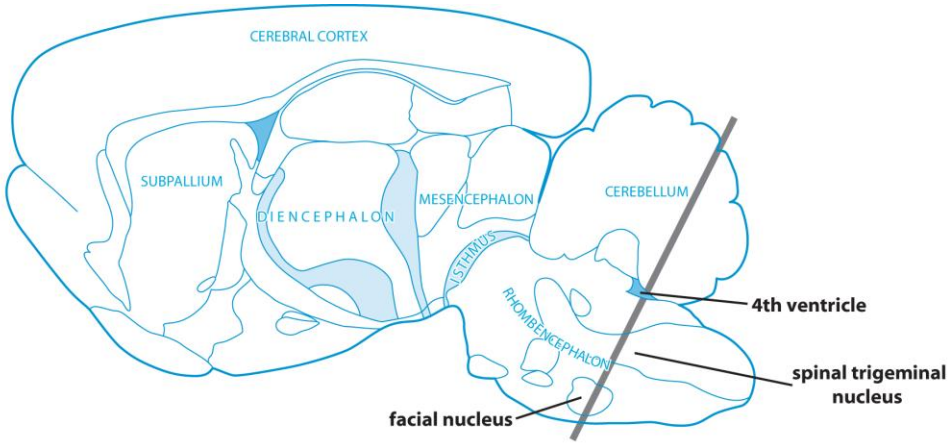
CEREBRAL CORTEX
SUBPALLIUM
DIENCEPHALON
MESENCEPHALON
CEREBELLUM
ISTHMUS
RHOMBENCEPHALON
4th ventricle
spinal trigeminal nucleus
facial nucleus

B

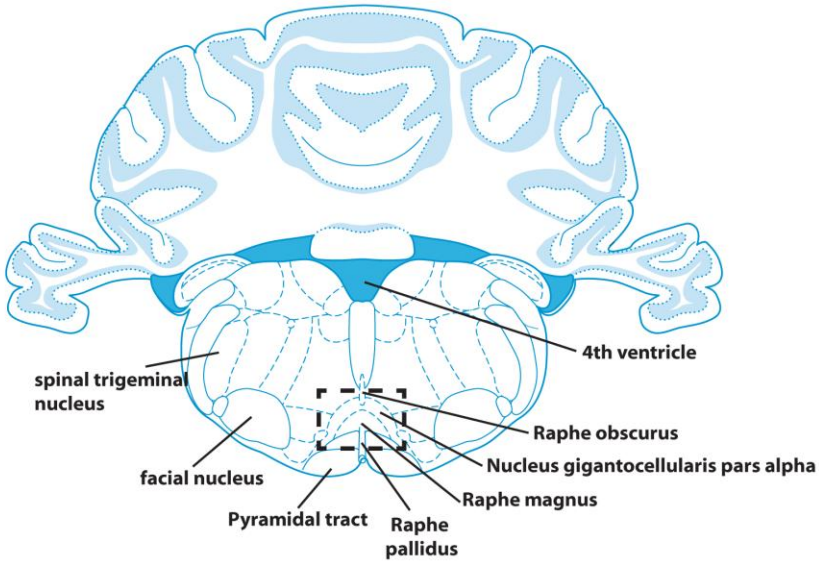
4th ventricle
spinal trigeminal nucleus
Raphe obscurus
Nucleus gigantocellularis pars alpha
facial nucleus
Raphe magnus
Pyramidal tract
Raphe pallidus

C

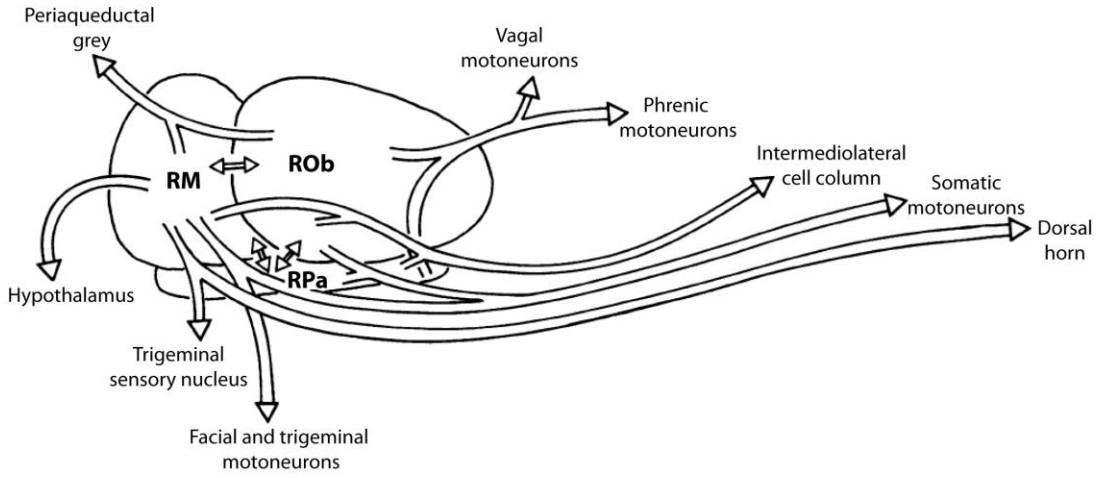
Periaqueductal grey
Vagal motoneurons
Phrenic motoneurons
Intermediolateral cell column
Somatic motoneurons
Dorsal horn
RM
ROb
RPa
Hypothalamus
Trigeminal sensory nucleus
Facial and trigeminal motoneurons

Figure 1: Anatomy of the RVM and surrounding regions.

A) The RVM is a region of the ventral brainstem medial to the facial nucleus, and extends through approximately the same the rostral-caudal boundaries. The dorsal edge of the facial nucleus also marks the dorsal boundary of the RVM. In the parasagittal view of the rat brain shows relative location of the facial nucleus and, by interference, the RVM. The grey line marks the section from which (B) is taken, approximately 2.6mm caudal to the interaural line.

B) An axial view of the brainstem shows the constituent nuclei of the RVM. In this view, the dashed box marks the boundaries of the RVM, which includes the raphe magnus, raphe pallidus, nucleus gigantocellularis pars alpha, and a portion of raphe obscurus.

C) Internal and external connections of raphe nuclei show the complexity of the region. Sagittal view. Abbreviations: RM, Raphe magnus; ROb, Raphe obscurus; RPa, Raphe pallidus.

(A) and (B) modified from *The Rat Brain in Stereotaxic Coordinates* (Paxinos and Watson 1997). (C) Reproduced from *The medullary raphe nuclei: a system for integration and gain control in autonomic and somatomotor responsiveness* (Lovick 1997)

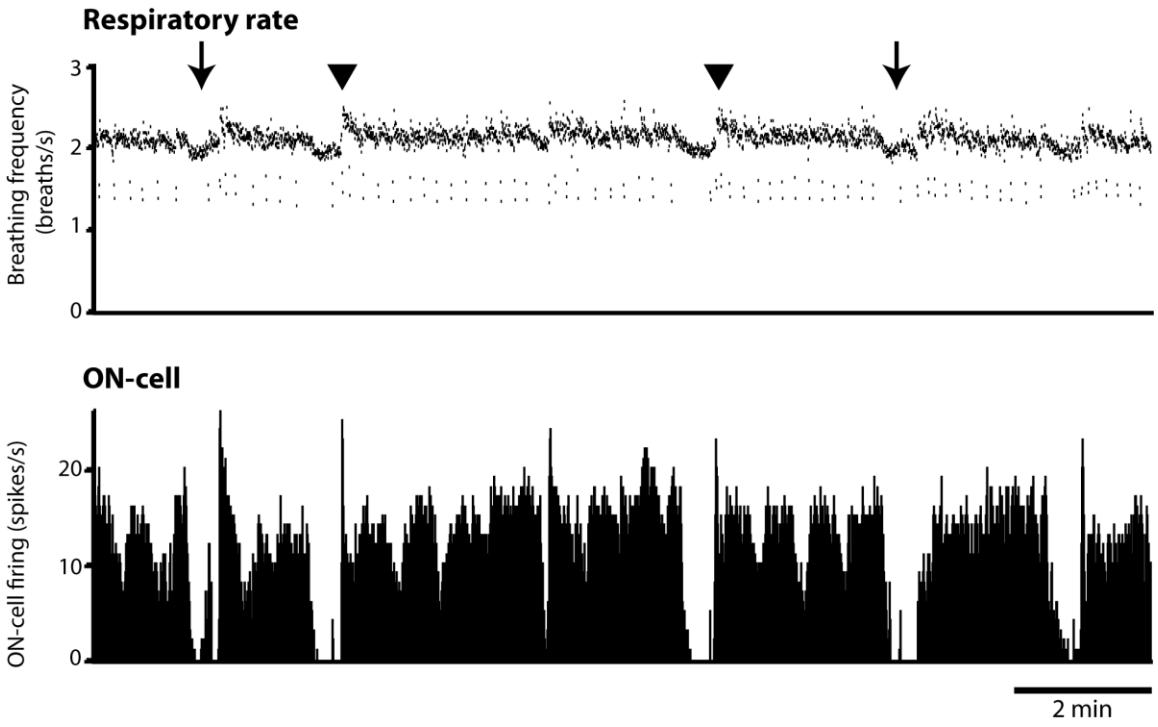
Respiratory rate
Breathing frequency (breaths/s)
3
2
1
0
ON-cell
ON-cell firing (spikes/s)
20
10
0
2 min

Figure 2: Correlation between ON-cell firing and breathing frequency.

Changes in respiratory rate (top) occur in synchrony with changes in ON-cell firing (bottom). Arrows indicate areas where both ON-cell firing is decrease and respiratory rate is lower than baseline. Arrowheads show points where a sudden increase in ON-cell activity is accompanied by a similar increase in breathing frequency. (Cleary et al, unpublished)

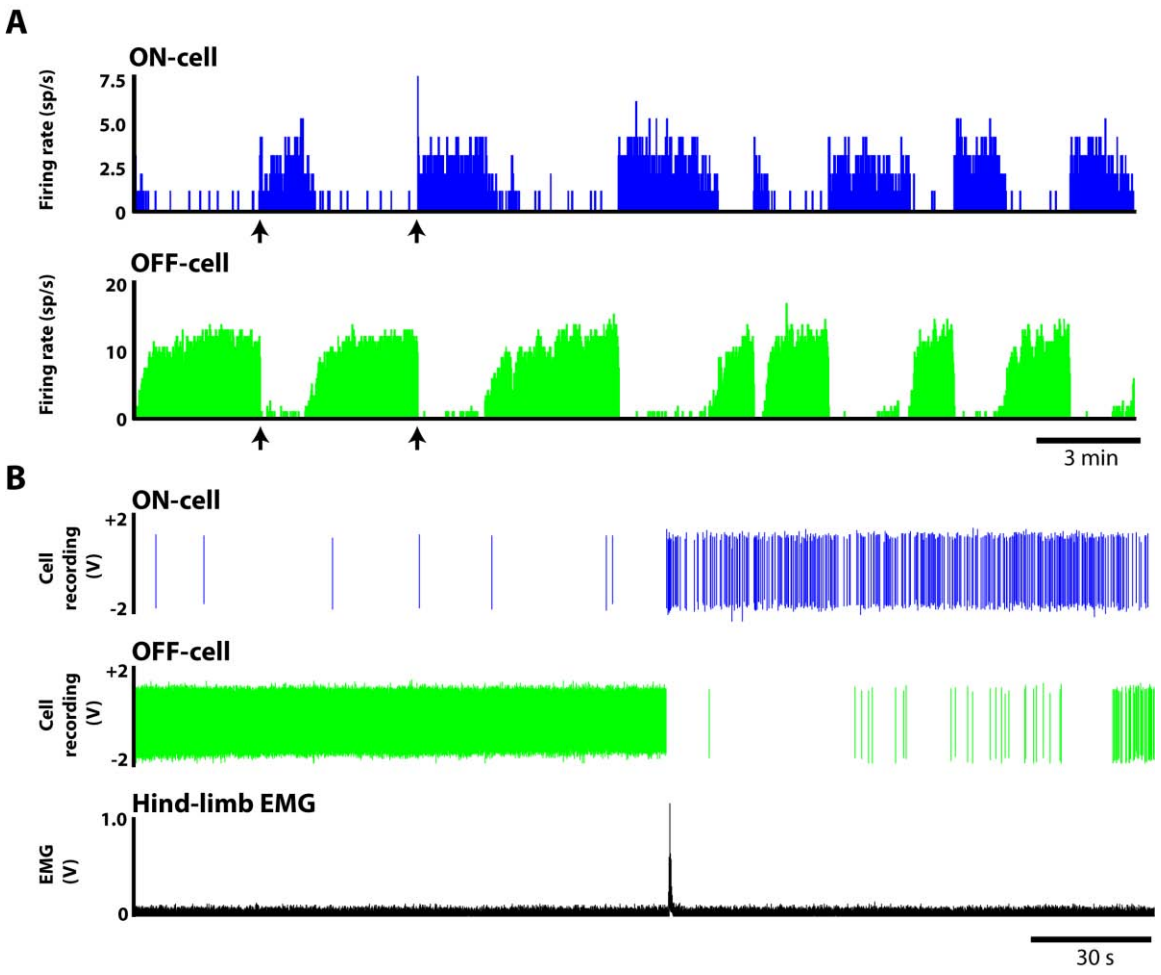
A
ON-cell
Firing rate (sp/s)
7.5
5.0
2.5
0
OFF-cell
Firing rate (sp/s)
20
10
0
3 min
B
ON-cell
Cell recording (V)
+2
-2
OFF-cell
Cell recording (V)
+2
-2
Hind-limb EMG
EMG (V)
1.0
0
30 s

Figure 3: Temporal patterns of ON- and OFF-cell firing.

A) Ratemeters from an ON-cell (top) and an OFF-cell (bottom) recorded together on a single electrode show the alternating periods of high and low activity of the two RVM cell classes. Periods of increased ON-cell activity correspond to low OFF-cell activity. Arrows indicate points of withdrawal from noxious thermal stimulus.

B) Individual action potentials from the ON-cell (top) and OFF-cell (middle) are shown during withdrawal from a noxious thermal stimulus. EMG recording from the calf muscles shows the moment of withdrawal (bottom). (Cleary et al, unpublished)

CHAPTER 2

Manuscript #1

Adaptations in responsiveness of brainstem pain-modulating neurons in acute compared to chronic inflammation

Daniel R. Cleary[a] and Mary M. Heinricher[a,b]

[a]Department of Neurological Surgery, Oregon Health & Science University, Portland, OR, USA

[b]Department of Behavioral Neuroscience, Oregon Health & Science University, Portland, OR, USA

2.1 Abstract

Despite similar behavioral hypersensitivity, acute and chronic pain have distinct neural bases. Here we used intraplantar injection of Complete Freund's Adjuvant (CFA) to directly compare activity of pain-modulating neurons in the rostral ventromedial medulla (RVM) in acute versus chronic inflammation.

Heat- and von Frey-evoked withdrawal reflexes and corresponding RVM neuronal activity were recorded in lightly anesthetized animals either during the first hour after CFA injection (acute) or 3-10 days later (chronic). Thermal and modest mechanical hyperalgesia during acute inflammation were associated with increases in the spontaneous activity of pain-facilitating ON-cells and suppression of pain-inhibiting OFF-cells. Acute hyperalgesia was reversed by RVM block, showing that the increased activity of RVM ON-cells is necessary for behavioral hypersensitivity. In chronic inflammation, thermal hyperalgesia had resolved, but mechanical hyperalgesia had become pronounced. The spontaneous discharges of ON- and OFF-cells were not different from controls, but the mechanical response thresholds for both cell classes were reduced into the innocuous range. In contrast to acute inflammation, RVM block in the chronic condition worsened mechanical hyperalgesia.

These studies identify distinct contributions of RVM ON- and OFF-cells to acute and chronic inflammatory hyperalgesia. During early immune-mediated inflammation, ON-cell spontaneous activity promotes hyperalgesia. However, after inflammation is established, the anti-nociceptive influence of OFF-cells is dominant, but the lowered threshold for the OFF-cell pause allows behavioral responses to stimuli that would normally be considered innocuous. The efficacy of OFF-cells in counteracting sensitization of ascending transmission pathways could therefore be an important determining factor in development of chronic inflammatory pain.

2.2 Introduction

Chronic pain is not merely prolonged activation of normal pain pathways, but instead reflects plasticity in both peripheral and central neuronal circuits. The rostral ventromedial medulla (RVM), the final output relay from a well-studied pain-modulating system (Fields et al. 2006). This system modulates nociceptive transmission pathways during acute injury, but is also thought to maintain sensitization during chronic pain (Heinricher et al. 2009; Porreca et al. 2002; Ren and Dubner 2002).

The transition from acute to chronic pain is accompanied by physiological and molecular changes in the RVM. For example, the effectiveness of electrical stimulation in inhibiting nociceptive behaviors fluctuates over the first 24 hours following injection of an inflammatory agent in the hindpaw (Guan et al. 2003; Guan et al. 2002; Terayama et al. 2000). In the days after induction, inflammation also produces changes in NMDA, AMPA , trkB, opioid, and neurokinin-1 receptor expression and function (Guan et al. 2004; Guan et al. 2003; Guan et al. 2002; Guo et al. 2006; Hurley and Hammond 2000; LaGraize et al. 2010; Ren and Dubner 2002; Schepers et al. 2008), as well as changes in local glial activation (Roberts et al. 2009). However, the functional significance of many of these molecular and cellular changes remains unclear. Because the RVM can independently facilitate and inhibit nociception (Fields 2004; Heinricher et al. 2009), enhanced behavioral sensitivity could reflect increased descending facilitation, reduced descending inhibition, or a combination of both.

The RVM inhibits and facilitates nociceptive transmission pathways through the actions of two classes of neurons, “OFF-cells” and “ON-cells”, respectively (Fields et al. 2006; Heinricher et al. 2009), but the specific contributions of the ON- and OFF-cell classes to different chronic pain states are not well understood. In acute neurogenic inflammation, the spontaneous firing of both cell classes is altered, with ON-cell discharge significantly increased and OFF-cell firing depressed. The increase in ON-cell activity is necessary for hyperalgesia (Brink et al. 2012; Kincaid et al. 2006). By extension, if chronic inflammation were simply a continuation of the acute condition, then ON-cells would be expected to show increased spontaneous firing in chronic pain states. However, in another model of chronic pain, nerve injury, RVM

ON-cells do not display abnormal spontaneous activity (Carlson et al. 2007; Pertovaara et al. 2001). Instead, both ON- and OFF-cells become sensitized and display abnormal responsiveness to innocuous tactile stimulation (Carlson et al. 2007). The dissimilar pattern of RVM activity in acute neurogenic inflammation compared to chronic nerve injury indicates that, despite clear evidence implicating the RVM in behavioral hypersensitivity in both conditions, the underlying RVM processes mediating hyperalgesia are not the same. This difference could relate to the type of injury (inflammatory vs. neuropathic) or to its time-course (acute vs. chronic).

The goal of the present experiments was to record the activity of identified ON- and OFF-cells at acute (1 hour) and chronic (3-10 days) time points during localized inflammation induced by injection of complete Freund's adjuvant (CFA) in the plantar hindpaw. This approach allowed us to compare directly the activity of pain-facilitating and pain-inhibiting RVM neurons under standard conditions during acute and chronic immune-mediated inflammation, and to test the net RVM contribution to thermal and mechanical hypersensitivity at both time points.

2.3 Materials and Methods

All experimental procedures followed the guidelines of the National Institutes of Health and the Committee for Research and Ethical Issues of the International Association for the Study of Pain. Methods used here were approved by the Institutional Animal Care and Use Committee at the Oregon Health & Science University.

2.3.1 Inflammation

For studies of acute inflammation, male Sprague-Dawley rats weighing between 250 and 350 g were anesthetized and stabilized in a lightly anesthetized state (described below). Saline (0.1 ml) or Complete Freund's Adjuvant (CFA, heat-killed Mycobacterium tuberculosis in mineral oil, 1 mg/ml, 0.1 ml, Sigma-Aldrich) was injected subcutaneously into the plantar surface of the left hindpaw. In a subset of animals, paw thickness and surface temperature was measured at the base of the ankle before and 15 minutes after hindpaw injection.

To induce chronic inflammation, rats weighing less than 250 g were briefly anesthetized with isoflurane (4%, 4-5 minutes). Saline (0.1 ml) or CFA (0.1 ml) was injected subcutaneously into the plantar surface of the left hindpaw. Animals were anesthetized 3-10 days later (mean ± SEM: 6.2 ± 0.5 days) for electrophysiological and behavioral studies, at which point they weighed between 250 and 350 g.

2.3.2 Experimental animals

A total of 112 animals was used in this work. For electrophysiological studies of RVM neurons in *acute* inflammation, we used a within-subject design comparing pre- and post-injection neuronal activity and thermal and mechanical nociception. Seventeen animals were treated with saline and 24 with CFA. We recorded 6 NEUTRAL-cells, 5 OFF-cells, and 6 ON-cells in the saline group and 10 NEUTRAL-cells, 7 OFF-cells, and 11 ON-cells in the CFA group. To determine the contribution of the RVM to behavioral hypersensitivity in these animals, the RVM was inactivated by lidocaine microinjection in additional animals following plantar saline (n = 8) or CFA (n = 6) injection.

For electrophysiological studies of RVM neurons during *chronic* inflammation, we used a between-subject design, comparing neuronal activity and mechanical and thermal nociception in CFA-treated animals with saline-treated and naïve control groups. Since data from saline-treated and naïve animals were not significantly different, those groups were combined for subsequent analyses. Twenty-three control animals and 22 CFA-injected animals were studied. We recorded 8 NEUTRAL-cells, 10 OFF-cells, and 12 ON-cells in control animals, and 8 NEUTRAL-cells, 11 OFF-cells, and 13 ON-cells in CFA-treated animals. To determine the contribution of the RVM to behavioral hypersensitivity in animals with chronic inflammation, the RVM was inactivated by lidocaine microinjection in an additional five control and seven CFA-treated animals.

2.3.3 Lightly Anesthetized Preparation

Electrophysiological recordings and RVM drug injections in lightly anesthetized animals were performed as described previously (Carlson et al. 2007; Kincaid et al. 2006; Martenson et al. 2009). Animals were initially deeply anesthetized with either sodium pentobarbital (60 mg/kg, i.p.) or isoflurane

(4% in oxygen). A catheter was placed in an external jugular vein for subsequent infusion of methohexital and the animal placed in a stereotaxic frame. While the animal was still deeply anesthetized, a craniotomy was drilled for access to the RVM.

After the surgical preparation was completed, the methohexital infusion was adjusted so that animals displayed no spontaneous movement or vocalization, but withdrew briskly from noxious heat or mechanical stimulation applied to an untreated hindpaw (15-30 mg/kg/hr). In animals initially induced using pentobarbital, we waited at least 2.5 hours before starting electrophysiological recording, since even minimal levels of pentobarbital mask mechanical hyperalgesia in lightly anesthetized rats (Carlson et al. 2007). Room temperature was kept around 25 °C, and body temperature maintained between 36 and 37 °C using a heating pad. Heart rate was monitored using EKG, and respiratory rate was monitored by recording changes in air pressure at the nares, a technique that has been described in detail elsewhere (Cleary et al. 2012). The experimental protocol was started once heart rate, core temperature, and respiratory rate were stable and methohexital flow rate not adjusted for a minimum of 45 min.

2.3.4 Electrophysiological Recording

Stainless-steel microelectrodes (Microprobe, Gaithersburg, MD) with gold- and platinum-plated tips were used for all recordings. Signals were amplified 10,000-fold, sampled at 20 kHz, bandpass filtered (150 Hz to 15 kHz), and displayed on an oscilloscope. The signal was simultaneously digitized and stored for off-line analysis.

RVM neurons were isolated and characterized as ON-cells, OFF-cells, or NEUTRAL-cells. This mutually exclusive and exhaustive classification is based on firing patterns relative to nocifensor withdrawals (Fields and Heinricher 1985). At the withdrawal, “ON-cells” become active (if not already active), “OFF-cells” stop firing (if active), and NEUTRAL-cells do not change firing rate. Both OFF-cells and ON-cells can fire steadily or cycle between periods of activity and inactivity. Because an ON-cell with high basal firing can be easily misclassified as a NEUTRAL-cell (Barbaro et al. 1986), possible NEUTRAL-cells with continuous spontaneous activity were verified as such prior to starting the protocol by giving a brief bolus of

anesthetic to the point that the withdrawal reflex was abolished. Firing of spontaneously active ON-cells slows or stops with this manipulation, which unmasks reflex-related responses.

2.3.5 Behavioral Testing

For thermal nociceptive testing, a Peltier device (Yale Instrumentation, New Haven, CT) was lightly applied to the plantar surface of the hindpaw, heated at a constant rate of 1.5 °C/s from 35 °C to a maximum of 53 °C. To avoid damage to the paw, the Peltier device was removed when the animal withdrew. Trials were initiated at 4-5 min intervals, with an attempt to capture a period when the cell under study was active (OFF-cells) or inactive (ON-cells), which allowed us to measure the withdrawal-related pause and burst that characterize these neurons. NEUTRAL-cells were tested at 4-5 min intervals irrespective of cell activity.

For mechanical testing, von Frey Fibers (4, 8, 15, 26, 60, and 100 g) were applied in ascending order to the interdigital webbing for a period of either 8 s or until a withdrawal was elicited, with three trials at each tested force. Three testing sites were rotated. Withdrawals were recorded via electromyograph (EMG) electrodes placed 1 cm apart in the muscles of the calf. Individual trials were initiated at intervals of at least 1 min, with longer interstimulus intervals used when necessary to capture a period when OFF-cells were active or ON-cells inactive.

2.3.6 Experimental Protocols

In electrophysiological studies of *acute* inflammation, the experimental protocol was initiated after isolation and characterization of one (or occasionally, two) well distinguished neuron or neurons as an ON-, OFF- or NEUTRAL-cell. The first 10-15 minutes of neuronal activity was recorded without any nociceptive testing; this period was used to measure baseline spontaneous activity in the absence of stimulation. Three thermal trials with the Peltier device were then performed on the experimental (left) hindpaw. To minimize the potential confound of secondary hyperalgesia from the recent noxious thermal trials, mechanical testing using von Frey fibers was initiated at least 5 min after the last thermal trial. Saline or CFA was then injected into the plantar surface of the left hindpaw. Spontaneous firing rate was

determined (10-min sample beginning 1-2 min after completing the hindpaw injection), followed by three thermal trials and a second round of mechanical testing of the treated paw. One hour after hindpaw injection, this was repeated, with a third 10-min sample of spontaneous firing, followed by three additional thermal trials and repeated mechanical testing. For all experiments, only one protocol was performed in each animal.

In behavioral studies of the role of the RVM in *acute* CFA-evoked hypersensitivity, we used a within-subject design. Baseline thermal and mechanical sensitivity was determined, and CFA or saline injected into the left hindpaw. Thermal and mechanical testing were repeated for the experimental paw, followed by lidocaine (4%, 200 nl) injection into the RVM to block all neuronal activity. Behavioral testing was again repeated.

In electrophysiological studies of *chronic* inflammation, activity of RVM neurons in controls was compared with that in animals injected with CFA 3-10 d previously. Following isolation and characterization of an RVM neuron or neurons, spontaneous firing rate was determined as above. Three thermal trials were then initiated for each hindpaw in alternating succession. Following a 5-10 min recovery period, mechanical threshold testing was performed for the two hindpaws. In some cases, the von Frey fiber thresholds had been determined prior to the initiation of the protocol, and mechanical testing then commenced at one level below that threshold. Otherwise, von Frey fibers between 4 and 100 g were applied.

In behavioral studies of the role of the RVM in *chronic* CFA-evoked hypersensitivity, thermal and mechanical responses for the treated hindpaw were measured before and after injection of lidocaine in the RVM (4%, 200 nl) in controls or animals injected 3-10 d previously with CFA in the left hindpaw.

2.3.7 Histology

At the conclusion of the protocol, recording sites were marked with an electrolytic lesion. RVM microinjection sites were marked by green fluorescent beads (Invitrogen, Eugene, OR), either mixed in with the lidocaine or injected separately at the completion of the experiment. Animals were overdosed

with methohexital and perfused transcardially with saline followed by 10% formalin. The brainstem was blocked, cut into 60 μm thick sections, and the recording or injection site visualized on a BX51 Olympus microscope. Sites were mapped in accordance with the atlas of Paxinos and Watson (1997). The RVM was defined as the area of the raphe magnus and adjacent reticular formation at the level of the facial nucleus (-1.04 to -2.6 mm IA, ± 0.6 mm lateral, and 9-10 mm ventral to the brain surface). Locations of neurons recorded in CFA-treated and control groups are plotted in Fig. 4. Neurons outside of the RVM boundaries were excluded from analysis.

2.3.8 Data Analysis

Neuronal and EMG activity, heart rate, respiratory rate, paw heat-stimulus temperature, and von Frey application timing were recorded using Spike2 (Cambridge Electronic Design, Cambridge, England). Action potentials were sorted using template matching on waveforms, and discriminated on an individual spike basis.

The behavioral threshold was defined as the lowest von Frey fiber force at which the animal withdrew its paw from stimulation in at least two of three trials. Latency to withdraw was the time difference between the onset of the heat or von Frey stimulus and the first point of positive inflection on the EMG. EMG magnitude was quantified by subtracting the baseline and then smoothing, rectifying, and integrating the resultant signal (Carlson et al. 2007). These data are therefore expressed as arbitrary units.

Reflex-related changes in activity for both ON- and OFF-cells were quantified by comparing firing rates at the time of the withdrawal (3 s interval beginning 0.5 s prior to the withdrawal) to that in the 10 s before stimulus onset. With mechanical stimulation, where withdrawal was not always evident, mean firing rate was measured over the entire 8 s period after the onset of the stimulus, regardless of when the stimulus was withdrawn, and compared to the 10 s period prior to stimulus onset.

2.3.9 Statistics

Data are presented as mean ± SEM, with *p* values of less than 0.05 considered statistically significant.

Effects of acute CFA on thermal withdrawal threshold and EMG magnitude were analyzed with ANOVA followed by Dunnett's test for comparison with baseline. Changes in mechanical withdrawal threshold from baseline were determined using either a Wilcoxon's signed-rank test or a Friedman's test with Dunn's post-hoc test. Effects of acute CFA treatment or RVM lidocaine injection on withdrawal magnitude and latency of response from mechanical stimuli were determined using a two-way ANOVA and Bonferroni post-hoc tests, with time (before/after hindpaw injection) as a repeated measure. Spontaneous activity after acute CFA injection was compared with baseline using a Friedman's test with Dunn's post hoc test. Changes in evoked activity (ON-cell increase and OFF-cell inhibition) were analyzed with a Wilcoxon's signed-rank test. Effects of lidocaine on thermal withdrawal thresholds were determined using two-way ANOVA, with time and treatment as factors, followed by Bonferroni post-hoc tests.

For the chronic CFA-treated and control groups, anesthetic requirements and heart rate were compared using *t*-tests for independent means. The thresholds for responses to von Frey probes were compared using a Kruskal-Wallis ANOVA followed by Dunn's post-hoc test. Thermal withdrawal thresholds for ON- and OFF-cell responses, areas under the curve for stimulus-responses, withdrawal latencies, and EMG magnitudes were compared using one-way ANOVA followed by Tukey's post-hoc tests. Spontaneous firing rates of the different groups were compared for each cell class using a Mann-Whitney U. For lidocaine injection experiments, magnitude and latency of response were compared using a two-way mixed-design ANOVA and Bonferroni post-hoc test, with force as one factor and pre- vs. post-lidocaine injection as the repeated factor. Correlations were calculated using Spearman's rho.

2.4 Results

2.4.1 Acute CFA injection produces thermal hyperalgesia and slight but measurable mechanical hypersensitivity in lightly anesthetized animals

In lightly anesthetized animals, plantar injections of CFA produced acute localized inflammation, edema, and small, spontaneous twitches of the injected hindpaw. Paw thickness was increased from 5.42 ± 0.06 mm to 6.26 ± 0.11 mm by 10 min after CFA injection ($p < 0.0001$). Paw temperature was increased from 29.5 ± 0.6 to 33.8 ± 0.3 °C ($p < 0.0001$), comparable to previous reports in awake behaving animals after CFA hindpaw injection (Hurley and Hammond 2000). Control injections of saline produced a smaller but statistically significant increase in paw thickness (from 5.36 ± 0.12 to 5.71 ± 0.08 mm, $p = 0.02$). Paw temperature was not altered (from 30.0 ± 0.7 to 30.6 ± 0.7 °C, $p = 0.2$). Heart rate and breathing frequency were both significantly increased following plantar injection of CFA (heart rate: 361.7 ± 4.5 to 369.8 ± 5.1 beats/min, $p = 0.007$; breathing rate: 1.61 ± 0.05 breaths/s to 1.65 ± 0.05 breaths/s, $p = 0.023$) but not saline (heart rate: 369.4 ± 7.2 to 366.1 ± 7.4 beats/min, $p = 0.29$; breathing rate: 1.67 ± 0.05 breaths/s to post-injection: 1.63 ± 0.05 breaths/s, $p = 0.41$).

Within 15 min of CFA injection, there was significant heat hyperalgesia, with the withdrawal threshold decreased by approximately 5 °C. This hyperalgesia was maintained for the entire 60-min observation period (Fig. 5A). Control injections of saline produced a slight (< 1 °C), but statistically significant, reduction in thermal withdrawal threshold (Fig. 5A). Withdrawal magnitude was not significantly increased in either group (Fig. 5B).

Mechanical sensitivity was modestly enhanced in both CFA- and saline-treated animals. The threshold for withdrawal from von Frey fibers was lowered (Fig. 5C), and the magnitude of withdrawals evoked by 60 and 100 g fibers was increased (Fig. 5D). The latency to withdraw to the 60 g fiber was also slightly reduced for both groups (Fig. 5E).

Lightly anesthetized animals thus develop potent thermal hyperalgesia within the first hour following acute injection of CFA. There is also a modest but measurable mechanical hypersensitivity in both CFA-treated and control animals.

2.4.2 Spontaneous and reflex-related activity of RVM neurons in acute inflammation

The behavioral hypersensitivity seen in the first hour following CFA treatment was associated with changes in the activity of RVM ON- and OFF-cells, but not NEUTRAL-cells. As shown in the examples in Fig. 6A, the spontaneous firing of ON-cells was increased within minutes of the injection, while that of OFF-cells was reduced, although not completely inhibited. These changes were not maintained however, and activity was no longer significantly different from baseline at 60 min post-injection (Fig. 6B). The reflex-related activation of ON-cells was unchanged following CFA, as was activity evoked by von Frey stimulation (Fig. 6C). Thus, the characteristic activation at the time of withdrawal was unaffected by acute inflammation, although the heat-evoked withdrawal occurred at a lower temperature. The OFF-cell pause was modestly enhanced following CFA, but only for heat-evoked withdrawal; suppression of firing during von Frey probing was not different from baseline (Fig. 6C). Saline injection had no effect on the spontaneous or reflex-related firing of ON-cells or OFF-cells.

Some NEUTRAL-cells have been reported to change firing properties to be more like ON- or OFF-cells during the development of inflammation following local administration of CFA (Miki et al. 2002). We therefore examined NEUTRAL-cells in the present experiments. NEUTRAL cells characterized using our protocol showed no change in spontaneous activity following CFA injection (Fig. 6B). Further, none developed ON- or OFF-like changes in firing.

2.4.3 RVM blockade reverses both thermal and mechanical hyperalgesia during acute inflammation

To determine whether RVM activity contributes to the behavioral hypersensitivity during acute inflammation in lightly anesthetized animals, we blocked RVM activity by microinjecting lidocaine into the RVM in a subset of animals without cell recording. After baseline testing, an injection was made into the hindpaw and thresholds determined. Lidocaine was then microinjected into the RVM. Blockade of RVM activity by lidocaine reversed CFA-induced thermal hyperalgesia, but had no effect in saline-injected controls (Fig. 7A).

Lidocaine also reversed CFA-induced decreases in mechanical withdrawal threshold (Fig. 7B), increases in response magnitude (Fig. 7C), and decreases in response latency (Fig. 7D). These data show

that facilitatory output from the RVM is necessary for both thermal and mechanical hypersensitivity during acute localized inflammation induced by CFA.

2.4.4 Chronic CFA injection produces mechanical hypersensitivity but not thermal hyperalgesia in lightly anesthetized animals

The second set of experiments used animals treated with CFA or saline 3 to 10 days prior to the recording session. Anesthetic requirements in the CFA-treated and control groups were similar (21.3 ± 1.2 mg/hr *vs*. 21.0 ± 1.3 mg/hr, respectively, $p = 0.95$). Heart rates were also comparable in the two groups (413.8 ± 10.3 vs. 393.3 ± 8.2 beats per min in CFA-treated and controls respectively, $p = 0.12$). Respiratory rates were not measured in these experiments.

CFA-treated animals did not show thermal hypersensitivity. Heat-evoked withdrawal thresholds of the chronic CFA-treated paw were not different from those on the contralateral side or from the saline-treated control group (Fig. 8A). There was also no difference between sides or groups in response magnitude (EMG, data not shown).

In contrast with the absence of thermal hypersensitivity, mechanical hypersensitivity in the chronic CFA-treated paw was substantial. The threshold for withdrawal to von Frey fiber probing of the treated paw was significantly reduced (Fig. 8B), response magnitude was increased across the range of tested fibers (Fig. 8C), and response latency was shorter (Fig. 8D) compared to the contralateral side and controls.

Animals subjected to chronic localized inflammation thus display profound mechanical hypersensitivity in the lightly anesthetized state, with thresholds significantly lower than that seen in the acute condition. Notably, only 8% of the animals that had been tested with acute CFA showed thresholds in the innocuous range (< 26 g). By contrast, 85% of animals tested in the chronic condition exhibited thresholds below 26 g ($\chi 2 = 26.1$, $p < 0.0001$). No saline-treated animal, acute or chronic, responded to fibers in the innocuous range. The increased sensitivity in the chronic condition can also be seen in comparisons of response magnitude (Figs. 5D and 8C). Comparison of the response to probing with the

100 g fiber showed a significantly enhanced response in the chronic compared to the acute condition (p = 0.035).

2.4.5 Activity of RVM neurons during chronic inflammation

The pattern of activity of RVM neurons in animals subjected to chronic inflammation was distinct from that seen in the first hour after CFA treatment. Unlike RVM neurons recorded during acute inflammation, ON- and OFF-cells showed comparable rates of spontaneous firing in the chronic CFA-treated and control animals (Fig. 9A).

In contrast to spontaneous firing, the mechanically evoked ON- and OFF-cell changes in activity were enhanced in the CFA-treated animals, and paralleled the shift in behavioral sensitivity. First, the threshold for evoking a change in cell activity was reduced (ipsilateral hindpaw: 14.2 ± 3.8 g; contralateral hindpaw: 74.1 ± 7.1 g, $p < 0.0001$). Not surprisingly, since the responses of these neurons are associated with behavior rather than with noxious stimulation *per se*, there was a high correlation between behavioral and neural thresholds (Spearman's rho = 0.84). Both cell classes also exhibited a leftward shift in the stimulus response curve (Fig. 9B,C). Finally, the response-related activation of ON-cells (Fig. 9B) was correlated with withdrawal magnitude (magnitude shown in Fig. 8C; rho = 0.24, $p < 0.0001$).

For thermal stimulation, there was no effect of CFA treatment on the response-related changes in activity for either ON- or OFF-cells (Fig. 6B and C; for ON-cells: p = 0.25, for OFF-cells: p = 0.75).

Firing of NEUTRAL-cells was comparable in chronic CFA-treated and control groups, with no difference in spontaneous firing rates (Fig. 6A). NEUTRAL-cells also did not respond to von Frey probing of any force, whether applied to inflamed or non-inflamed hindpaws (Fig. 9D), and no difference was observed among groups during thermal stimulation (Fig. 9D, p = 0.45).

2.4.6 RVM blockade potentiates mechanical hypersensitivity in animals subjected to chronic inflammation

We next blocked activity of the RVM in order to determine whether this region contributes to mechanical hypersensitivity after chronic inflammation, as it does to thermal hyperalgesia in acute

inflammation. The threshold for heat-evoked withdrawal was not changed by lidocaine injection into the RVM in either chronic CFA-treated or control animals (Fig. 10A). However, the response magnitude was significantly reduced in both groups (Fig. 10B).

Unlike thermal responsiveness, mechanical hypersensitivity in the treated paw was potentiated by RVM block. Mechanical threshold, already lower than controls in baseline, was further reduced following RVM lidocaine in animals subjected to chronic hindpaw inflammation. RVM block had no effect on withdrawal threshold in control animals (Fig. 10C). There was a small, but statistically significant increase in the magnitude of the EMG evoked by innocuous stimuli at the lowest levels of stimulation (Fig. 10D), and the responses to innocuous stimulation occurred with a shorter latency (Fig. 10E). Therefore, the net influence of the RVM on mechanical sensitivity in the chronic CFA group was not facilitatory, but rather inhibitory.

2.5 Discussion

Molecular, pharmacological, and behavioral evidence demonstrate that plasticity in the central nervous system maintains and reinforces chronic pain. The present experiments considered the physiology of individual RVM neurons as another area of potential plasticity in the transition from acute to chronic pain. Single-unit recording from identified RVM ON-, OFF-, and NEUTRAL-cells was combined with behavioral measures of thermal and mechanical sensitivity to test the role of RVM neurons in acute, compared to chronic, immune-mediated inflammation. Firing of RVM neurons in the first hour of inflammation following administration of CFA strongly resembled that seen in other acute inflammatory conditions (Brink et al. 2012; Kincaid et al. 2006; Sanoja et al. 2010; Xu et al. 2007). However, cell activity recorded 3-10 days later was similar to that seen in a different persistent pain state, chronic nerve injury (Carlson et al. 2007). Thus, while acute and chronic pain conditions appear similar at the behavioral level, the underlying mechanisms of descending control are distinct, and differentiate acute from chronic hypersensitivity.

2.5.1 Activity of physiologically identified RVM ON- and OFF-cells in acute vs. chronic immune-mediated inflammation

In the first hour following local administration of CFA, RVM ON- and OFF-cells exhibited clear changes in spontaneous activity: overall firing of ON-cells was increased, while that of OFF-cells was suppressed. This pattern of altered spontaneous firing of ON- and OFF-cells is similar to what has been reported previously during acute neurogenic inflammation (Brink et al. 2012; Kincaid et al. 2006; Sanoja et al. 2010; Xu et al. 2007). These changes were relatively short-lived, with recovery towards baseline by the end of the first hour after CFA injection. The restoration of spontaneous activity of the ON- and OFF-cells may represent a compensatory process, and is consistent with the report of Miki et al. (Miki et al. 2002), who found little alteration in the spontaneous firing of ON- and OFF-cells sampled at various intervals over the first day following CFA injection. Reflex-related changes in the activity of these two classes were not markedly altered from baseline.

Recordings at later time points (3-10 days post-treatment) revealed a different pattern of cell activity. The spontaneous discharges in the CFA-treated and control groups were similar for both cell classes. However, in the CFA group, both ON- and OFF-cells were more sensitive to mechanical stimulation of the treated paw, exhibiting both lowered thresholds and increased response magnitudes. This finding is similar to the observations of Montagne-Clavel (1994), who recorded activity of RVM neurons in awake, behaving animals several weeks after induction of polyarthritis produced by injecting large doses of CFA in the tail. As in the present studies, they reported little change in the spontaneous discharges of the recorded neurons, but increased sensitivity to light touch.

These data show that changes in ON- and OFF-cell firing seen in the first hour following CFA injection are not maintained in later stages of inflammation. Instead, ON- and OFF-cell activity in chronic inflammation closely resembles that seen following nerve injury (Carlson et al. 2007). Spontaneous firing rates return to control levels, but both cell classes become responsive to innocuous tactile stimulation of the affected limb. The similar adaptation of the RVM output in two chronic pain states, one neuropathic

and the other inflammatory, suggests that time-course, rather than mode of injury, is the important factor underlying altered activity of RVM pain-modulating neurons in persistent pain states. The parallel changes with two different forms of insult also argue that the RVM is not simply mirroring ongoing or abnormal peripheral input.

2.5.2 NEUTRAL-cells in acute and chronic inflammation

All RVM neurons that do not exhibit the reflex-related changes in firing that define ON- and OFF-cells are classified as NEUTRAL-cells, a separation that is confirmed by pharmacological differences among cell classes (Harasawa et al. 2000; Heinricher et al. 1992; Heinricher et al. 1994; Heinricher and Neubert 2004; Potrebic et al. 1994). The role of NEUTRAL-cells in the genesis and modulation of acute and chronic pain remains controversial. Miki et al. (Miki et al. 2002) reported that some NEUTRAL-cells developed ON- or OFF-cell properties in the early phases of CFA-induced inflammation. However, these authors did not have baseline data for the recorded neurons, which makes direct comparison with our findings tenuous. In the present studies, NEUTRAL-cell firing was unchanged during the acute phase of CFA-induced inflammation, and we found no evidence of NEUTRAL-cells developing ON- or OFF-like properties. Similar stability of NEUTRAL-cell properties has also been reported in acute neurogenic inflammation (Brink et al. 2012; Kincaid et al. 2006).

2.5.3 Contribution of the RVM to behavioral hypersensitivity in acute vs. chronic immune-mediated inflammation

Descending control from the RVM is generally agreed to be altered in chronic inflammation, but there has been considerably less consensus as to when and whether descending inhibition and/or descending facilitation are recruited (Ren and Dubner 2002; Terayama et al. 2000; Vanegas and Schaible 2004). Hypersensitivity measured behaviorally could reflect increased descending facilitation, decreased or insufficient inhibition, or both. In our paradigm, changes in behavioral sensitivity were monitored in parallel with RVM cell activity, which allowed us to pinpoint the contributions of the pain-facilitating and pain-inhibiting outputs from this region at different time points.

In the first hour following CFA injection, the treated paw showed RVM-dependent thermal and mechanical hypersensitivity. Thermal hyperalgesia was much more pronounced, and the injection *per se* appeared to have contributed to the modest mechanical hyperalgesia. Since CFA injection resulted in a reduction in OFF-cell firing and did not increase the *evoked* responses of ON-cells, the reversal of thermal hyperalgesia by RVM block implies that behavioral hyperalgesia was driven by the increased *spontaneous* firing of the ON-cells. This has been shown previously for acute neurogenic inflammation (Kincaid et al. 2006; Sanoja et al. 2010; Xu et al. 2007).

Three to 10 days after CFA treatment, spontaneous activity was restored to control levels, but ON- and OFF-cells showed novel responsiveness to innocuous mechanical stimuli. In these animals, prominent mechanical hypersensitivity was potentiated, not reversed, by inactivation of the RVM. This finding discounts a critical role for ON-cells in mechanical hyperalgesia after CFA, and is consistent with evidence that descending inhibition from the RVM increases as immune-mediated inflammation develops (Coutinho et al. 1998; Guan et al. 2003; Guan et al. 2002; Randich et al. 2008; Ren and Dubner 1996; Terayama et al. 2000). It further implies that OFF-cell output to some extent holds sensitized dorsal horn transmission in check. However, this compensation is not complete, since the animals nonetheless exhibit behavioral hypersensitivity. Moreover, the mechanical lowered threshold for the OFF-cell pause would disinhibit behavioral responses to innocuous tactile stimuli. Mechanical hypersensitivity in the chronic condition therefore reflects not an overall shift towards ON-cell output, as seen in acute inflammation (Bederson et al. 1990; Brink et al. 2012; Heinricher et al. 2004; Kincaid et al. 2006; Martenson et al. 2009; Ramirez and Vanegas 1989; Sanoja et al. 2010; Xie et al. 2005), but a lowered response threshold or “tipping point” at which descending inhibition is removed. Although descending inhibition is the dominant output, the lowered threshold for ON-cell activation may still contribute to increased sensitivity, as reported for inflammation of visceral and deep tissues (Da Silva et al. 2010a; Da Silva et al. 2010b; Sugiyo et al. 2005; Vera-Portocarrero et al. 2006a).

Thermal hyperalgesia had resolved by three to ten days after CFA in these experiments. This finding is consistent with the observation that the spontaneous activity of RVM ON- and OFF-cells had returned to normal at this point (since, as noted above, thermal hyperalgesia is closely tied to an increase in the spontaneous activity of ON-cells). However, others have reported that heat thresholds are lowered for a week or more after plantar CFA injection, although the effect is reported to be maximal within the first 24 hours (Guan et al. 2002; Okun et al. 2011; Ren et al. 1992; Wei et al. 1999). A number of differences could account for this discrepancy. Our animals were anesthetized, which could suppress activating inputs to ON-cells from higher centers. We also used contact, rather than radiant heat, and a holding temperature (35 °C) that was above skin temperature of both normal and inflamed paws. Paw temperature is not controlled in most studies, and the fact that the inflamed paw is substantially warmer could contribute to the reduced withdrawal latencies reported elsewhere (Carrive et al. 2011; Duggan et al. 1978; Hole and Tjolsen 1993). In addition, the slow linear heat-ramp used here is thought to activate C-fibers selectively, even in inflamed tissue. By contrast, thermal stimuli used in studies in awake animals typically have a logarithmic rise, which would more likely activate A-fibers (McMullan et al. 2004; Yeomans et al. 1996). Since increased sensitivity of dorsal horn neurons in chronic inflammatory hyperalgesia has been tied to A-fiber afferents (Baba et al. 1999; Torsney 2011; Woolf et al. 1994), it is possible that our thermal stimulus failed to activate the inputs relevant to thermal hyperalgesia.

Although RVM inactivation during chronic inflammation did not change thermal withdrawal *thresholds*, the *magnitude* of the heat-evoked EMG response was reduced in both CFA-treated and control animals. This finding is consistent with the suggestion of Jinks and colleagues (Jinks et al. 2004) that the ON-cell reflex-related burst contributes to the magnitude of the heat-evoked withdrawal, which may be more related to perception of suprathreshold stimuli rather than threshold.

2.5.4 Conclusion

The present studies show that changes in the RVM during chronic inflammation are distinct from those observed during acute inflammation (Kincaid et al. 2006), and instead mimic the lowered

mechanical thresholds seen following chronic nerve injury, (Carlson et al. 2007), with lowered response thresholds but no difference in ongoing firing. In acute inflammation, increased ON-cell spontaneous activity and the early engagement of ON-cells drive both thermal and mechanical hyperalgesia, whereas in chronic inflammation the sensitization of ON-cells no longer plays a role in hyperalgesia. Rather, decreased descending inhibition and OFF-cell influence underlie the contribution of the RVM to chronic pain.

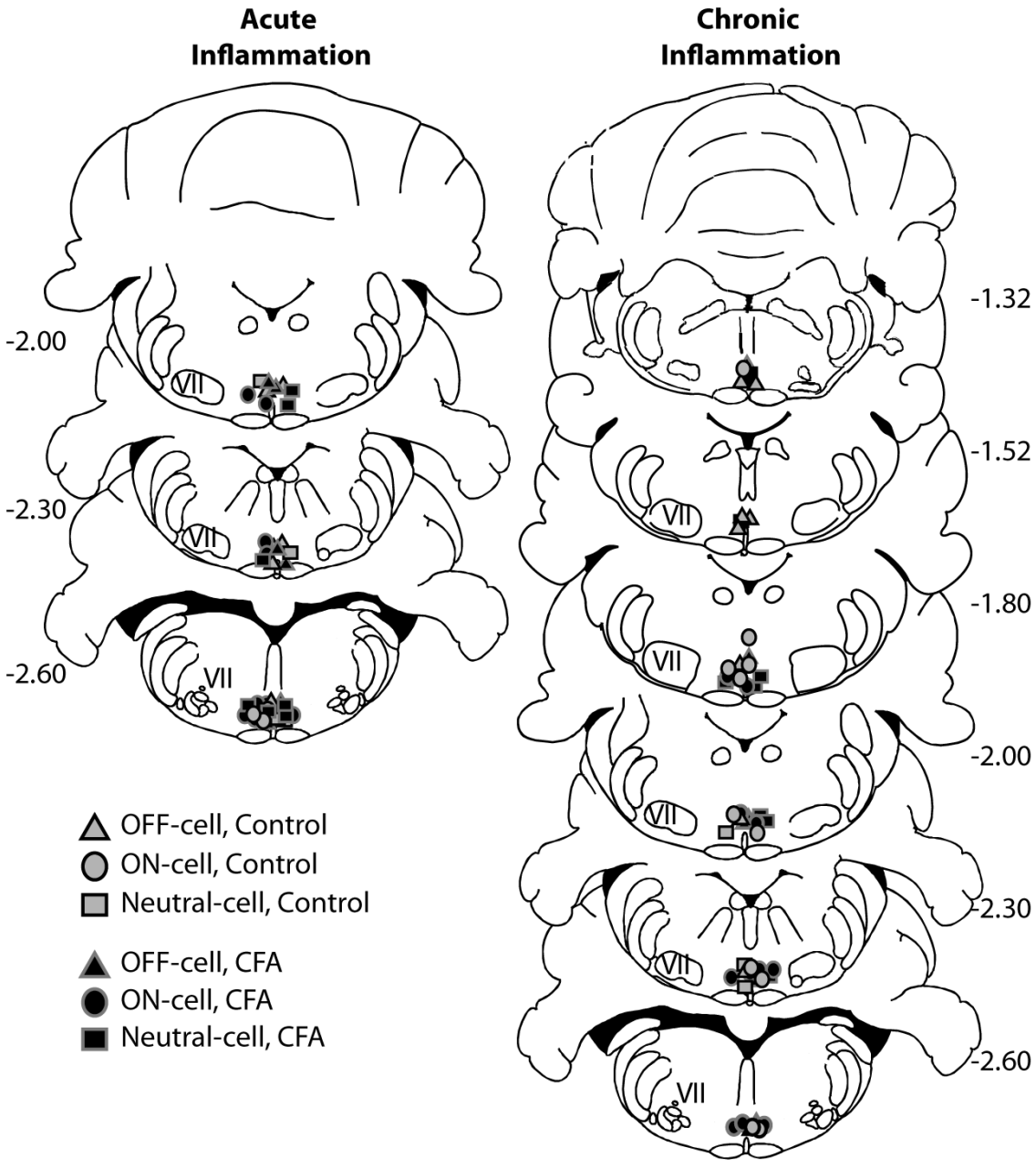
Acute
Inflammation
Chronic
Inflammation
-2.00
-2.30
-2.60
-1.32
-1.52
-1.80
-2.00
-2.30
-2.60
VII
OFF-cell, Control
ON-cell, Control
Neutral-cell, Control
OFF-cell, CFA
ON-cell, CFA
Neutral-cell, CFA

Figure 4: Locations of recordings sites within the RVM.

ON-cells, OFF-cells, and NEUTRAL-cells were distributed between sections at -1.04 mm and -2.60 mm relative to the interaural line, with the majority of the cells recorded between -1.80 mm and -2.60 mm. Adapted from Paxinos and Watson (1997).

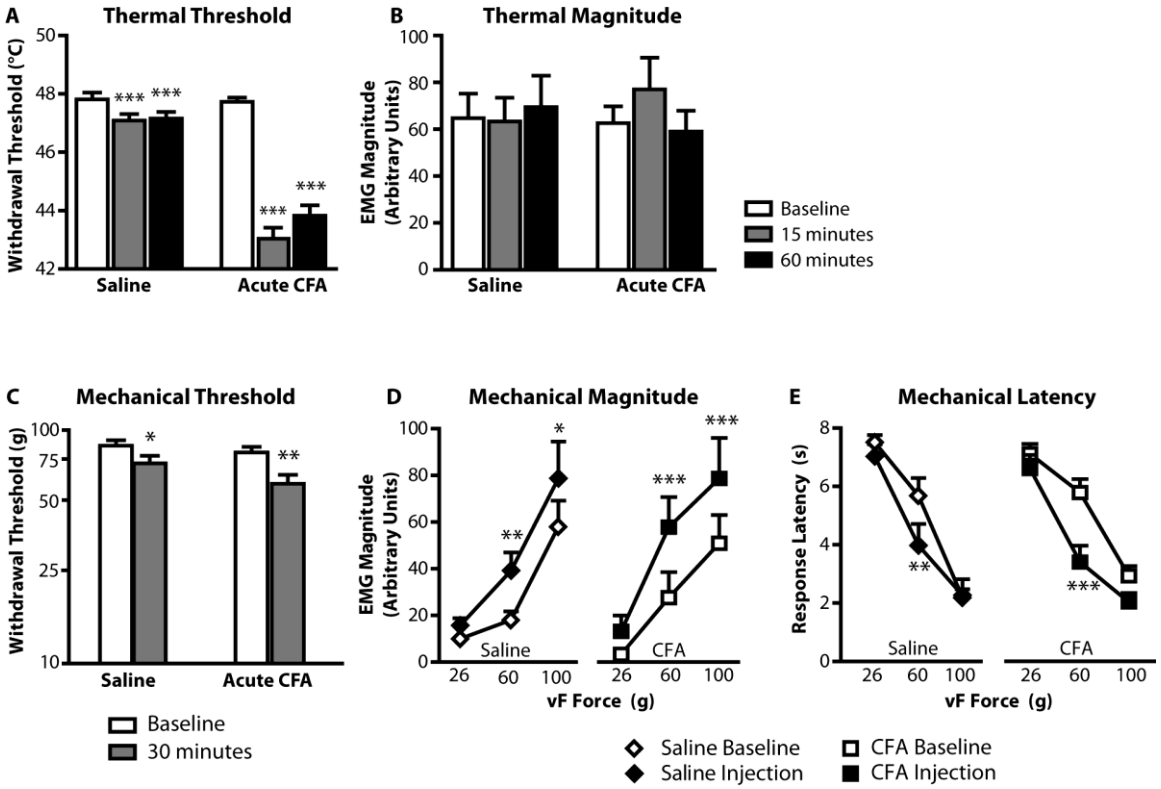
A
Thermal Threshold
Withdrawal Threshold (°C)
50
48
46
44
42
***
***
***
***
Saline
Acute CFA
B
Thermal Magnitude
EMG Magnitude (Arbitrary Units)
100
80
60
40
20
0
Saline
Acute CFA
Baseline
15 minutes
60 minutes
C
Mechanical Threshold
Withdrawal Threshold (g)
100
75
50
25
10
*
**
Saline
Acute CFA
Baseline
30 minutes
D
Mechanical Magnitude
EMG Magnitude (Arbitrary Units)
100
80
60
40
20
0
*
**
***
Saline
CFA
26
60
100
vF Force (g)
E
Mechanical Latency
Response Latency (s)
8
6
4
2
0
**
***
Saline
CFA
26
60
100
vF Force (g)
Saline Baseline
Saline Injection
CFA Baseline
CFA Injection

Figure 5: Thermal and mechanical hyperalgesia from acute hindpaw injection.

A) Threshold for heat evoked withdrawal was substantially reduced in CFA-treated animals ($F_{2,46}$ =102.0, $p < 0.0001$, n = 24). Reduced threshold in saline-treated animals was small but statistically significant ($F_{2,32} = 12.0$, $p < 0.0001$, n = 17). The two groups had comparable thresholds in baseline (unpaired t-test, $p = 0.85$).

B) Withdrawal magnitude given as arbitrary units (AU) from thermal stimuli were not affected by injection of CFA or saline (saline: $F_{2,32} = 0.96$, $p = 0.39$; CFA: $F_{2,46} = 1.55$, $p = 0.22$). Baseline response magnitudes were not different (unpaired t-test, $p = 0.68$).

C) Mechanical withdrawal thresholds were also reduced, although only two animals, both in the CFA-treated group, responded to fibers normally considered innocuous (Wilcoxon signed ranks test, $p = 0.003$ and $p = 0.048$ for CFA and saline injections, respectively)

D,E) Withdrawal magnitude was increased (two-way ANOVA, $F_{1,44} = 17.3$, $p < 0.0001$ for saline; $F_{1,66} = 33.3$, $p < 0.0001$ for CFA-injected) and response latency reduced (two-way ANOVA, $F_{1,44} = 13.0$, $p < 0.001$ for saline; $F_{1,66} = 21.0$, $p < 0.0001$ for CFA-injected). Acute CFA with RVM lidocaine*$p <$ 0.05, **$p < 0.01$, ***$p < 0.001$ compared to pre-injection baseline at the same force.

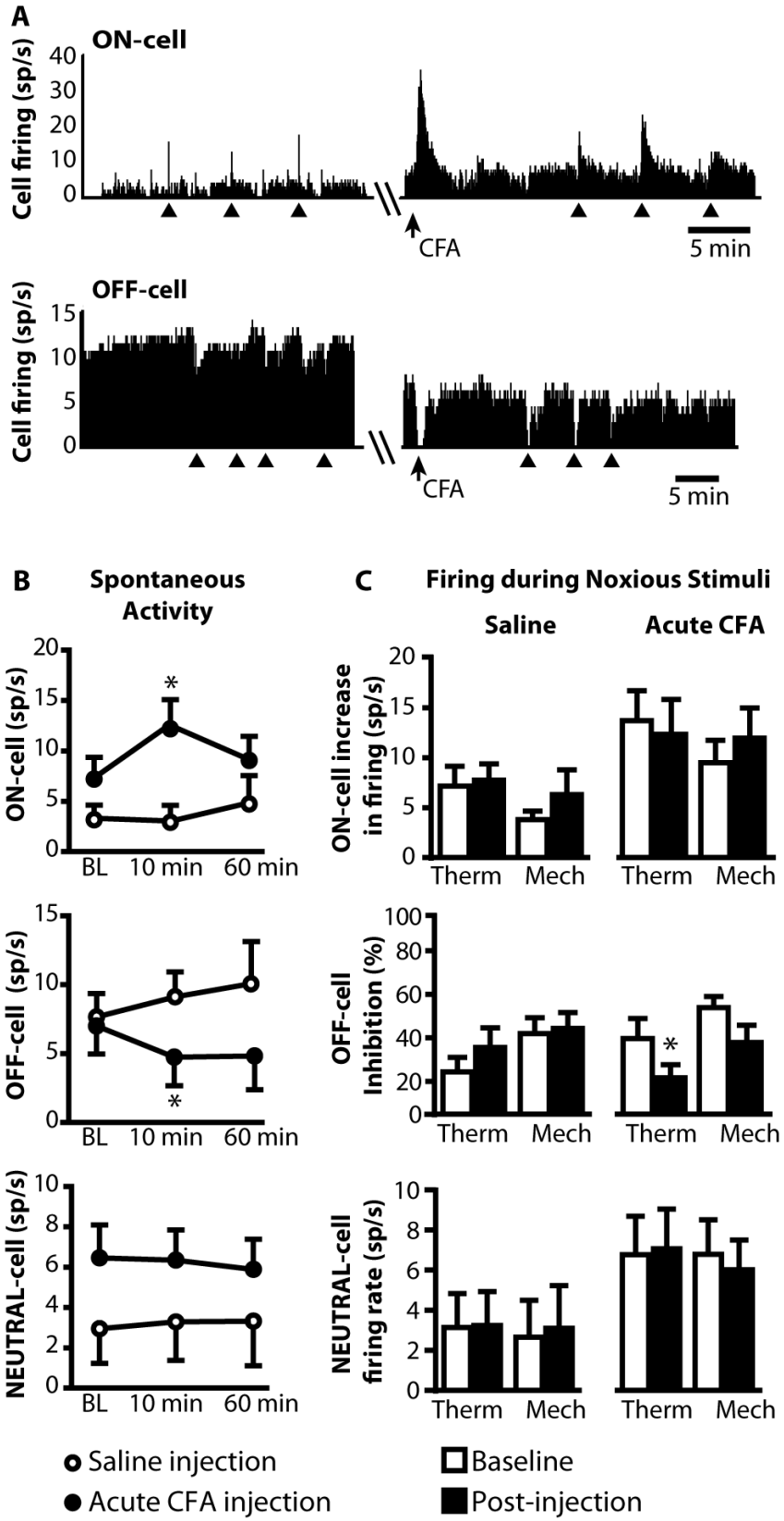
A
ON-cell
Cell firing (sp/s)
40
30
20
10
0
CFA
5 min
OFF-cell
Cell firing (sp/s)
15
10
5
0
CFA
5 min
B
Spontaneous Activity
ON-cell (sp/s)
20
15
10
5
0
BL
10 min
60 min
OFF-cell (sp/s)
15
10
5
0
BL
10 min
60 min
NEUTRAL-cell (sp/s)
10
8
6
4
2
0
BL
10 min
60 min
C
Firing during Noxious Stimuli
Saline
Acute CFA
ON-cell increase in firing (sp/s)
20
15
10
5
0
Therm
Mech
Therm
Mech
OFF-cell Inhibition (%)
100
80
60
40
20
0
Therm
Mech
Therm
Mech
NEUTRAL-cell firing rate (sp/s)
10
8
6
4
2
0
Therm
Mech
Therm
Mech
Saline injection
Acute CFA injection
Baseline
Post-injection

Figure 6: Spontaneous and withdrawal-related activity of ON-, OFF-, and NEUTRAL cells during acute inflammation.

A) Ratemeters showing spontaneous and thermal withdrawal-related activity from a typical ON-cell and OFF-cell before and after CFA injection.

B) CFA but not saline injection increased spontaneous activity of ON-cells (Wilcoxon's signed ranks test, CFA: $p = 0.019$, n = 11; Saline: $p = 0.96$, n = 6) and decreased that of OFF-cells (CFA: $p = 0.016$, n = 7; Saline: $p = 0.37$, n = 5). NEUTRAL cell spontaneous activity was unaffected by either treatment (CFA: $p = 0.37$, n = 10; Saline: $p = 0.99$, n = 6). BL: baseline

C) Firing associated with noxious stimulation trials was generally unaffected by CFA. However, the reflex-related OFF-cell inhibition from thermal stimulation was significantly enhanced after CFA injection.

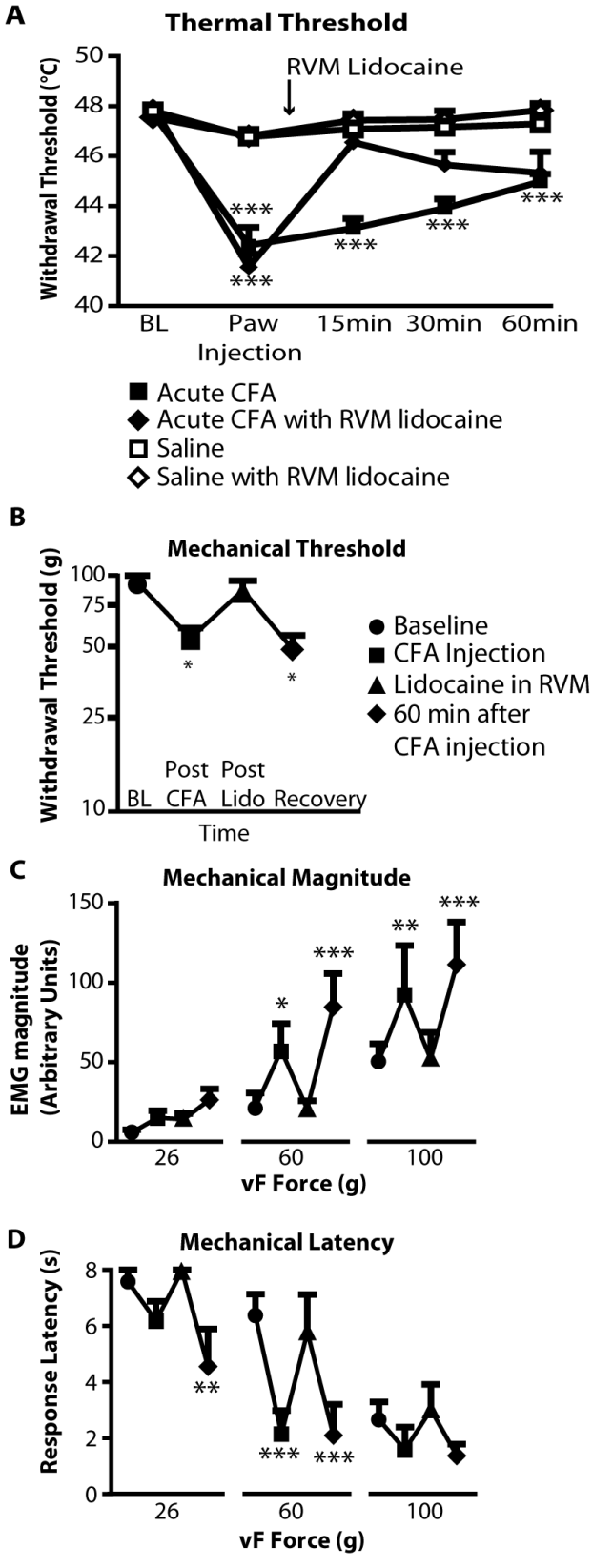
A
Thermal Threshold
Withdrawal Threshold (°C)
50
48
46
44
42
40
RVM Lidocaine
***
***
***
***
***
BL
Paw Injection
15min
30min
60min
Acute CFA
Acute CFA with RVM lidocaine
Saline
Saline with RVM lidocaine
B
Mechanical Threshold
Withdrawal Threshold (g)
100
75
50
25
10
*
*
Post CFA
Post Lido
BL
Recovery
Time
Baseline
CFA Injection
Lidocaine in RVM
60 min after CFA injection
C
Mechanical Magnitude
EMG magnitude (Arbitrary Units)
150
100
50
0
*
***
**
***
26
60
100
vF Force (g)
D
Mechanical Latency
Response Latency (s)
8
6
4
2
0
**
***
***
26
60
100
vF Force (g)

Figure 7: RVM blockade attenuates both thermal and mechanical hyperalgesia in acute inflammation.

A) CFA injection produced immediate thermal hyperalgesia that partially recovered over the subsequent hour. This effect was reversed by RVM lidocaine. X-axis gives time since hindpaw injection. Two-way repeated-measures ANOVA, with significant effects of both time ($F_{4, 204} = 21.2$, $p < 0.0001$) and treatment on threshold ($F_{3,51} = 38.35$, $p < 0.0001$). *** $p < 0.001$ post-hoc Bonferroni comparison against hindpaw saline/RVM lidocaine group.

B-D) RVM lidocaine reversibly eliminated the decrease in withdrawal threshold (B), increase in withdrawal magnitude (C), and reduction in withdrawal latency (D) produced by CFA. Hypersensitivity returned approx. 40 min after lidocaine administration (60 min after CFA).
For mechanical threshold, Friedman's test was followed by Dunn's post hoc test ($p<0.001$, n = 6). ANOVA was used to analyze magnitude ($F_{3,45} = 19.1$, $p < 0.0001$) and latency ($_{F3,45} = 14.9$, $p < 0.0001$). *$p < 0.05$, **$p < 0.01$, ***$p < 0.001$ compared to pre-CFA baseline.

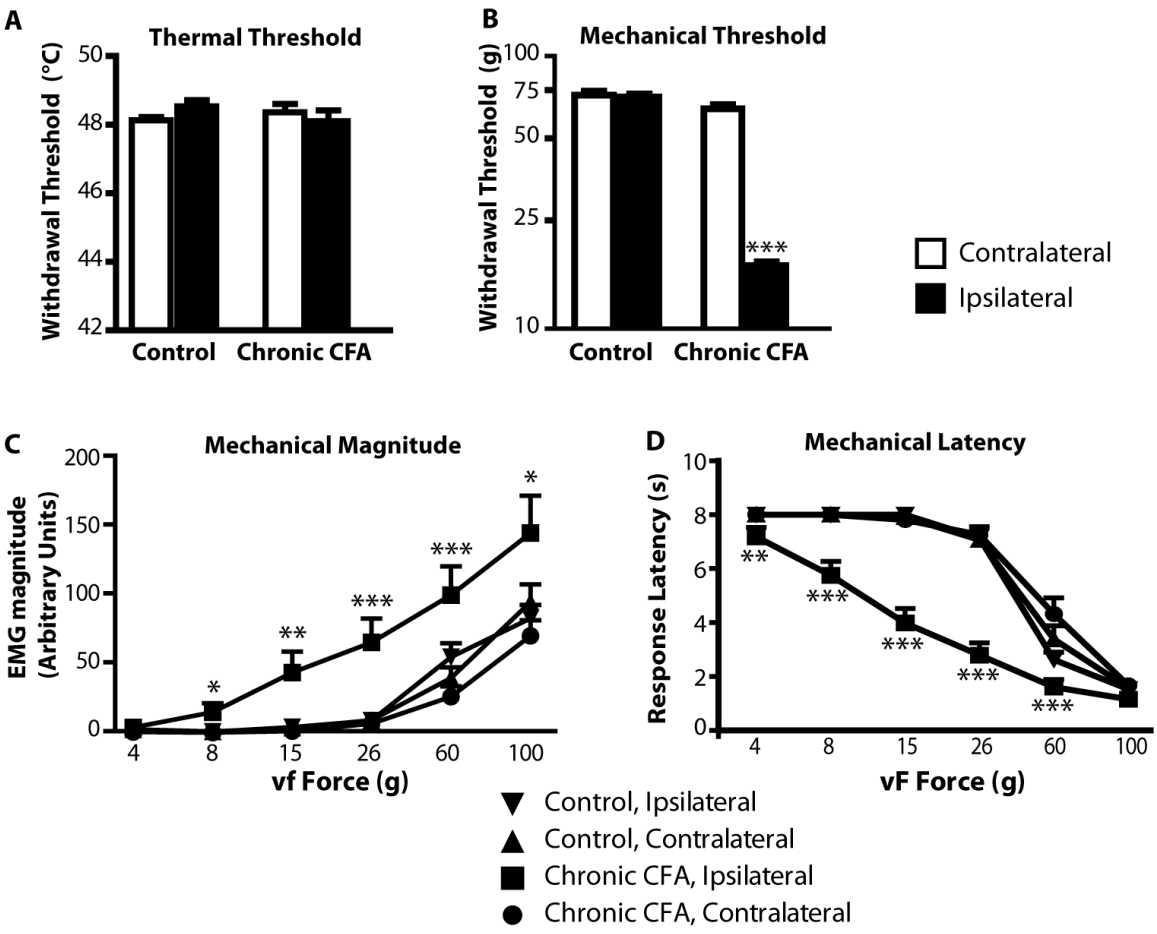
A
Thermal Threshold
Withdrawal Threshold (°C)
50
48
46
44
42
Control
Chronic CFA
B
Mechanical Threshold
Withdrawal Threshold (g)
100
75
50
25
10
***
Control
Chronic CFA
Contralateral
Ipsilateral
C
Mechanical Magnitude
EMG magnitude (Arbitrary Units)
200
150
100
50
0
*
**
***
***
*
4
8
15
26
60
100
vf Force (g)
D
Mechanical Latency
Response Latency (s)
10
8
6
4
2
0
**
***
***
***
***
4
8
15
26
60
100
vF Force (g)
Control, Ipsilateral
Control, Contralateral
Chronic CFA, Ipsilateral
Chronic CFA, Contralateral

Figure 8: Mechanical but not thermal hyperalgesia in chronic inflammation.

A) In lightly anesthetized animals at 3-10 days after initial CFA injection, thermal hyperalgesia was not detectable ($F_{3,86} = 0.84$, $p = 0.47$).

B-D) Mechanical hyperalgesia was fully developed, with lowered threshold (B), a left and upward shift in the stimulus-response magnitude relationship (C), and a reduction in response latency evident throughout the stimulus range tested (D). When an overall ANOVA was significant, a Tukey's post-hoc test was used to compare groups at each fiber force. $*p < 0.05$, $**p < 0.01$, $***p < 0.001$ compared to contralateral paw, which was not different from ipsilateral or contralateral controls at any force.

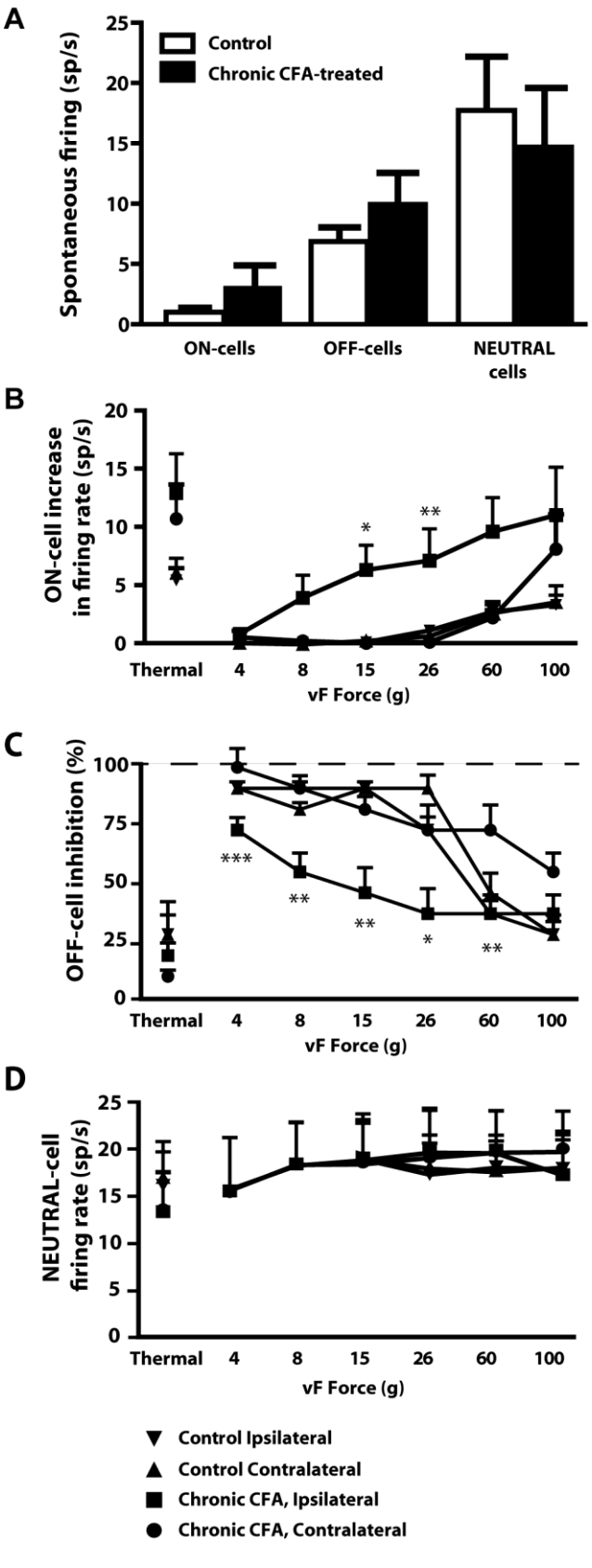
A
Spontaneous firing (sp/s)
Control
Chronic CFA-treated
ON-cells
OFF-cells
NEUTRAL cells
B
ON-cell increase in firing rate (sp/s)
Thermal
vF Force (g)
C
OFF-cell inhibition (%)
D
NEUTRAL-cell firing rate (sp/s)
Control Ipsilateral
Control Contralateral
Chronic CFA, Ipsilateral
Chronic CFA, Contralateral

Figure 9: Spontaneous and withdrawal-related activity of ON-, OFF-, and NEUTRAL-cells during acute inflammation.

A) Spontaneous firing rates were not significantly different in CFA-treated and control animals. (Wilcoxon's test: ON-cells, $p = 0.16$; OFF-cells, $p = 0.35$, NEUTRAL-cells, $p = 0.54$, n = 8-12 group).

B-D) Evoked responses of ON-cells (B), OFF-cells (C) and NEUTRAL-cells (D). Activity during thermal and mechanical trials is plotted on the same graph for each class. Both ON- and OFF-cells recorded in CFA-treated animals showed significant shifts in the mechanical force vs. response relationship for stimulation of the treated paw compared to the contralateral side or in controls. There was no effect of group or side on responses during heat trials. NEUTRAL-cells did not respond to thermal or mechanical stimulation. When an overall ANOVA was significant, a Tukey's post-hoc test was used to compare groups at each fiber force. $*p < 0.05$, $**p < 0.01$, $***p < 0.001$ compared to contralateral paw, which were not different from ipsilateral or contralateral controls at any force.

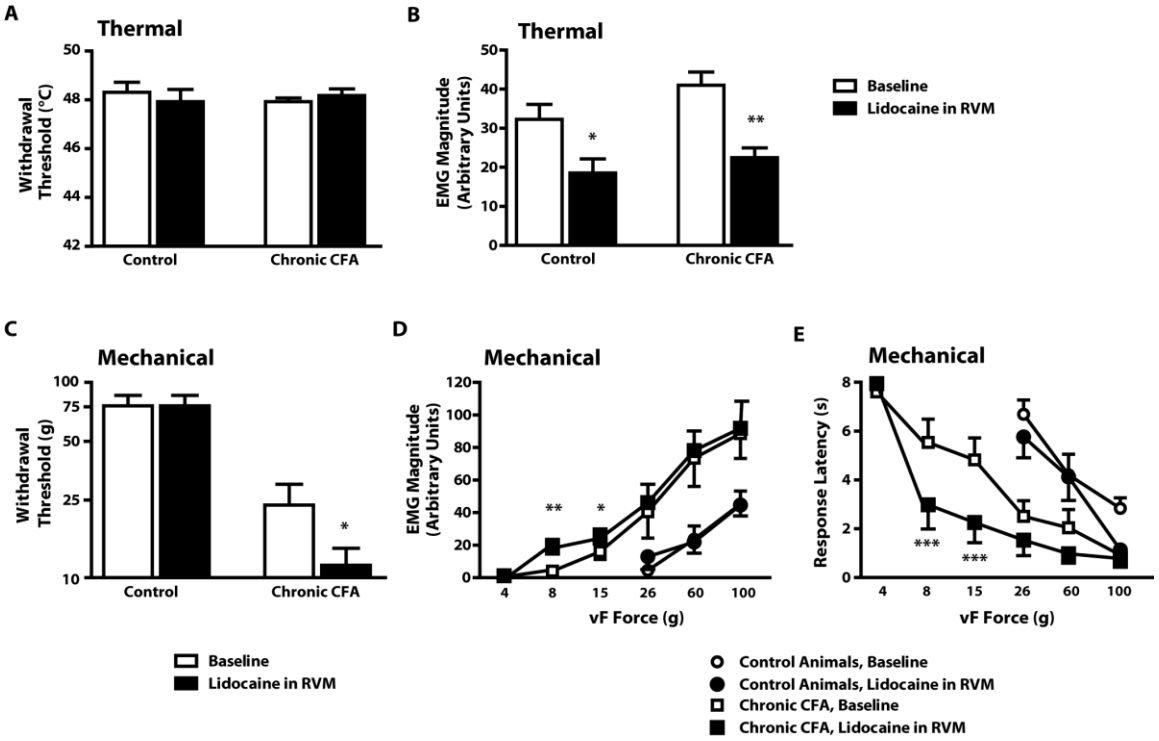
A
Thermal
Withdrawal Threshold (°C)
50
48
46
44
42
Control
Chronic CFA
B
Thermal
EMG Magnitude (Arbitrary Units)
50
40
30
20
10
0
*
**
Control
Chronic CFA
Baseline
Lidocaine in RVM
C
Mechanical
Withdrawal Threshold (g)
100
75
50
25
10
*
Control
Chronic CFA
Baseline
Lidocaine in RVM
D
Mechanical
EMG Magnitude (Arbitrary Units)
120
100
80
60
40
20
0
**
*
4
8
15
26
60
100
vF Force (g)
E
Mechanical
Response Latency (s)
8
6
4
2
0
***
***
4
8
15
26
60
100
vF Force (g)
Control Animals, Baseline
Control Animals, Lidocaine in RVM
Chronic CFA, Baseline
Chronic CFA, Lidocaine in RVM

Figure 10: Effects of RVM lidocaine on behavioral responses to heat (A, B) and von Frey stimulation (C, D, E) in animals subjected to chronic inflammation.

A) Thermal withdrawal thresholds were not significantly altered by lidocaine in the RVM in control (n = 5) or CFA-treated (n = 7) animals.

B) RVM blockade significantly reduced the magnitude of the heat-evoked reflex in both groups (paired *t*-test, $p = 0.024$ for control animals, $p = 0.005$ for CFA-injected animals).

C) RVM block potentiated mechanical hypersensitivity in CFA-treated animals (Wilcoxon's test, $p = 0.03$, n = 7), with no effect in controls ($p = 0.99$, n = 5).

D) RVM block resulted in a small but statistically significant increase in the magnitude of withdrawals evoked by innocuous stimulation of the treated paw, with no effect on the response to noxious stimuli.

E) RVM block resulted in a significant decrease in the latency of the response evoked by innocuous stimulation of the treated paw, with no effect on the response to noxious stimuli. For D and E, $*p < 0.05$, $**p < 0.01$, $***p < 0.001$, compared to post RVM lidocaine injection, paired t-tests at innocuous forces.

CHAPTER 3

Manuscript #2

A novel, non-invasive method for respiratory monitoring for use in stereotactic procedures

Daniel R. Cleary[a], Ryan S. Phillips[a], Michael Wallisch[b], Mary M. Heinricher[a,c]

[a]Department of Neurological Surgery, Oregon Health & Science University, Portland, OR, USA

[b]Department of Physiology and Pharmacology, Oregon Health & Science University, Portland, OR, USA

[c]Department of Behavioral Neuroscience, Oregon Health & Science University, Portland, OR, USA

3.1 Abstract

Accurate monitoring of respiration is often needed for neurophysiological studies, as either a dependent experimental variable or an indicator of physiological state. Current options for respiratory monitoring of animals held in a stereotaxic frame include EMG recordings, pneumotachograph measurements, inductance-plethysmography, whole-body plethysmography (WBP), and visual monitoring. While powerful, many of these methods prevent access to the animal's body, interfere with experimental manipulations, or require deep anesthesia and additional surgery.

For experiments where these issues may be problematic, we developed a non-invasive method of recording respiratory parameters specifically for use with animals held in a stereotaxic frame. This system, ventilation pressure transduction (VPT), measures variations in pressure at the animal's nostril from inward and outward airflow during breathing. These pressure changes are detected by a sensitive pressure transducer, then filtered and amplified. The output is an analog signal representing each breath.

VPT was validated against WBP using 10% carbon dioxide and systemic morphine (4 mg/kg) challenges in lightly anesthetized animals. VPT accurately represented breathing rate and tidal volume changes under both baseline and challenge conditions. This novel technique can therefore be used to measure respiratory rate and relative tidal volume when stereotaxic procedures are needed for neuronal manipulations and recording.

3.2 Introduction

Many *in vivo* experiments in neuroscience employ stereotaxy, which allows manipulations or neuronal recordings in specifically targeted areas in the central nervous system (Depuy et al. 2011; Subramanian and Holstege 2011; Zhang et al. 2009). Monitoring breathing of the anesthetized animal is critical for such studies, as animal health and anesthetic depth can drastically affect experiments. Non-invasive methods of respiratory monitoring are often preferred or even required, such as with non-terminal experiments.

The most commonly used methods for respiratory monitoring during stereotaxic procedures include EMG (electromyography) from respiratory muscles (Gray et al. 2001; Montandon et al. 2011a), intubation or tracheotomy with pneumotachograph (Spoelstra et al. 2007; Weksler et al. 1994; Yasaki and Dyck 1991), and capnography (Colman and Krauss 1999). EMG electrodes can monitor the diaphragm, the intercostals, the genioglossus, or abdominal muscles, and depending on the muscle group, the resulting signal is associated with either inhalation or exhalation (Subramanian and Holstege 2011). Although EMG is easily recorded in animals held in a stereotaxic frame, this method is subject to electrical artifacts and challenges of interpretation (O'Neil and Raub 1984). Pneumotachograph accurately measures air flow, but to be compatible with stereotaxy it requires additional invasive procedures (tracheotomy or endotracheal intubation) and deep anesthesia. Capnography (monitoring carbon dioxide output) is a powerful method but is subject to environmental and metabolic interference (Bhavani-Shankar et al. 1992).

Less invasive methods of respiratory monitoring are available, although these methods also have limitations. One widely used non-invasive approach is respiratory plethysmography, which measures changes in volume of the chest and/or abdomen during breathing. Whole-body plethysmography (WBP) involves placing the animal in a closed chamber and measuring volume of air displaced during breathing (Dubois et al. 1956a; Dubois et al. 1956b; Enhorning et al. 1998; Glaab et al. 2007; O'Neil and Raub 1984; Palecek 1969). WBP allows absolute measurements of volume of air displaced, but the system is

cumbersome when combined with stereotaxy, and prevents access to the animal's body during the experiment. A newer, non-invasive method is accelerometry-based inductive plethysmography (ACC, Devonshire et al. 2009) Instead of measuring volume expansion, ACC uses a microchip to measure acceleration during movement of the chest or abdomen, and therefore has promise for noninvasively monitoring the breathing of animals in a stereotaxic frame. This method is similar to inductance plethysmography, which measures changes in the position of the chest and abdomen with breathing (Carry et al. 1997; Stromberg et al. 1993). However, acceleration as a surrogate for positional changes of the chest has not so far been validated by comparison to a standard method such as WBP.

Here we present a novel non-invasive method for measuring respiratory parameters during stereotaxic procedures. The method, ventilation pressure transduction (VPT), uses a sensor to pick up changes in air pressure at the nares during breathing. We compared VPT to whole-body plethysmography (WBP), as well as to accelerometry-based inductive plethysmography (ACC). We find that VPT provides an accurate, reliable, and easy-to-use solution for non-invasive measurement of breathing compatible with stereotaxy.

3.3 Material and Methods

3.3.1 Animals

All experimental procedures were approved by the Institutional Animal Care and Use Committee at Oregon Health & Science University. Research methods followed the guidelines of the Committee for Research and Ethical Issues of the International Association for the Study of Pain (Zimmermann 1983). Experiments were conducted on 6 male Sprague-Dawley rats (Charles River, Wilmington, MA, USA) weighing between 250 and 350 g.

3.3.2 Preparation and Surgery

Animals were initially anesthetized with inhaled 4% isoflurane in humidified oxygen (1.25 l/min) for 4-5 min (Martenson et al. 2005). An incision was made and a catheter (PE50) placed in the jugular vein for

subsequent drug administration (morphine). The incision was covered with 5% lidocaine ointment and closed using wound clips. Animals were placed in a stereotaxic frame with a loose-fitting nasal mask for continuous flow isoflurane anesthesia, and the isoflurane concentration stepped down gradually to 1.25-1.5%. Waste gases were exhausted through a low pressure scavenger system.

3.3.3 Lightly Anesthetized Model

The lightly anesthetized model is an anesthetic preparation that permits stable *in vivo* stereotaxic electrophysiology experiments while maintaining important neuronal circuits, behavioral reflexes, and other characteristics of awake animals (Heinricher and Kaplan 1991; Lanier et al. 1994; Morel et al. 1987; Reed et al. 2008).). The experimental protocol was not started until anesthetic flow, heart rate, and breathing frequency were stable for least 25 minutes. For the duration of the experimental protocol, the anesthetic concentration and gas flow were maintained at a constant level, consistent with previous work in lightly anesthetized animals (Heinricher et al. 2010a; Heinricher et al. 2010b).

3.3.4 Respiratory Monitoring

The three methods of respiratory monitoring, VPT, WBP and ACC, were used simultaneously in all experiments (Figure 11). The simultaneous use of these three non-invasive methods permitted within-subject comparisons of the characteristics of each approach.

3.3.4.1 Ventilation Pressure Transduction (VPT)

VPT is based on the idea that subtle changes in pressure fields from inhalation and exhalation can be detected externally as the animal breathes. The incisors and head were locked in place in the stereotactic frame, and a small piece of polyethylene tubing (2 mm outer diameter, 1 cm length) was connected to one port on the pressure transducer (BLVR-L01D, BLVR Series Low Pressure Sensors, All Sensors, Morgan Hill, CA). This sensor and tubing were placed in the frame such that the open end of the tubing was 1-5 mm from the nostrils, inside the nasal mask used for isoflurane delivery (Figure 11, nasal mask not

shown in the figure for clarity). The sensor body was then set in place on the stereotaxic frame such that the tubing remained in a fixed position relative to the nostrils for the entire experiment.

The conceptual design of the VPT system is represented in Figure 12. Changes in pressure were measured through physical displacement of an impermeable membrane inside the sensor body. The two-port sensor was positioned such that the port attached to the tubing was in close approximation to the animal's nostril and the other port was open to the air. The electrical output of the sensor is relative to the pressure difference across the two ports, so leaving the second port open to air ensured that environmental changes would affect both ports equally and not disturb the recording. The sensor output was fed into a custom processing system, although any commercially available signal amplification and filtering unit would suffice. Our system used hardware-based band-pass filtering (0.01 to 10 Hz) to remove low- and high-frequency noise, and a 2-stage amplifier to boost the signal 10,000 to 20,000-fold. The final output signal was digitized, stored, and displayed using Spike2 software (CED, Cambridge, England). All data were digitized at a minimum of 1 kHz and saved for off-line analysis.

3.3.4.2 Accelerometry-based induced plethysmography (ACC)

ACC constitutes a variant of inductance plethysmography, but instead of a chest or abdominal band to measure displacement, a small electronic accelerometer was used to quantify movement. This method provides only an indirect measure of chest movement, since the signal is not based on actual displacement but instead on acceleration, the second derivative of positional changes.

The ACC system was assembled similar to published circuit diagrams (Devonshire et al., 2009). In short, a commercially-available accelerometer chip (ADXL330K-CPZ, Analog Devices, Norwood, MA, USA) was hooked to ground and 3.5 V power source, and the output from the chip fed into an amplifier and filtering box (Grass General Purpose Amplifier, Grass Technologies, West Warwick, RI, USA). The chip was attached along the lateral chest wall caudal to the scapula (Figure 11) using quick-set dental impression material (Patterson Reflection, Patterson Dental, Saint Paul, MN). This material is non-toxic and adheres well to skin and hair, but is elastic enough to be easily peeled away at the end of the experiment to

retrieve the accelerometer chip. The signal from the chip was high-pass filtered at 0.01 Hz to remove the DC offset, low-pass filtered at 15 Hz, notch filtered at 60 Hz, and amplified 1000-fold. The output signal was digitized and recorded as above.

3.3.4.3 Head-Out Whole-Body Plethysmography (WBP)

WBP measures changes in volume of an organ or body by quantifying pressure changes in a closed chamber (Bar-Yishay 2009; Cumming 1961; Dubois et al. 1956a; Jacky 1978). In head-out whole-body plethysmography, an animal's head is left free while the body is sealed inside the chamber, which is equipped with an external port for measuring pressure changes (Figure 11). Using Boyle's law, measurements of pressure changes in the container can be converted to volumes of air displaced. The volume of air in one breath (tidal volume) is an integration of these measurements over time.

Here, WBP data were gathered using a single head-out chamber plethysmography system (Buxco Electronics, Sharon, CT, USA), as described previously (Nettleton et al. 2008; Wallisch et al. 2011). A flexible membrane was placed around the animal's neck, tight enough to prevent airflow around the membrane when in the sealed chamber but not tight enough to occlude circulation or the airway. The line for the jugular catheter was passed out along the edges of the membrane. The animal was mounted in the stereotaxic apparatus and the rear portion of the chamber sealed around the animal's body. Pressure changes in the body chamber were filtered and amplified by Buxco's proprietary equipment and then digitized as above.

3.3.5 Experimental Design

The purpose of the experiment was to validate measurements of VPT against WBP as a well-established non-invasive method for respiratory monitoring (Bar-Yishay 2009; Coggins et al. 1981; Enhorning et al. 1998), and to determine the relative merits of VPT and ACC. The comparisons were made under basal conditions and during increased and decreased respiratory drive.

Baseline activity was first recorded for 10-15 min. Then, to increase respiratory drive, the pure oxygen in the gas anesthetic mix was switched to a 10% carbon dioxide and 90% oxygen mix for 3-5 minutes. Flow rate and anesthetic concentration were held constant during this process. The gas mixture was then switched back to pure oxygen, and the animal was given 10 minutes to recover. In the next part of the experiment, an intravenous injection of 4 mg/kg morphine was used to produce a decrease in respiration and periods of apnea. Figure 13A shows examples of the gross changes for the different treatments using the three recording methods.

3.3.6 Breathing Frequency

Breathing frequency for all three methods was measured using threshold detection on the periodic signals. The specific detection points were often slightly off-set due to differences in the detection points between methods, so for each successive breath detected, instead of using absolute time at the breath, the inter-breath interval was calculated and this value was converted to an instantaneous readout of breaths per second.

3.3.7 Tidal Volume

For measurements of tidal volume, the area under the curve for the WBP signal was integrated for each individual breath, and then normalized to the mean magnitude in the baseline period of the experiment. The normalized measurements thus represent the relative tidal volume, as compared to the baseline period. Although WBP can measure absolute tidal volume, normalized rather than absolute measurements were used here with WBP because future measures of tidal volume using only VPT or ACC alone could not be calibrated absolutely. This is because the baseline amplitudes of the VPT and ACC signals depend largely on placement of the devices.

A number of different analyses of the VPT and ACC signals were carried out to identify the metric that best matched the WBP measurements of tidal volume. Absolute peak value, area under the curve, double integral, and peak-to-peak amplitude were all considered. A correlation analysis using all breaths during baseline in each individual experiment showed that peak-to-peak amplitude of VPT and ACC (difference

between the highest point and lowest point for each individual breath) correlated best with measurements of WBP tidal volume (WBP tidal volume vs. ACC peak-to-peak: $R^2 = 0.65$; WBP tidal volume vs. VPT peak-to-peak: $R^2 = 0.67$). We therefore chose peak-to-peak measurement of VPT and ACC outputs for comparison to WBP in all analyses of tidal volume.

3.3.8 Statistical Analysis

The Bland-Altman method was used for assessing the level of agreement between methods (Bland and Altman 1986). Mean difference (bias), the limits of agreement, and the standard error for the limits of agreement are reported for comparisons of WBP with VPT and with ACC. This analysis was conducted on data from 120 measurements of individual breaths from each of the three methods during a quiescent period of steady breathing in baseline (approximately 2-3 minutes of activity), with the required correction for repeated measures, giving n = 6 (Bland and Altman 2007; 1999). With the correction for repeated measures, the traditional Bland-Altman plot does not accurately convey the limits of agreement, and a graphical plot is therefore not shown here.

Between-method comparisons of measured rate and tidal volume during increased and decreased respiration were made using a two-way ANOVA, with both time and method of measurement as within-subject factors. Averages of 30-s samples taken in baseline, during CO_2, and after morphine administration were compared. A Bonferroni post-hoc test was used to test for specific differences. Results are expressed as mean ± SEM.

3.4 Results

3.4.1 Measurements of Respiration

All three methods (WBP, VPT, and ACC) provided reliable baseline respiratory signals (Figure 13A). Signals were steady, regular, and consistent, and events such as sighs were clearly visible across all three methods (Figure 13B). Occasionally, an adjustment in the ACC placement would have to be made before

the start of the experiment, but once the protocol was started, no further adjustments were made to any of the devices.

3.4.2 Breathing Frequency

A Bland-Altman analysis of the three different methods for measuring breathing frequency showed strong agreement between WBP and each of the other two methods. The mean difference in measurements of individual breaths between WBP and VPT was 0.0025 Hz, and the 95% limits of agreement ranged between -0.084 Hz and 0.089 Hz, with a standard error for the confidence interval of 0.016 Hz. Since the confidence interval crosses zero, measurements of breathing frequency for VPT showed no bias relative to WBP.

For ACC, measurements of breathing frequency also agreed with WBP. The mean difference in measurements of individual breaths between WBP and ACC was 0.00002 Hz, and the limits of agreement were from -0.086 Hz to 0.086 Hz, with a standard error for the confidence interval of 0.04 Hz. Measurements of breathing frequency made using ACC therefore have no significant bias relative to WBP.

3.4.3 Relative Tidal Volume

Low systematic bias of VPT or ACC relative to WBP was also found for relative tidal volume. The mean difference between VPT and WBP was 1.4% for measurements of relative tidal volume. The 95% limits of agreement ranged between -18.7 and 21.5%, with a standard error of 6.9%. Similarly, ACC was not significantly biased relative to WBP, with a mean difference of measurement of -3.9%. The 95% limits of agreement were from -30.1 to 23.1%. The standard error for these limits was 7.6%.

3.4.4 Detection and Quantification of Changes in Respiration

A carbon dioxide challenge drove an increase in respiration, while systemically administered morphine severely depressed respiration. Both changes were grossly evident in output from all three systems (Figure 13A).

Carbon dioxide produced significant increases in both breathing frequency and tidal volume, as measured using WBP, VPT, and ACC (Figure 14). For breathing frequency, we saw a significant effect of treatment ($F_{2,15} = 8.40$, $p = 0.011$), but no difference among measurement methods ($F_{2,15} = 0.00$, $p = 0.99$). Relative tidal volume showed a similar pattern, with a significant effect of treatment ($F_{2,15} = 44.72$, $p < 0.001$), and no effect of method ($F_{2,15} = 1.04$, $p = 0.38$).

Respiratory depression was next induced by administration of morphine (4 mg/kg, i.v.). Morphine produced a significant decrease in breathing frequency ($F_{2,15} = 14.11$, $p < 0.01$) , with no difference among measurement methods ($F_{2,15} = 0.01$, $p = 0.99$). Although relative tidal volume was significantly reduced by morphine treatment ($F_{2,15} = 47.72$, $p < 0.001$), the three methods were not equivalent ($F_{2,15} = 3.99$, $p < 0.05$). Post-hoc tests showed that VPT accurately tracked WBP measurement of tidal volume after morphine, whereas ACC significantly overestimated the decrease in tidal volume relative to WBP (Figure 14). This difference in measurement occurred because some lower-amplitude breaths after morphine were indistinguishable from noise when using ACC (Figure 15).

3.5 Discussion

We present a novel method for measuring respiratory parameters compatible with stereotaxy. This method, VPT, provides an accurate and reliable measure of breathing frequency and relative changes in tidal volume. The low profile and unobtrusive design allow surgical and behavioral perturbations of the body without concern over disturbing the respiratory signal. VPT is therefore a useful tool for measuring respiration, either as an experimental dependent variable or as an indicator of anesthetic stability (Steffey et al. 2003).

3.5.1 Sensitivity of VPT

With VPT, the relative amplitude of the respiratory signal depends on the detection of small pressure changes, and filtering and amplification are required to extract a workable signal from the noise. The sensors used in this experiment have a working pressure range of ±1 inH2O (~250 Pas or ~2.5 mBar), and the sensor's normal electrical output for this pressure range is from 4.5 to 11.5 mV. The output is graded

relative to pressure, and the sensor manufacturer claims excellent linearity in the pressure-to-signal ratio (0.3% linearity). In the present experiments, the raw electrical output with the animal's breathing was in the tens of μV for each breath. Assuming the sensors have consistent linearity, the pressure changes being measured by these sensors were in the range of single Pascals or tens of μBar. In an open environment, these small pressure perturbations from airflow at the nostril drop off exponentially with distance from the source to the sensor, so the sensor should be placed as close to the source as possible, although we were able to obtain a usable signal at distances of up to 5 mm from the nostril. Sensors less sensitive than those used here may not be able to register a signal or may need to be placed much closer to the nostril.

3.5.2 VPT compared to WBP

VPT showed good agreement with WBP in measuring respiratory frequency and relative tidal volume, as demonstrated by the Bland-Altman analysis. The negligible difference in measurements of rate between these two methods was reflected in the average rates seen during increased and decreased respiratory drive, with no detectable difference in the response to carbon dioxide or morphine obtained with these two methods.

While the estimates of relative tidal volume obtained with VPT did not systematically over- or underestimate tidal volume determined using WBP, the Bland-Altman analysis of individual breaths showed variation of as much as 25% on some individual breaths between the two measures. However, this variation should not pose a problem in most experimental applications. Because the VPT system shows no systematic bias, aggregate measures that average tidal volume over a period of time would substantially reduce this source of error. This idea was applied here in the practical measurements of effects of morphine and carbon dioxide, where we used the average of a 30-second sample. With this approach, measures obtained using WBP and VPT were not significantly different.

Finally, the waveform for VPT closely matched that of WBP for individual breaths. The similarity of waveform would allow advanced analyses on VPT signals using the same techniques that are applied to

WBP, including measuring relative inspiratory and expiratory times, quantifying number of sighs in a given period, or considering irregularities in breathing patterns (Subramanian and Holstege 2011; Zhang et al. 2009).

3.5.3 VPT compared to other methods

Our data show that for rate and relative volume, VPT measurements were in close agreement with those obtained using WBP, a well-validated method of measuring respiration (Glaab et al. 2007; Hantos and Brusasco 2002). The principal advantage of VPT over WBP is the ease and simplicity of obtaining respiratory signals in the stereotaxic environment. WBP requires the animal's entire body be enclosed in a sealed chamber, and opening the chamber to manipulate the animal or change the configuration affects measurements. By contrast, VPT uses only one sensor placed in close proximity to the head, fixed to the stereotaxic frame. Shifts in the animal's body, surgical procedures, sensory testing, or repeated injections do not perturb the signal obtained from the animal. Further, since the transducer measures the pressure difference across two ports, the system is resistant to ambient changes in environmental pressures, such as a door opening or an experimenter moving around the room.

We also compared VPT to ACC, since both methods provide non-invasive respiratory monitoring in a manner compatible with stereotaxic frames or other head restraint. The two methods perform comparably in detecting respiratory rate, but VPT provides a more accurate measure of tidal volume during respiratory depression. In addition, interpretation of the ACC signal in terms of inspiration and expiration would not be possible. Further, with ACC any movement of the animal, the sensor, or the connecting wires can change the placement and distort further measurements of relative tidal volume, a problem that does not arise with VPT. Lastly, since animals can use both chest and abdominal muscles for breathing (O'Neil and Raub 1984), the placement of a single accelerometer in relation to specific muscle groups increases possible error in measurement.

For survival surgeries or experiments that need to minimize surgical procedures, other non-invasive methods are also available for monitoring respiration. Hot-wire anemometry measures changes in wire

impedance from flow of gas over a small, heated filament. This method provides an accurate representation of airflow under physiological conditions, but the direction of flow (inspiration vs. expiration) cannot be discriminated without additional equipment (Godal et al. 1976; Lundsgaard et al. 1979; Yoshiya et al. 1979). Capnography is a commonly used clinical method for monitoring breathing, but has shortcomings that limit its use in the research environment. The accuracy of carbon dioxide readings are affected by atmospheric pressure, gas anesthetic, oxygen concentration, and water vapor, and metabolic activity will change the actual excretion of carbon dioxide (Bhavani-Shankar et al. 1992).

Invasive methods of respiratory measurement in anesthetized animals include EMG recordings, pneumotachograph measurement, or even deriving respiratory rate from blood pressure. EMG recordings offer advantages in dissecting the neuromuscular components of respiration, although for simply monitoring physiological state EMG does not necessarily represent tidal volume well (Campbell et al. 1995; Hodges et al. 2001). EMG recordings are also subject to electrical noise from the heart, animal movements, and the environment (Bartolo et al. 1996). Deriving respiratory rate from blood pressure avoids having an additional measurement device for respiration, but the method requires an arterial cannula and is limited to measurements of breathing rate (Mason et al. 2007). Pneumotachograph measurements via tracheotomy or an endotracheal tube is a powerful approach that can be employed with stereotaxy in deeply anesthetized animals. However, while possibly more accurate, invasive pneumotachograph measurements are incompatible with light anesthesia and survival experiments. Also, in some cases the maintenance of the laryngeal valve is preferred, such as with the investigation of airway dysfunction related to neurodegeneration (Dutschmann et al. 2010; Menuet et al. 2011).

3.5.4 Limitations of VPT

VPT does not provide an absolute measure of tidal volume, so tidal volume and minute volume could only be compared between subjects by calculating change relative to baseline. However, the inability to calculate absolute tidal volumes for these systems is not necessarily a significant experimental limitation. With a treatment, the change in absolute tidal volume may differ between animals, but the relative

change may be the more consistent and relevant value (e.g. with a treatment, a large animal may have a larger absolute change in tidal volume than a small animal, but the relative change could be equal between the two animals). The variability in agreement of VPT with WBP measures of tidal volume is largely inconsequential, although WBP is slightly better for detecting subtle changes in tidal volume when only sampling a small number of breaths. Additionally, variations in experimental conditions, such as changes in anesthetic gas viscosity or ambient humidity, as well as altered airway patency, could also increase the variance in the measurements of tidal volume. However, these variables should not affect measurements of breathing frequency.

3.5.5 Conclusion

Various methods of measuring respiratory function provide quantitative and qualitative information related to breathing rate, tidal volume, and gas exchange. Depending on the specific question addressed and the experimental paradigm, some technologies may be more appropriate. Here we present and validate a novel, non-invasive method for use with anesthetized animals in a stereotaxic frame. Respiratory rate and relative tidal volume are quantified via detection of small pressure variations that occur with the inward and outward flow of air during breathing. This method is compatible with stereotaxy, allows surgical and experimental access to the entire animal, and accurately measures breathing rate and relative tidal volume.

3.5.6 Acknowledgements

Andy Rekito of OHSU Dept. of Neurological Surgery provided illustrations. We thank John Hunt of the OHSU Dept. of Biomedical Engineering for circuit design assistance.

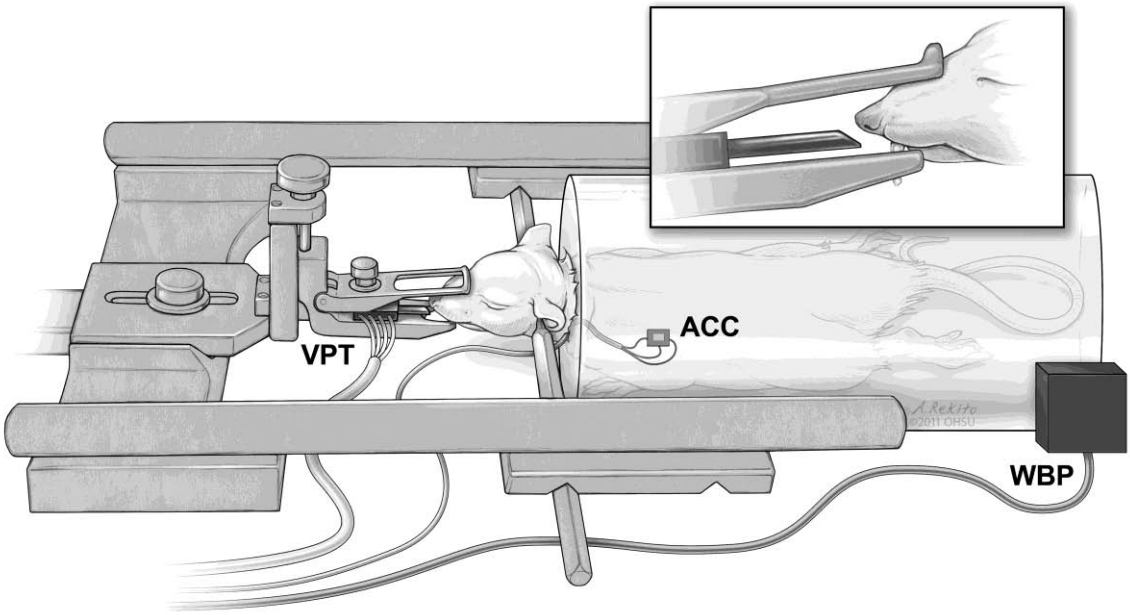
VPT
ACC
WBP

Figure 11: Placement of respiratory monitoring devices.

The measurement device for VPT was locked in place in the stereotaxic frame in front of the animal's nose, so that the sensor was 1 to 5 mm from the nostril. The sensor for ACC was glued to the shaved chest wall using a flexible dental epoxy. WBP used an enclosed plastic chamber that completely surrounds the animal's body, with subtle air displacements being picked up by pressure sensors in the system. (The isoflurane delivery method is not shown in this figure to highlight the positioning of the VPT sensor.)

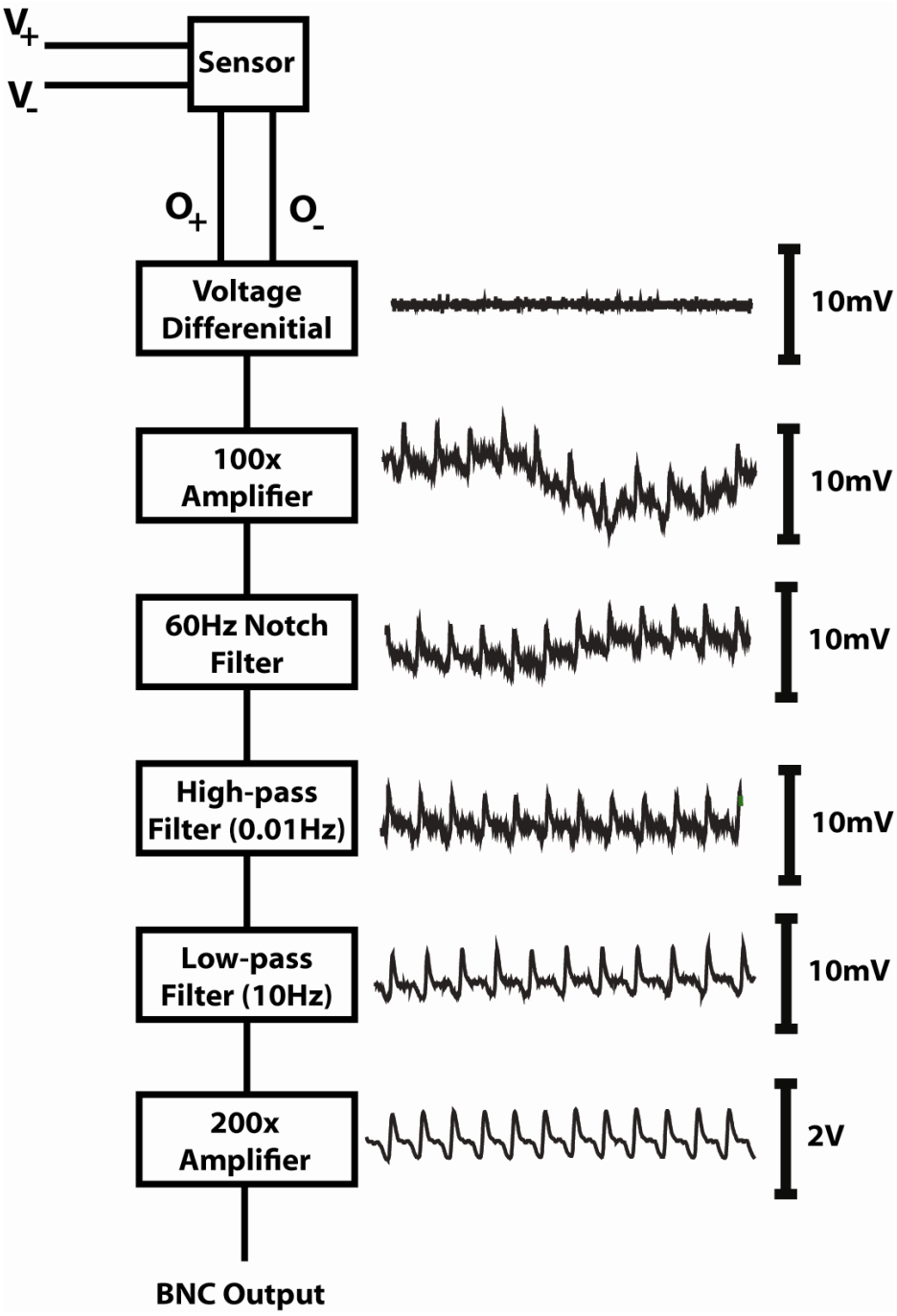
V+
V-
Sensor
O+
O-
Voltage Differenitial
10mV
100x Amplifier
10mV
60Hz Notch Filter
10mV
High-pass Filter (0.01Hz)
10mV
Low-pass Filter (10Hz)
10mV
200x Amplifier
2V
BNC Output

Figure 12: Schematic of VPT system.

The VPT measurement device takes as power a voltage between 2.5 and 3.5 V, and outputs two signals whose differential represents the strength of the measured changes in pressure. Differential, amplification, and filters were all implemented through hardware processing. The final output was passed to an analog-to-digital converter, and the signal then fed into a computer.

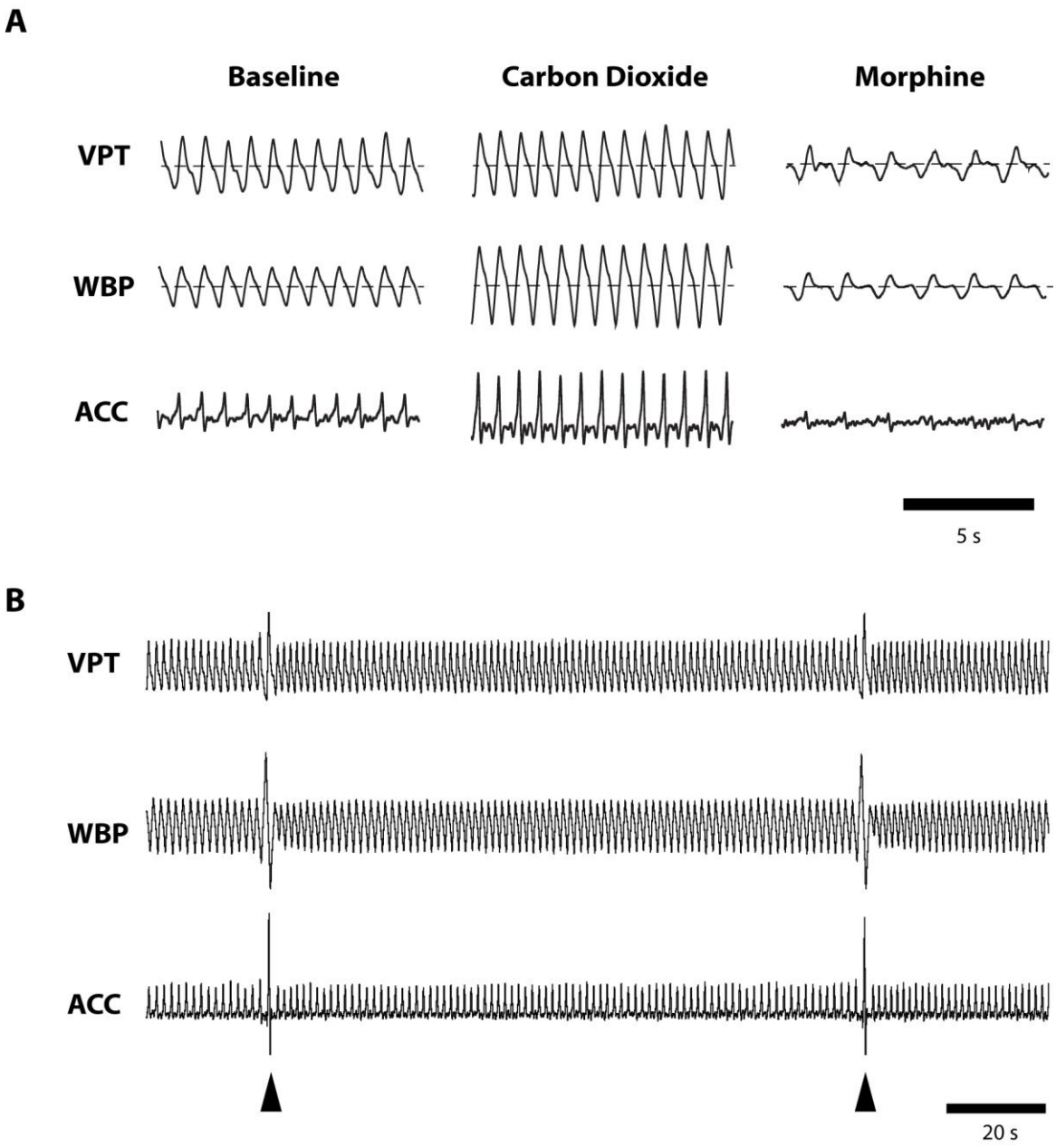
A
Baseline
Carbon Dioxide
Morphine
VPT
WBP
ACC
5 s
B
VPT
WBP
ACC
20 s

Figure 13: Example data from experimental protocol.

A) Following a baseline period, 10% carbon dioxide was administered for 5 minutes, which significantly increased respiratory drive. After a recovery period, morphine was administered at a dose (4 mg/kg) that produced respiratory depression. Dashed line indicates zero-point of signal.

B) At intervals, anesthetized animals exhibited sighs (arrowheads), brief increases in inspiration that open alveoli and prevent atelectasis (Orem and Trotter 1993). Recordings in this figure were taken from the same animal, using all three methods simultaneously.

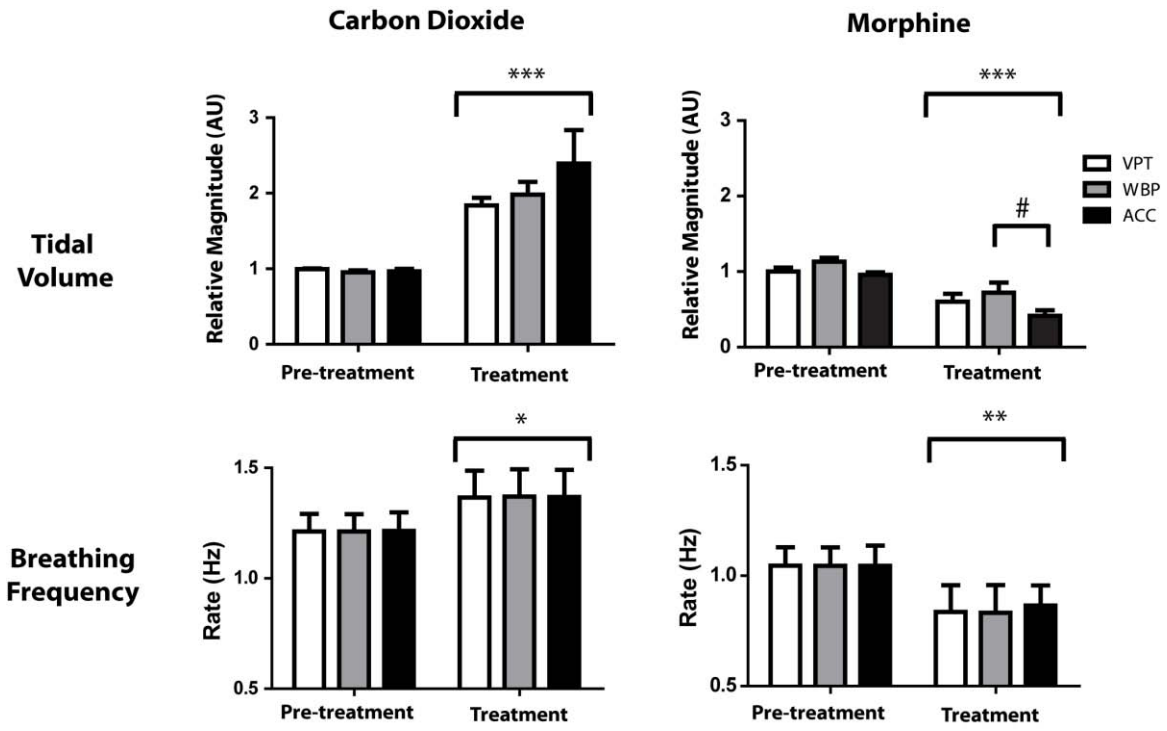
Carbon Dioxide
Morphine
Tidal Volume
Breathing Frequency
Relative Magnitude (AU)
Rate (Hz)
Pre-treatment
Treatment
VPT
WBP
ACC
***
*
**
#

Figure 14: Mean effect of 10% carbon dioxide and 4 mg/kg morphine on breathing frequency and tidal volume.

Administration of carbon dioxide produced an increase in rate and tidal volume detected by all three methods. Morphine produced a decrease in breathing frequency and tidal volume evident with all three methods, but ACC significantly overestimated the effect of morphine on tidal volume. *$p < 0.05$, ** $p < 0.01$, and *** $p < 0.001$ compared to pre-treatment; # $p < 0.05$ compared to WBP.

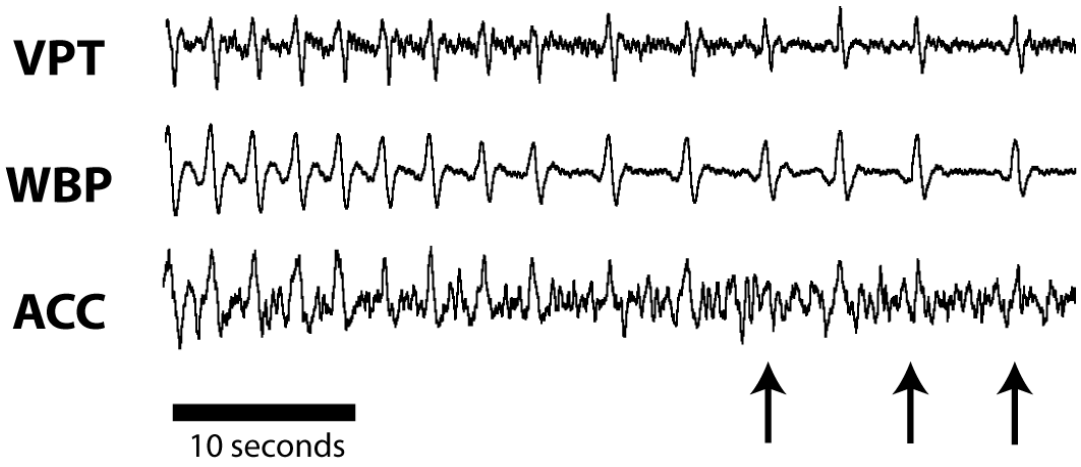
VPT
WBP
ACC
10 seconds

Figure 15: Breaths lost to detection by ACC during respiratory depression.

Administration of morphine produced respiratory depression bordering on apnea. While the periodic breaths were still detectable using VPT and WBP, the waveform for ACC was indistinguishable from noise (arrows indicate breaths lost to detection).

CHAPTER 4

Manuscript #3

Pain-facilitating medullary neurons contribute to opioid-induced respiratory depression

*Ryan S. Phillips[1], *Daniel R. Cleary[1], Julia W. Nalwalk[2], Seksiri Arttamangkul[3], Lindsay B. Hough[3], Mary M. Heinricher[1,4]

[1]Department of Neurological Surgery, Oregon Health & Science University, Portland, OR.

[2]Center for Neuropharmacology and Neuroscience, Albany Medical College, Albany, New York

[3]Vollum Institute, Oregon Health & Science University, Portland, OR

[4]Department of Behavioral Neuroscience, Oregon Health & Science University, Portland, OR

* Denotes authors contributed equally.

4.1 Abstract

Respiratory depression is a therapy-limiting side effect of opioid analgesics, yet our understanding of the brain circuits mediating this potentially lethal outcome remains incomplete. Using direct microinjection of the non-selective antagonist naltrexone in lightly anesthetized rats, we found that the rostral ventromedial medulla (RVM), a region long implicated in pain modulation and homeostatic regulation, contributes to both the analgesic and respiratory depressant properties of systemically administered morphine. However, RVM-dependent antinociception can be separated from respiratory depression. That is, microinjection of the μ-opioid agonist DAMGO in the RVM produced both analgesia and respiratory depression, whereas the non-opioid analgesic improgan produced similar antinociception but stimulated breathing. The distribution of neurons directly inhibited by RVM opioid microinjection was determined using a fluorescent opioid peptide, dermorphin-Alex594, and found to be concentrated in and around the RVM. μ-Opioids, including DAMGO, are known to activate RVM OFF-cells, and suppress the firing of RVM ON-cells. We recorded the activity of identified OFF- and ON-cells during improgan microinjection, and found that this agent activated neurons from both cell classes. The differential respiratory response to these two analgesic drugs is therefore best explained by their opposing effects on the activity of RVM ON-cells. These findings show that pain relief can be separated pharmacologically from respiratory depression, and identify RVM OFF-cells as important central targets for continued development of potent analgesics with fewer side effects.

4.2 Introduction

While opioids remain the most powerful tool available for treating moderate to severe pain, their utility is limited by side effects, especially potentially lethal respiratory depression. Given this risk and the low therapeutic index for many opioids, clinicians often under-treat pain (Nickerson and Attaran 2012; Webster et al. 2011). Despite the clinical and social significance of opioid-induced respiratory depression, the underlying neural mechanisms and circuits are still not fully understood.

In contrast to respiratory depression, the analgesic actions of opioids have been studied intensely, and we now know that these agents produce pain relief by engaging an endogenous brainstem pain modulatory system. This system is the driving force behind the natural suppression or enhancement of pain in different behavioral states (Fields 2004). Its output influences pain behavior via projections from the rostral ventromedial medulla (RVM) to dorsal horn nociceptive circuits. Inactivation or lesion of the RVM can interfere with the analgesic effects of systemically administered opioids, and μ-opioid agonists applied directly in the RVM produce a potent analgesia (Fields et al. 2006).

Two classes of RVM neurons, the "ON-cells" and "OFF-cells," respond to opioids (Fields et al. 2006; Heinricher et al. 2009). ON-cells facilitate nociception, and these neurons are defined by activation during nociceptive withdrawal behaviors. Conversely, OFF-cells suppress nociception, and this cell class is defined by a withdrawal-related pause in activity. Drugs that prevent the OFF-cell pause produce behavioral antinociception, independent of whether ON-cell activity is changed (Heinricher and Ingram 2008; Heinricher et al. 2010b; Neubert et al. 2004). μ-Opioids, for instance, given systemically or locally in the RVM, produce continuous OFF-cell firing while inhibiting ON-cell activity. Whether these changes in OFF-cell and ON-cell activity collectively or separately relate to other effects of opioids, including respiratory depression, is not yet known.

The constituent regions of the RVM, including portions of raphe magnus, raphe pallidus, and raphe obscurus at the level of the facial nucleus, have also been tied to other regulatory functions, including thermogenesis and cardiovascular control (Cao et al. 2004; Lovick 1997; Nakamura and Morrison 2007).

Although these areas have not been strongly implicated in opioid-mediated respiratory depression, they have been linked to respiratory modulation (Dias et al. 2012; Dias et al. 2007; Hellman et al. 2009; Madden and Morrison 2005; Menuet et al. 2011; Rice et al. 2009; Taylor et al. 2006; Verner et al. 2004). Nevertheless, the neuronal and physiological overlap of these homeostatic functions with pain modulation is not well-understood, in part due to the relatively few mechanistic studies that include both parameters.

Here we show that the RVM contributes to opioid-induced respiratory depression at doses that simultaneously produce behavioral analgesia. In the same brain region, the non-opioid analgesic improgan also relieves pain, yet stimulates respiration. This functional separation reflects independent actions of the two distinct populations of opioid-sensitive RVM neurons, the ON-cells and the OFF-cells. Thus, while these results demonstrate an overlap of opioid-induced respiratory depression and analgesia within a common brainstem region, they also show promise for dissociating these two effects pharmacologically, at the level of functionally distinct neuronal populations.

4.3 Methods

4.3.1 Animals

All experimental procedures were approved by the Institutional Animal Care and Use Committee at Oregon Health & Science University and followed the guidelines of the Committee for Research and Ethical Issues of the International Association for the study of Pain.

4.3.2 Surgical Preparation and Anesthesia

Deep surgical anesthesia was induced in male Sprague-Dawley rats (250-350 g, Charles River) using 4% isoflurane in humidified O_2 at 1.25 l/min, and placed in a stereotaxic apparatus. For surgical preparation (no more than 20 min) the isoflurane concentration was reduced to 3% and a small craniotomy performed to allow placement of a recording electrode and/or glass microinjection pipette in the RVM. Animals were placed on a circulating warm-water pad to support body temperature.

After surgical preparation the isoflurane concentration was reduced from 3% to 1.5% over 30 minutes (-0.5% every 10 minutes), and then further adjusted in increments of 0.25% until a tail flick reflex was evoked (see *Nociceptive Testing* below) without other signs of discomfort. This concentration was maintained for at least 30 min prior to the initiation of the experimental protocol. Isoflurane concentration and gas flow rate were fixed for the duration of the protocol.

4.3.3 Nociceptive Testing

Nociceptive thresholds were measured using tail flick (TF) latency. The ventral side of the animal's tail was maintained at 34 °C between trials, and then heated, using a radiant heat source, at a constant rate of 1.7 °C/s until a tail movement was detected or the cut-off temperature of 53 °C was reached. A motion transducer detected movement of the tail. Three locations, at 2, 4, and 6 cm from the tip of the tail, were tested in rotation to avoid sensitization and tissue damage. The holding temperature allowed us to rule out the possibility that any changes in latency could be attributed to changes in skin temperature. TF latency was defined as the difference in time between the point at which the tail surface temperature reached 36 °C and the occurrence of the reflex. This protocol, with trials at 5 min intervals, produces a stable measure of nociceptive responsiveness over several hours (Martenson et al. 2005). The baseline threshold was the average withdrawal latency of three trials taken immediately prior to the drug injection. To aid in comparisons of drug effect among groups, TF latency is sometimes expressed as percent of maximum possible effect: % MPE = (post-drug latency – baseline latency) / (cut-off latency – baseline latency).

4.3.4 Respiration, Heart Rate, and Rectal Temperature

Breathing was monitored by using two different noninvasive methods, both of which provide accurate measurements of breathing rate and relative tidal volume as compared to whole-body plethysmography (Cleary et al. 2012). Initial experiments used accelerometry-based plethysmography (Devonshire et al. 2009), where an accelerometer was attached to the chest wall of the animal to detect movements associated with breathing . In later experiments, respiration was monitored using ventilation

pressure-transduction, which measures small changes in pressure just outside the animal's nose resulting from inhalation and exhalation. The respiratory signals were amplified, filtered, and recorded for off-line analysis (Spike2; CED, Cambridge, UK). Respiratory rate was determined by averaging the inter-breath interval over the 60-s period before each TF. Relative respiratory amplitude was determined by expressing peak-to-peak amplitude, a correlate of tidal volume as a percentage of the pre-drug baseline (Cleary et al. 2012). Heart rate was derived from the electrocardiogram. Body temperature was measured using a rectal thermometer (TH-5; Physitemp, Clifton, NJ).

4.3.5 RVM Recording

A gold- and platinum-plated stainless-steel recording microelectrode (Microprobe, Gaithersburg, MD) was placed in the RVM using anatomical landmarks. Cell recordings were stored for later off-line analysis to ensure accurate discrimination throughout the recording. All neurons were clearly identified and classified as an ON-, OFF, or NEUTRAL-cell prior to the start of the experimental protocol using standard criteria (Fields et al. 1983). ON- and OFF-cells are defined by a sudden activation or cessation in firing rate, respectively, beginning just prior to a nociceptive reflex such as the TF response. NEUTRAL-cells show no change in firing rate correlated with the occurrence of a nociceptive reflex. Spontaneous firing was determined by measuring firing rate in a 30-s period immediately prior to each tail flick trial (5-min intervals). Reflex-related changes in firing were determined in a 3-s period beginning 0.5 s prior to the tail flick response.

4.3.6 Experimental Protocols

In the first set of experiments, the contribution of neurons in the RVM to the antinociceptive and respiratory depressant actions of systemically administered morphine was determined by microinjection of the locally acting opioid antagonist naltrexone in the RVM. Tail flick trials were initiated at 5-min intervals throughout the protocol. Following a 15-min baseline period, morphine (0.66 mg/kg, i.v.) was given. Ten minutes later, naltrexone (3 μg/200 nl) or artificial CSF (aCSF, 200 nl) was microinjected into the RVM, or into surrounding regions as off-site controls. Naloxone (0.27 mg/kg, i.v.) was given

systemically at the end of the experiment to show that morphine effects were receptor-mediated and reversible.

In the second set of experiments, we examined the effects of direct RVM microinjection of DAMGO ([d-Ala2, n-MePhe4, Gly-ol]-enkephalin, 200 pmol) or the non-opioid analgesic improgan (15 or 30 nmol, Hough et al. 2000) on the activity of RVM neurons, nociception, respiratory parameters, heart rate, and body temperature. A 15-min baseline was established followed by microinjection of drug or vehicle (injected over five to ten minutes, beginning immediately after the last baseline TF). TF, respiratory measurements, heart rate, and rectal temperature were recorded for the next hour.

In the third set of experiments, we microinjected either GABAA receptor antagonist bicuculline (22 pmol) to disinhibit RVM neurons, or the GABAA receptor agonist muscimol (18 pmol) to suppress activity of RVM neurons. The protocol in this third set was identical to that for DAMGO and improgan, with TF, respiration, heart rate and rectal temperature recorded before and after microinjection of bicuculline or muscimol.

4.3.7 Verification of microinjection and recording sites

Microinjection locations and recording sites were marked by either fluorescent beads injected with the drug or by an electrolytic lesion created after the experimental protocol. Animals were overdosed with isoflurane and then transcardially perfused with physiological saline followed by 10% formalin. Brains were removed and stored overnight in 10% formalin. The brainstem was sectioned at 60 μm and mounted for microscopic examination.

4.3.8 Identification of opioid-sensitive brainstem neurons

To identify neurons in the region of the RVM that contain post-synaptic μ-opioid receptors and that could thus drive RVM opioid-induced changes in nociception and respiration, we injected a peptide μ-opioid agonist, dermorphin, that was fluorescently labeled using Alexa Fluor 594 (Arttamangkul et al.

2000; Arttamangkul et al. 2008) into the RVM. Dermorphin-A594 was dissolved in either 3% DMSO in saline (6 pmol/200 nl injections) or 30% DMSO in saline (66 pmol/200 nl).

For injection of dermorphin-A594 into the RVM, animals were initially anesthetized using 5% isoflurane for placement of a jugular catheter, and the anesthetic then switched from inhaled isoflurane to intravenous methohexital (30 – 60 mg /hr). After achieving a stable baseline for at least 25 minutes, dermorphin-A594 was injected into the RVM. In some experiments, 45 minutes prior to the injection of dermorphin-A594, an injection of the irreversible mu-opioid antagonist, β-funaltrexamine (β-FNA, 300 nl, 6 nmol, Tocris Bioscience), was injected into the RVM. Heart rate, respiratory rate, and rectal temperature were measured as described above. Nociceptive threshold was measured by placing a peltier device on the left hindpaw, slowly increasing temperature from 35 to 53 C, and noting the temperate at which a withdrawal was initiated. EMG recordings from the left calf were used to determine the beginning of the withdrawal. Antinociception is expressed as percent of maximum possible effect (%MPE). These experiments allowed a comparison of the analgesic efficacy and respiratory and autonomic depressive effects of dermorphin-A594 with those of DAMGO and improgan.

Physiological and nociceptive parameters were monitored before and after injection of dermorphin-A594. Sixty minutes after injection, animals were overdosed with methohexital and perfused transcardially with solutions of physiological saline and of 10% formalin. The brains were removed, fixed overnight in 10% formalin, and sectioned at 60 µm. Sections were mounted on glass slides with permount, visualized on an Olympus BX51 fluorescent microscope (Olympus, Center Valley, PA), and photographed using a Microfire A/R camera attachment (Optronics, Inc., Goleta, CA). For each brain, an experimenter blinded to the treatment conditions photographed eight representative brainstem sections between -1.08 and -3.96 mm (relative to the interaural line), with the same intensity and exposure for each photograph.

Mean fluorescence for each section was quantified using the open-source image processing package Fiji (http://www.fiji.sc). Fluorescence was measured in the RVM, a midline area roughly 2 mm in width

and 1 mm in height directly dorsal to the pyramidal tracts at the level of the facial nucleus. Background intensity for each section was also measured and then subtracted from the overall fluorescence.

4.3.9 Statistical analysis

All data are represented as mean + SEM. Drug effects on TF latency, hindpaw withdrawal threshold, respiratory rate, heart rate, and rectal temperature were determined using one- or two-way ANOVA, with post-hoc comparisons used where indicated. Differences in mean RVM fluorescence between treatment groups and the effects of dermorphin-A594 relative to baseline were analyzed using unpaired and paired t-tests, respectively. Respiratory amplitude was analyzed using a Friedman's analysis of variance by rank. Cell firing data post-treatment were compared to baseline using a Wilcoxon's signed ranks test. Analyses were performed using GraphPad Prism or Statview. $P < 0.05$ was considered statistically significant.

4.4 Results

4.4.1 The RVM contributes to antinociceptive and respiratory-depressant actions of systemically administered morphine.

The RVM is defined functionally, as the area where low-current electrical stimulation produces behavioral antinociception, and includes the nucleus raphe magnus and adjacent reticular formation at the level of the facial nucleus (Fields and Heinricher 1985). We first determined whether this region is required for respiratory depressant actions of systemically administered morphine, as well as for analgesia. Respiratory parameters (rate and amplitude) were measured in parallel with the TF response evoked by noxious radiant heat. The latter is an index of nociception widely employed in awake behaving animals that can also be used in lightly anesthetized subjects (Fields and Heinricher 1985).

As shown in Figure 16, systemically administered morphine produced both potent analgesia and a significant decrease in respiratory rate (ANOVA, $p < 0.05$ compared to baseline for all groups). Both effects were reversed by focal application of the opioid antagonist naltrexone in the RVM, but not by aCSF vehicle. Naltrexone microinjections in areas immediately surrounding the RVM (dorsal, rostral, and

caudal) were ineffective (Figure 16, naltrexone placement control group). Subsequent systemic administration of naloxone, a highly lipophilic, short-acting opioid antagonist, reversed antinociception and respiratory depression in RVM-vehicle and placement control groups, showing that both effects were opioid receptor-mediated and reversible. These data demonstrate that opioid receptors in the RVM contribute to respiratory depression, as well as to antinociception, produced by systemically administered morphine.

4.4.2 Distribution of neurons in the RVM driving opioid-induced changes in respiration, heart rate, and pain threshold

We next determined the distribution of neurons in the RVM and surrounding areas that could be the direct target of μ-opioid agents. By microinjecting the μ-opioid agonist dermorphin labeled with an Alexa Fluor 594 fluorophore (dermorphin-A594), we could identify individual cells in the RVM and surrounding regions that bind the agonist and internalize the μ-opioid receptor. These labeled neurons are potential drivers for the physiological and behavioral effects produced by opioid microinjections into the RVM.

Microinjection of dermorphin-A594 (66 pmol/200 nl) into the RVM produced significant effects on heat-evoked withdrawal (%MPE: 64.6 ± 18.4, $n = 5$, $p < 0.05$), respiratory rate (-16.2 ± 3.6 breaths/min, $p < 0.05$), heart rate (-23.0 ± 7.9 beats/min, $p < 0.05$), and body temperature (-0.28 ± 0.10 ^{o}C, $p < 0.05$), consistent with results from microinjections of DAMGO into the RVM (see next section). To identify the minimal subset of neurons that could produce these effects, we used the lowest dose of dermorphin-A594 (6 pmol/200 nl) that consistently produced measurable, albeit small, antinociception (%MPE: 9.5 ± 3.5, $n = 4$, $p < 0.05$). With this lower dose, respiratory rate was significantly decreased (-10.8 ± 3.0 breaths/min, $p < 0.05$), and there were no changes in heart rate (-25.0 ± 11.0 beats/min, $p > 0.05$) or body temperature (-0.21 ± 0.09 ^{o}C, $p > 0.05$).

Many neurons with strong A594 fluorescence were visible in the area immediately surrounding the injection site (Figure 17), including numerous cells in the nucleus raphe magnus, nucleus raphe pallidus, raphe obscurus, and reticularis gigantocellularis pars alpha. Distinctly fluorescent single neurons were

visible as far as 1 mm rostral and caudal to the injection site. Some larger neurons were also visible in the area dorsal to the injection site (nucleus reticularis gigantocellularis), predominantly in the sections containing the injection site or the track of the injector.

In control experiments, injecting the irreversible mu-opioid antagonist beta-funaltrexamine (beta-FNA) 45 minutes prior to dermorphin-A594 injection significantly attenuated mean fluorescent labeling in the RVM (dermorphin-A594: 6.4 ± 1.1 arbitrary units averaged across all rostro-caudal levels, $n = 4$; beta-FNA pretreatment: 1.8 ± 0.63, $n = 4$; $p < 0.05$ by unpaired t-test, Figure 17f).

4.4.3 The RVM supports opioid-induced respiratory depression

To compare the analgesic and respiratory effects of direct local RVM administration of the μ-opioid agonist DAMGO with those of the non-opioid analgesic improgan (Hough et al. 2000), we recorded nociception, respiration, autonomic parameters (heart rate and body temperature) simultaneously before and after microinjection of the two agents. We also recorded RVM neuronal activity in the improgan experiments, but not in the DAMGO experiments, since the effects of local DAMGO injection on activity of RVM neurons has been defined previously (Heinricher et al. 1994).

Microinjections of DAMGO or improgan in the RVM at sites shown in Figure 18 produced potent antinociception. TF latency was increased significantly by both agents, but not by vehicle (Figure 19). The peak antinociceptive effects of improgan and DAMGO were seen at 10-20 and 35-45 min post-injection, respectively, consistent with the known time-courses of these agents. Injections of improgan in areas surrounding the RVM, mostly dorsal and rostral (see Figure 18) resulted in a small, but statistically significant, increase in TF latency (1.8 ± 0.5 s, n = 23, $p < 0.01$).

Although both DAMGO and improgan produced antinociception when microinjected into the RVM, only DAMGO produced a significant respiratory depression, decreasing both respiratory rate and amplitude (Figure 19). In marked contrast, improgan in the RVM stimulated both respiratory rate and amplitude. The peak effects of improgan and DAMGO were seen at 10-20 and 35-45 min post-injection, respectively, for both rate and amplitude. Vehicle injection had no effect on respiration, and injections of

improgan in areas surrounding the RVM produced only a modest increase in respiration (4.8 ± 0.18 breaths/min, $p < 0.05$). These data demonstrate that the analgesic actions of drugs in the RVM are not inextricably linked to respiratory depression.

4.4.4 Autonomic effects of DAMGO and improgan are also distinct

DAMGO microinjection resulted in a decrease in heart rate while improgan induced a substantial increase (Figure 19). Peak effects on heart rate were evident at 10-20 min and 35-45 min post-injection with improgan and DAMGO, respectively. A small but statistically significant decrease in heart rate (6.0 ± 2.0 beats/min) was seen in vehicle-treated controls over the course of the experiment. Injections of improgan in areas surrounding the RVM produced a statistically significant increase in heart rate (25 ± 6.6 beats/min, $p < 0.01$).

Like heart rate, body temperature was also differentially affected by DAMGO and improgan. DAMGO microinjection decreased, whereas improgan increased, body temperature (Figure 19). The peak effects of improgan and DAMGO on temperature were seen at 35-45 min post-injection. The delayed time-course for improgan in this case presumably reflects the kinetics of whole-body temperature change. Injections of improgan in areas surrounding the RVM produced a small but statistically significant increase in body temperature (0.1 ± 0.03 °C, $p < 0.01$).

Thus, like respiratory depression, reduced autonomic output following manipulations of the RVM can also be dissociated from analgesia.

4.4.5 Changes in RVM neuronal activity from DAMGO and improgan administration

To understand how opioids and improgan produced similar antinociception but opposing effects on respiration, we recorded the activity of physiologically identified neurons within the RVM. From a pain-modulating perspective, all neurons recorded in the RVM can be assigned to one of three mutually exclusive classes: OFF-cells (defined by nociceptive reflex-related inhibition of activity), ON-cells (characterized by nociceptive reflex-related activation), and NEUTRAL-cells (unresponsive to noxious

stimuli, Fields et al. 2006). Both OFF-cells and ON-cells function as pain-modulating neurons, respectively suppressing and facilitating spinal nociceptive processing.

The effects of μ-opioids on the firing of these RVM cell classes have been well documented and provide pharmacological validation of the physiological classification. Local or systemically administered μ-opioid receptor agonists, including morphine and DAMGO, indirectly activate OFF-cells through presynaptic disinhibition, suppress ON-cell firing through direct inhibition, and do not affect NEUTRAL-cell firing (Fields et al. 2006; Heinricher and Ingram 2008). However, the effects of locally administered improgan on the different RVM cell classes have not been studied. Since this agent produced analgesia with respiratory stimulation, we determined the effects of local administration of improgan on identified RVM neurons in order to establish where the actions of improgan and μ-opioids diverged.

Improgan, like μ-opioids, activated the pain-inhibiting OFF-cells in the RVM. Ongoing firing of these neurons was increased substantially (Figure 20). Further, improgan prevented the characteristic inhibition of OFF-cell firing during noxious stimulation (p = 0.03, n = 7, Wilcoxon's signed rank test compared to baseline, data not shown). Improgan activation of OFF-cells thus mimics the net opioid effect of increasing the firing of these neurons. However, unlike opioids, improgan also strongly activated both ON-cells and NEUTRAL-cells (Figure 20).

The differential effects of RVM DAMGO and improgan on respiration and autonomic parameters must therefore be due to the effects on the ON-cells, since only this cell classes responds differentially to the two drugs.

4.4.6 Functional effects of stimulating or blocking all RVM neurons

To corroborate the behavioral and physiological effects of RVM DAMGO and improgan, we examined the effects of non-selective excitation or inhibition of all RVM neurons on nociception, respiration, and autonomic parameters. The goal of these experiments was to contrast effects of selective manipulations of ON- and OFF-cells using opioids with non-selective activation or inhibition to confirm the contributing role of these two cell classes to analgesia, heart rate, thermogenesis, and respiratory control.

To non-selectively excite RVM neurons, we microinjected the $GABA_A$ receptor antagonist bicuculline into the RVM. Like improgan, bicuculline activates both ON- and OFF-cell classes (Heinricher et al. 1994). The physiological response to bicuculline generally mimicked the response to improgan rather than DAMGO, with antinociception accompanied by increases in respiratory rate, heart rate, and body temperature (Figure 21). These data verify the above finding with improgan that concurrent activation of ON- and OFF-cells in RVM stimulates respiration at the same time that it produces analgesia.

To confirm that suppression of activity of a subset of RVM neurons was relevant to opioid-induced respiratory depression, we blocked activity of all RVM neurons by microinjecting the $GABA_A$ receptor agonist muscimol (Martenson et al. 2009). Breathing, heart rate, and body temperature were all significantly reduced following RVM blockade, although nociceptive threshold was not altered (Figure 21). Inhibiting all RVM neurons thus reproduces the respiratory depressant actions of DAMGO, and further, points to a role for this region in maintenance of basal respiratory function.

4.5 Discussion

These experiments show that the RVM, a region long implicated in pain modulation and homeostatic regulation, contributes to both the analgesic and respiratory depressant properties of μ-opioids. To determine whether RVM mechanisms of antinociception can be separated from those mediating respiratory depression, we compared the behavioral, physiological and neuronal effects of DAMGO with those of improgan, a non-opioid analgesic (Table 2). While both drugs produced analgesia when microinjected into the RVM, DAMGO produced respiratory depression, whereas improgan stimulated breathing. Locally applied DAMGO, like systemically administered morphine, is known to activate OFF-cells and suppress ON-cell firing (Heinricher et al. 1994). Here, local improgan activated both ON- and OFF-cells. Thus, while OFF-cells show the same response to both DAMGO and improgan, the two drugs have opposing effects on ON-cells. The differential respiratory response to these two analgesic drugs in the RVM is therefore most readily explained by their opposing effects on the activity of ON-cells. By

contrast, the common analgesic response to the agents is accounted for by their ability to activate OFF-cells.

4.5.1 Neural basis for analgesia and respiratory depression mediated by the RVM

While histochemical and anatomical approaches to the study of RVM neurons are as yet incomplete, their physiological classification is comprehensive. That is, by definition, every RVM neuron recorded can be identified as an ON-, OFF-, or NEUTRAL cell. These three cell classes have been identified in barbiturate-, ketamine- and isoflurane-anesthetized rats as well as in decerebrate-unanesthetized and awake animals (Clarke et al. 1994; Heinricher et al. 2010b; Leung and Mason 1995; 1999; McGaraughty et al. 1993a; b). ON-cells facilitate nociception, and local or systemically administered μ-opioids suppress ON-cell activity. OFF-cells suppress nociception, and opioids increase OFF-cell firing through disinhibition. Sustained OFF-cell activity mediates the analgesic action of morphine and other μ-opioids. The NEUTRAL-cells do not respond to μ-opioid agonists, whether given systemically or locally (Fields et al. 2006; Heinricher and Ingram 2008). Therefore, one or both of the two opioid-sensitive cell classes, the ON-cells and OFF-cells, must mediate the physiological and behavioral effects of μ-opioids in the RVM, including respiratory depression and analgesia.

To better understand how μ-opioids act in the RVM to depress respiration, we compared the effects of opioids with those of improgan, a non-opioid analgesic. This compound does not cross the blood-brain barrier, but when administered intracerebroventricularly, it acts at an unknown receptor site to stimulate descending antinociception through RVM OFF-cell activation (Heinricher et al. 2010b; Nalwalk et al. 2004), a finding consistent with the present results. The surprising observation in the current study was that improgan, applied directly in the RVM, produced a powerful respiratory stimulation in parallel with analgesia, allowing us to investigate the cellular basis for the differential influence on respiratory control and nociception. Locally administered improgan activated not only OFF-cells, mimicking the effect of μ-opioids on these neurons, but also ON-cells, an effect opposite to that of μ-opioids. Although NEUTRAL-cell firing was also increased by local improgan, these neurons do not respond to opioids (Barbaro et al.

1989), which argues against a role for this cell class in opioid-induced respiratory modulation via the RVM. These data therefore confirm the already substantial evidence that the OFF-cells are the analgesic output from the RVM (Fields et al. 2006; Heinricher and Ingram 2008), but more important, suggest that RVM effects on respiration are mediated by ON-cells. A role for ON-cells in opioid-induced respiratory depression was unexpected but fits well with established interactions between pain and respiration. For instance, acute noxious stimuli, which activate ON-cells, have long been recognized to attenuate opioid-induced respiratory depression (Borgbjerg et al. 1996; Kamei et al. 2011; McQuay 1988). Should OFF-cells play any role in modulating respiration or autonomic parameters, that influence is masked by the overriding effect of the ON-cells.

4.5.2 Dissociation of analgesia from respiratory depression at the level of the RVM

Since OFF-cells appear to mediate analgesia but not respiratory depression, our data imply that further separation of respiratory depression from analgesia is possible, based on both neural substrate and pharmacology. μ-Opioid activation of OFF-cells is indirect, through a presynaptic mechanism, whereas inhibition of ON-cells is a direct postsynaptic effect (Heinricher and Ingram 2008; Heinricher et al. 1992; Pan et al. 1990). Because the pre- and post-synaptic actions of μ-opioids invoke distinct second-messengers and channels (Heinricher and Ingram 2008), this finding points to presynaptic mechanisms as critical targets for "pure" opioid-like analgesia. Focusing on OFF-cell-selective pathways, including the presynaptic μ-opioid receptors and downstream molecules, therefore has the potential to provide potent pain relief without the risk of respiratory depression. Indeed, cannabinoids, like opioids, act in the RVM to produce analgesia, but do not produce significant respiratory depression. This disparity between opioid and cannabinoid actions could be explained by the fact that cannabinoids do not have direct post-synaptic inhibitory actions on RVM ON-cells (Vaughan et al. 1999).

The RVM has the potential to modulate respiration through several pathways. Raphe magnus and raphe obscurus both send direct projections to the phrenic motor nucleus (Holtman et al. 1986; Holtman et al. 1984; Hosogai et al. 1998), and stimulation of either raphe magnus or pallidus influences activity of

phrenic motoneurons (Lalley 1986; Millhorn 1986). Alternatively, the RVM has numerous afferent and efferent connections within the brainstem, and could modulate relays at various stages of the chemosensory pathways or contribute to chemosensory-evoked activations (Guyenet et al. 2010; Huckstepp and Dale 2011; Nattie 2011; Pattinson et al. 2009). For example, medullary raphe regions are recognized to modulate chemosensory function of the retrotrapezoid nucleus (Depuy et al. 2011; Dias et al. 2008; Hilaire et al. 2010; Mulkey et al. 2007; Viemari and Tryba 2009).

4.5.3 Distribution of opioid-inhibited neurons in the RVM and surrounding brainstem

Due to technical challenges with the use of MOR1 antibodies in the medullary core, the distribution of neurons with postsynaptic μ-opioid receptors in the RVM and surrounding brainstem regions has not been defined precisely, and attempts to quantify or visually identify RVM neurons that express the μ-opioid receptor have met with limited success. We found that the fluorescent μ-opioid dermorphin-A594 microinjected into the RVM labeled somata of neurons that bound and internalized this ligand. This approach holds significant promise for labeling functional receptors where immunohistochemical techniques are not optimal. In addition, it gives a more direct measure of the spread of the injected drug than traditional dye approaches or calculations of injectate volumes.

Labeled neurons were found primarily in raphe magnus and nucleus reticularis gigantocellularis pars α, but were also concentrated in raphe pallidus. Neurons in the area of raphe magnus and reticularis gigantocellularis pars α that exhibit inhibitory responses to μ-opioid agonists have been found without exception to be ON-cells (Barbaro et al. 1989). Whether opioid-sensitive neurons in raphe pallidus also exhibit the physiological properties of ON-cells has not been investigated systematically. Raphe pallidus is strongly implicated in homeostatic regulation, especially control of body temperature (Cao and Morrison 2003; Madden and Morrison 2005; Morrison 2011). However, raphe pallidus has significant anatomical and functional overlap with more dorsal aspects of the RVM, and neurons from throughout the RVM project to the intermediolateral cell column (Berner et al. 1999; Henry and Calaresu 1974; Loewy 1981; Morrison and Nakamura 2011). Functional projections to the IML from the medullary raphe raise core

temperature by engaging multiple mechanisms of thermogenesis, including brown-adipose tissue activation, vasoconstriction, and fusimotor activity (Blessing and Nalivaiko 2001; McAllen et al. 2010; Nakamura et al. 2004). Control of thermogenesis by opioid-sensitive ON-cells fits with previous observations that DAMGO injected into the RVM attenuates stimulus-evoked increases in activity of brown adipose tissue (Nason and Mason 2006).

Some labeled neurons were also found immediately rostral and caudal to the RVM, at the level of the superior olive and in the area of raphe obscurus dorsal to the inferior olive. Opioid-sensitive cell populations rostral and caudal to the RVM have also not been characterized, but neurons with respiration-related activity have been identified in the medial medulla immediately caudal to the RVM (Lindsey et al. 1994; Pilowsky et al. 1995). The observation that an opioid microinjected in the RVM can directly influence neurons beyond the conventional boundaries of this region raises the possibility that opioid-induced analgesia and respiratory depression are mediated not by RVM OFF- and ON-cells but by opioid-responsive neurons in surrounding regions (Depuy et al. 2011; Zhang et al. 2007a). However, it seems unlikely that these areas were the primary target of the injected analgesic drugs, since local application of an opioid antagonist in areas surrounding the RVM did not prevent the analgesic or respiratory-depressant effects of systemically administered morphine. Further, it has been shown that microinjections of DAMGO caudal and lateral to the RVM, at the level of raphe obscurus, do not activate OFF-cells or produce behavioral antinociception (Heinricher et al. 1994). Nevertheless, it is doubtful that a clear functional boundary can be drawn between the RVM and adjacent reticular areas, and there is likely to be significant anatomical overlap in the distributions of neurons important in pain modulation, respiration, and autonomic function (Kerman 2008; Lovick 1997; Rathner et al. 2001; Strack et al. 1989).

4.5.4 Integration of pain modulation, respiratory control and autonomic function in the RVM

Control of respiration occurs through the cooperative actions of a network of brain regions, with contributions from the cerebral cortex, hypothalamus, and multiple sites in the brainstem (Dean and Nattie 2010; Feldman et al. 2003; Guyenet et al. 2010; Guyenet et al. 2008; Horn and Waldrop 1998;

Nattie and Li 2009). While the outputs of these areas may converge before reaching respiratory motor neurons, no single brain site is responsible for all aspects of breathing. Systemically administered opioids may depress respiration through concurrent actions in multiple brain areas, including rostral ventrolateral medulla, pre-Bötzinger complex, nucleus ambiguus, and cortex (Gray et al. 1999; Hassen et al. 1983; Lalley 2006; Miyawaki et al. 2002; Montandon et al. 2011b; Pattinson et al. 2009; Stucke et al. 2008; Zhang et al. 2007b). The present findings complement these results by showing that activation of opioid receptors in the RVM, a well-known pain-modulating region, can depress breathing rate significantly. While these data show that the RVM contributes to decreases in respiration at clinically relevant opioid doses, higher, potentially lethal doses almost certainly have multiple targets, including direct effects on respiratory premotor neurons (Lalley 2003; Mustapic et al. 2010; Stucke et al. 2008).

While the contribution of RVM ON-cells to opioid-induced respiratory depression is novel, the finding is not out of line with a long-standing view of this region as important for coordinating physiological and behavioral aspects of defense in response to both internal and external challenges to homeostasis (Bandler and Shipley 1994; Lovick 1997). The neuronal basis of this coordination of function deserves further study. Whether a single neuron can modulate nociception, respiration and autonomic parameters in parallel, or if defined cell populations or subpopulations separately regulate each of these functions is a long-standing question that is yet to be resolved (Brazier and Hobson 1980) .

4.5.5 Conclusion

Given the multiple functions integrated within the RVM, it has been argued that separating opioid-mediated analgesia from side effects would be impossible (Mason 2011). While the present data show that respiration, body temperature, and heart rate can be modulated by altering the activity of opioid-sensitive neurons in the RVM, the effects on all three homeostatic parameters are separable from pain inhibition.

An important clinical and scientific goal is to develop drugs that effectively relieve pain without producing respiratory depression. Our findings demonstrate a common central site of opioid action for

respiratory depression and analgesia, but also show promise for further dissociation of these effects pharmacologically at the level of functionally distinct neuronal populations within the RVM.

Treatment	Change in Firing		Behavioral or Physiological Effect			
	ON-cell	OFF-cell	Tail Flick	Resp. Rate	Heart Rate	Temperature
Vehicle	No effect	No effect	No effect	No effect	Mild effect	No effect
DAMGO	↓	↑	Hypoalgesia	↓	↓	↓
Improgan	↑	↑	Hypoalgesia	↑	↑	↑
Bicuculline	↑	↑	Hypoalgesia	↑	↑	↑
Muscimol	↓	↓	No effect	↓	↓	↓

Table 2: Summary of the responses of RVM neurons and the associated changes in tail flick latency, respiratory rate, heart rate, and temperature to local application of vehicle, DAMGO, improgan, bicuculline, and muscimol in the RVM. Activation of OFF-cells is coupled to hypoalgesia, whereas changes in respiratory rate and autonomic parameters are linked to drug effects on the ON-cells.

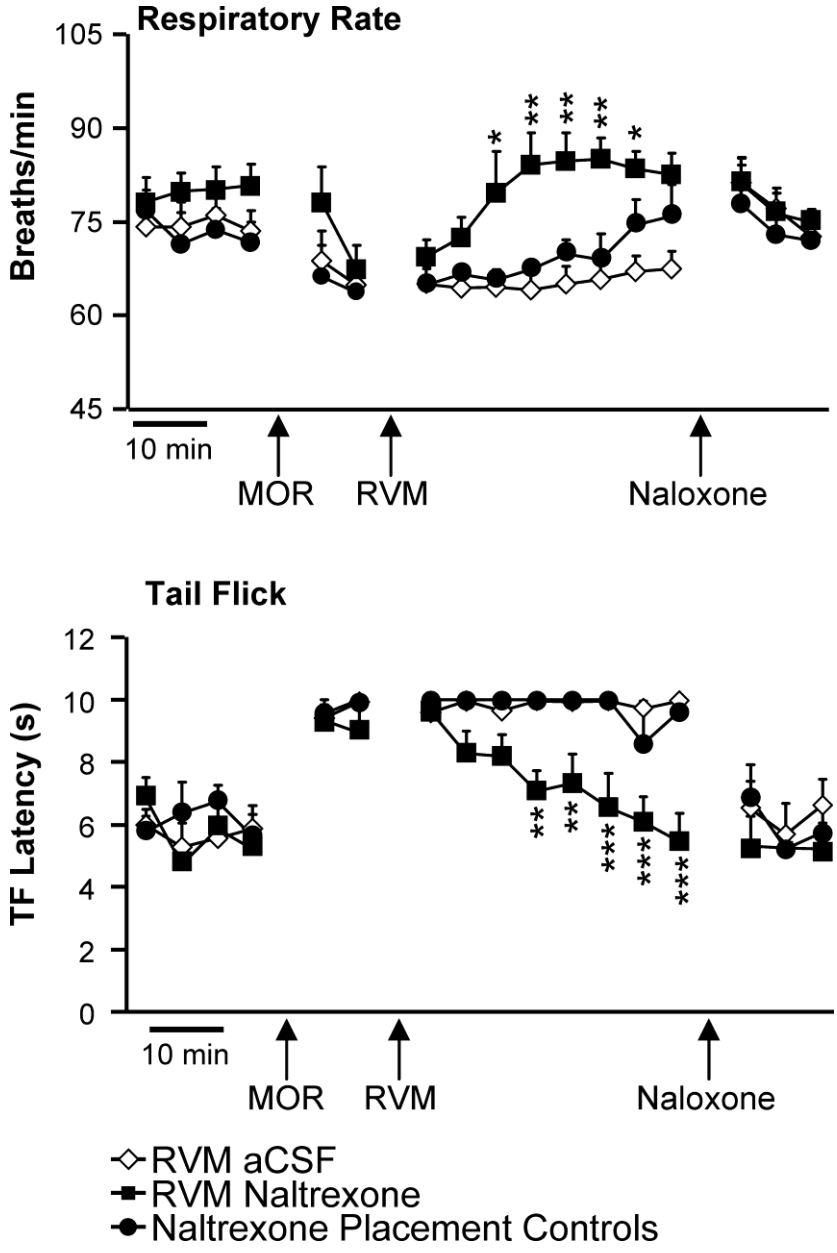
Respiratory Rate
Breaths/min
105
90
75
60
45
10 min
MOR
RVM
Naloxone
Tail Flick
TF Latency (s)
12
10
8
6
4
2
0
10 min
MOR
RVM
Naloxone
RVM aCSF
RVM Naltrexone
Naltrexone Placement Controls

Figure 16*:* Respiratory depression and antinociception produced by systemically administered morphine are blocked by an opioid-receptor antagonist in the RVM.

Animals underwent baseline testing and were given morphine systemically (**MOR**). At the point labeled **RVM**, naltrexone or aCSF was microinjected into the RVM. Injections that missed the RVM are shown as placement controls. All animals then received naloxone systemically, to verify the reversibility of any effect. Respiration was quantified and tail flick trials were initiated at 5-min intervals throughout the protocol. (6-9 animals/group, no difference among groups in baseline, *$p < 0.05$, **$p < 0.01$, ***$p < 0.001$ compared to aCSF using a repeated-measures ANOVA followed by a Bonferroni post-hoc test).

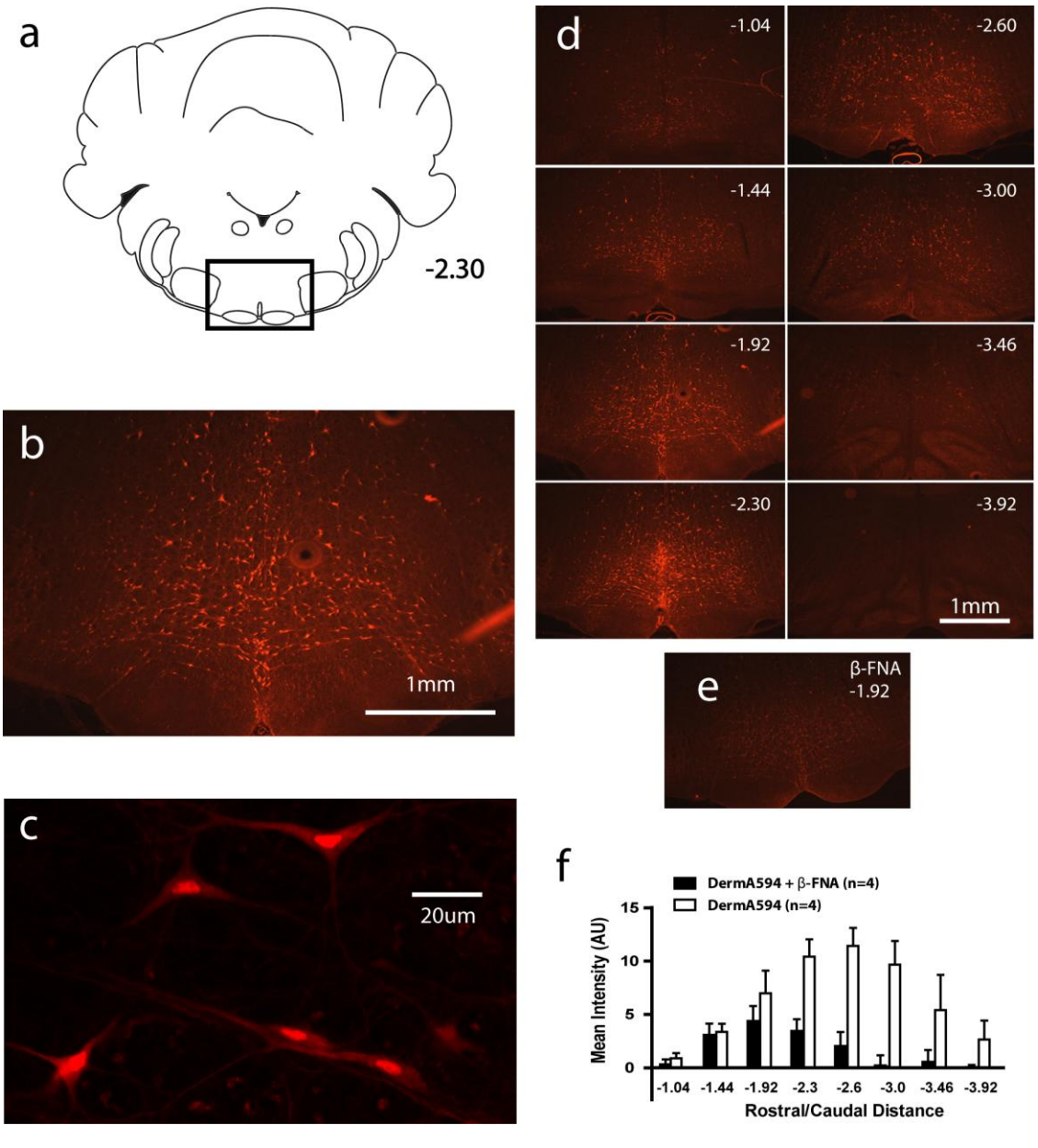
a
-2.30
b
1mm
c
20um
d
-1.04
-2.60
-1.44
-3.00
-1.92
-3.46
-2.30
-3.92
1mm
e
β-FNA
-1.92
f
DermA594 + β-FNA (n=4)
DermA594 (n=4)
Mean Intensity (AU)
15
10
5
0
-1.04 -1.44 -1.92 -2.3 -2.6 -3.0 -3.46 -3.92
Rostral/Caudal Distance

Figure 17*:* Dermorphin-A594 labeling of single neurons in and around the RVM.

a. Images were taken of a ventral area of the sections representing the RVM and rostrally and caudally adjacent brainstem.

b. Representative image showing the distribution of fluorescent cells at 1.92 caudal to the interaural line after a 200 nl microinjection of dermorphin-A594. **c.** View of individual RVM neurons with dermorphin-A594 labeling.

d. Representative sections from same animal as in b showing the distribution of fluorescent neurons at different rostral/caudal levels. Distance from interaural line is given.

e. Labeling for dermorphin-A594 from representative animal pretreated with beta-FNA.

f. Pre-treatment with beta-FNA significantly attenuated fluorescence from dermorphin-A594 microinjection. 4 animals/group. Schematics showing the extent of the RVM, including raphe pallidus, can be found in Figure 18.

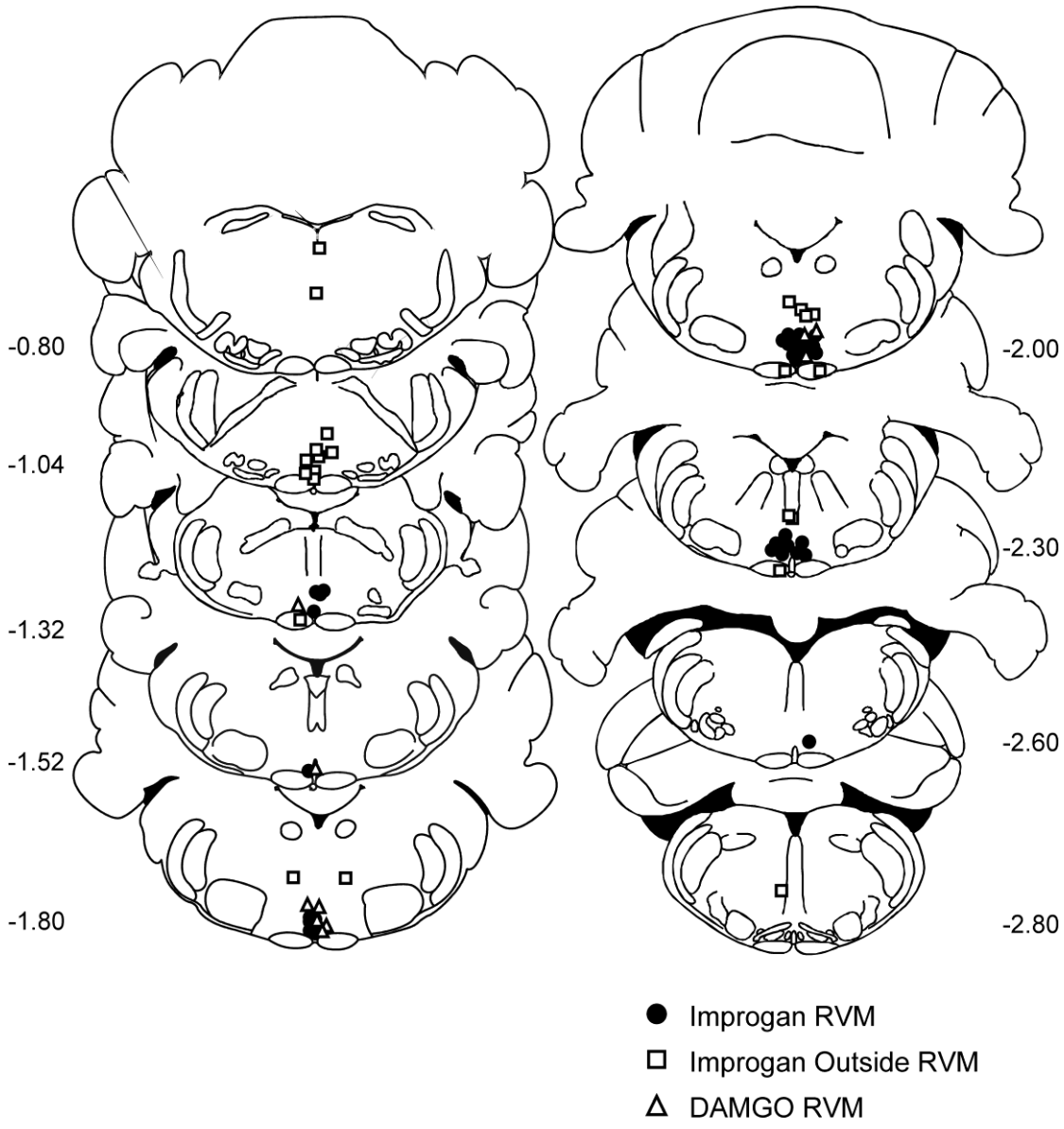
-0.80
-1.04
-1.32
-1.52
-1.80
-2.00
-2.30
-2.60
-2.80
Improgan RVM
Improgan Outside RVM
DAMGO RVM

Figure 18: Locations of improgan and DAMGO microinjection sites in and around the RVM.

There were 36 microinjections of improgan inside, and 23 outside, the RVM. Ten DAMGO microinjections were inside the RVM. Distances from lambda are indicated adjacent to each section. Sections adapted from Paxinos and Watson (1997). The RVM encompasses the ventromedial medulla at the level of the facial nucleus, ventral to a line drawn across the dorsal aspect of the facial nucleus and medial to the lateral edges of the pyramidal tracts.

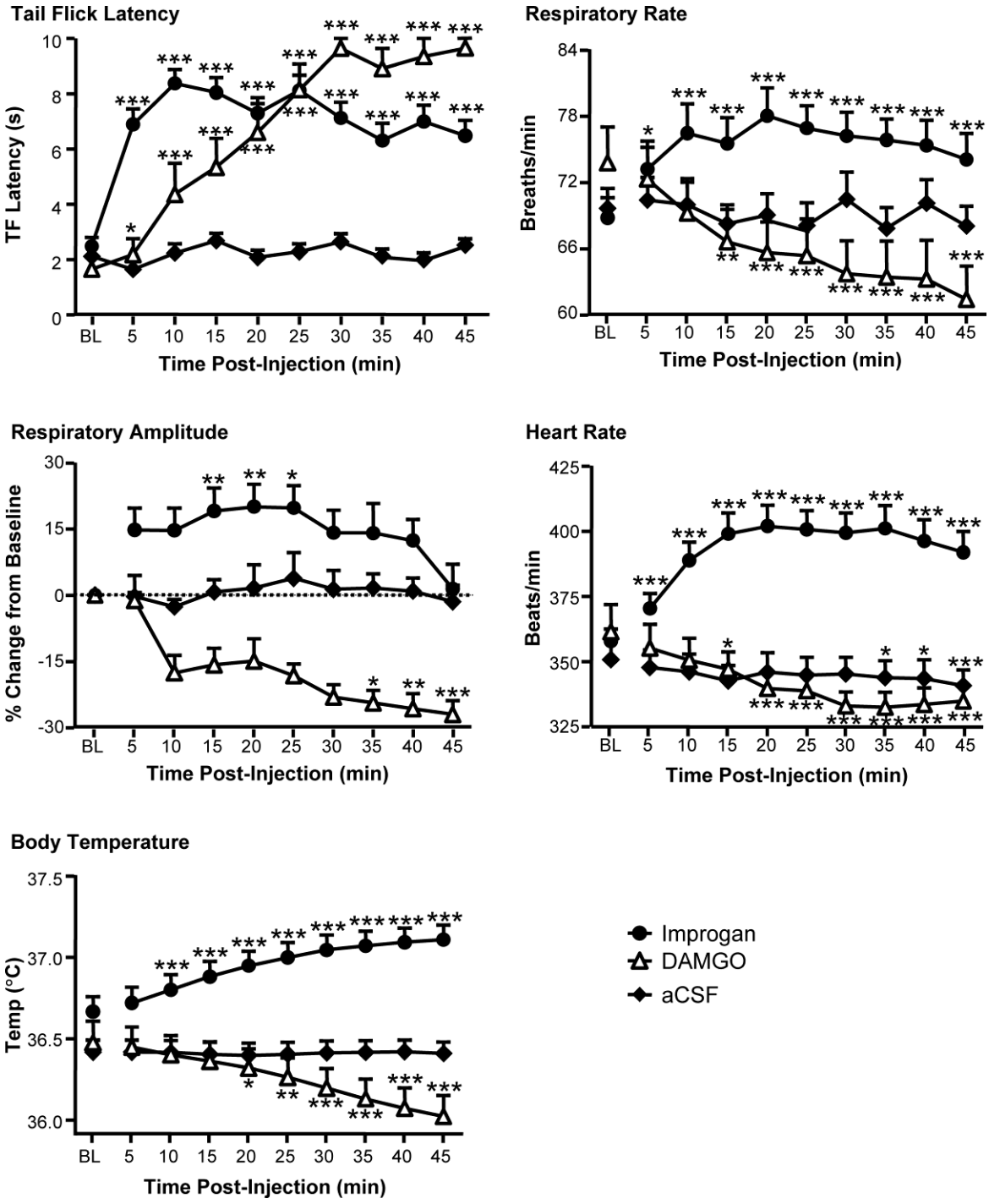
Tail Flick Latency
TF Latency (s)
Time Post-Injection (min)
Respiratory Rate
Breaths/min
Time Post-Injection (min)
Respiratory Amplitude
% Change from Baseline
Time Post-Injection (min)
Heart Rate
Beats/min
Time Post-Injection (min)
Body Temperature
Temp (°C)
Time Post-Injection (min)
Improgan
DAMGO
aCSF

Figure 19: Effects of improgan and DAMGO microinjections into the RVM on TF latency, respiratory rate, respiratory amplitude, heart rate, and body temperature.

Improgan and DAMGO were injected immediately following a three trials over a 15-min baseline (BL). There were no differences among groups in any of these parameters in baseline (one-way between-groups ANOVA, 10 – 36 animals/group). *$p < 0.05$, **$p < 0.01$, ***$p < 0.001$ compared to pre-injection baseline using repeated-measures ANOVA followed by Dunnett's test (respiratory rate, heart rate, body temperature) or Friedman's analysis of variance by ranks followed by a Dunn's test (respiratory amplitude).

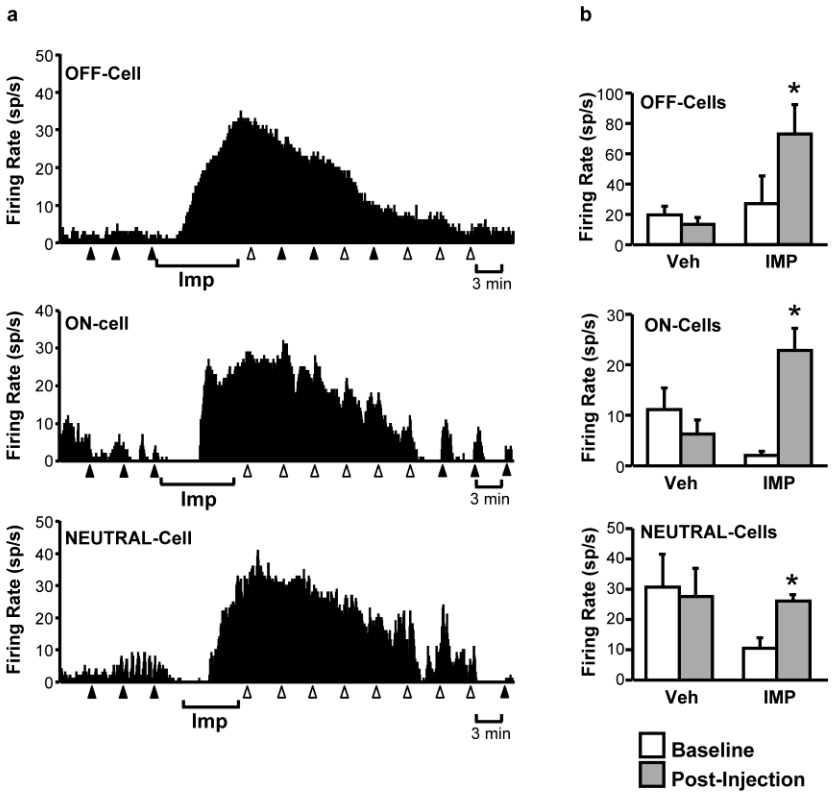
a
b
OFF-Cell
ON-cell
NEUTRAL-Cell
Firing Rate (sp/s)
Imp
3 min
OFF-Cells
ON-Cells
NEUTRAL-Cells
Veh
IMP
*
Baseline
Post-Injection

Figure 20: All RVM neuronal classes are activated following local application of the non-opioid analgesic improgan.

a. Ratemeter records showing firing rate (in spikes/s) of a typical OFF-cell, ON-cell and NEUTRAL-cell before and after local microinjection of improgan during the period indicated below the trace. Triangles indicate TF trials, with closed triangles indicating that the animal responded to the heat, open triangles that there was no response prior to the cut-off time.

b. Group data confirm that all three RVM cell classes exhibit an increase in firing rate following improgan, but not vehicle, microinjection. 6-8 cells/group, $*p < 0.05$ compared to pre-injection baseline, Wilcoxon's signed-ranks test.

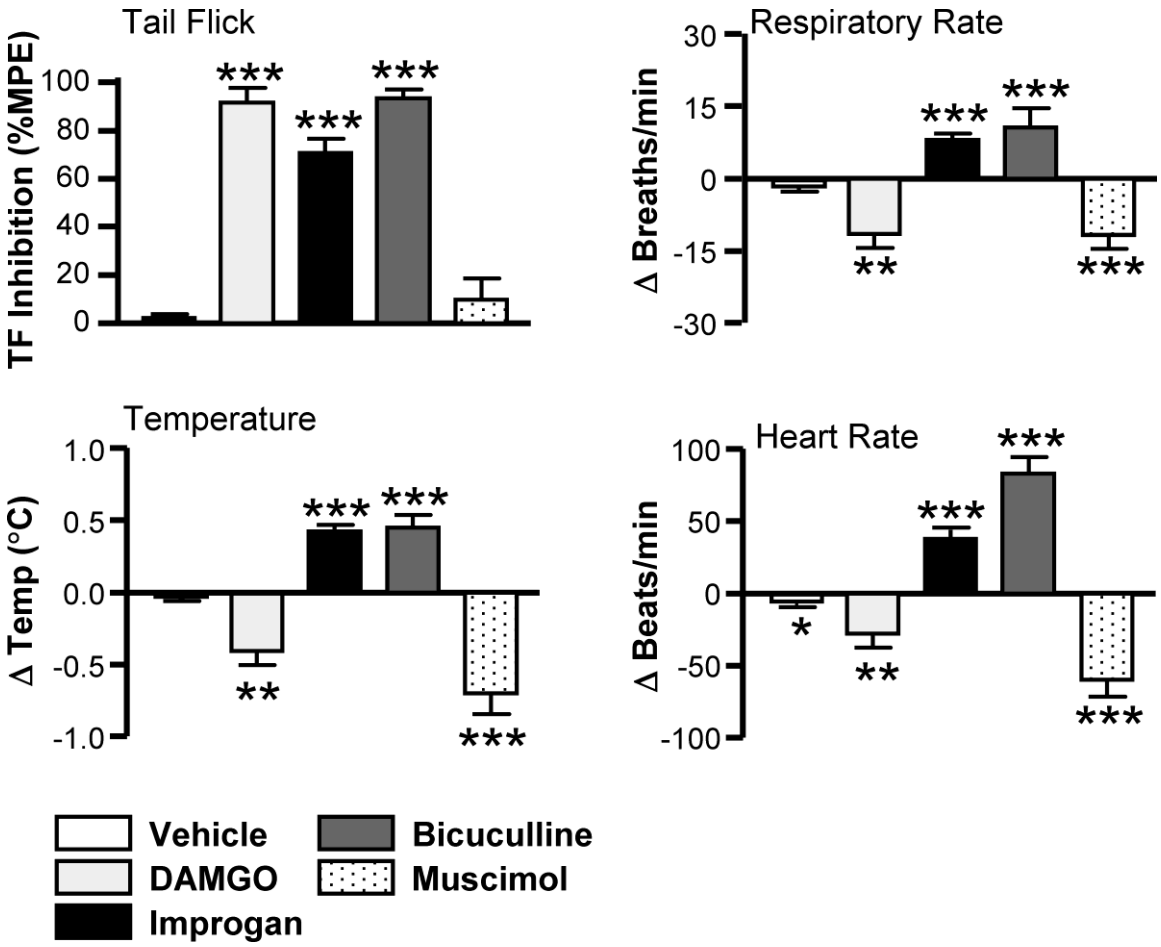
Tail Flick
TF Inhibition (%MPE)
100
80
60
40
20
0
***
***
***
Respiratory Rate
Δ Breaths/min
30
15
0
-15
-30
***
***
**
***
Temperature
Δ Temp (°C)
1.0
0.5
0.0
-0.5
-1.0
***
***
**
***
Heart Rate
Δ Beats/min
100
50
0
-50
-100
***
***
*
**
***
Vehicle
DAMGO
Improgan
Bicuculline
Muscimol

Figure 21: Effects of RVM improgan and DAMGO, compared to bicuculline and muscimol.

TF latency (expressed as percent maximum possible effect, %MPE), change in respiratory rate, change in heart rate, and change in body temperature. Each data set was analyzed using a 1-way ANOVA followed by a Dunnett's test for comparison to aCSF vehicle. 9 – 36 animals/group, $^{**}p < 0.01$, $^{***}p < 0.001$ compared to aCSF group.

CHAPTER 5

DISCUSSION

5.1 Key findings

- Acute inflammatory hyperalgesia is mediated by increased ON-cell activity, whereas sensitization of OFF-cells to stimuli is more important in chronic inflammatory hyperalgesia, which further illustrates that chronic pain is not a simple continuation of the acute condition.
- A novel method of recording respiratory rate and relative tidal volume (ventilatory pressure transduction) allows for improved monitoring of physiological parameters during stereotaxic experiments.
- Monitoring of respiration reveals RVM-mediated respiratory depression in conjunction with analgesia from opioid microinjection, as well the demonstration that such respiratory depression is separable from analgesia.
- Neurons controlling nociceptive, respiratory, cardiovascular, and thermogenic effects of opioids can be fluorescently labeled. The labeled neurons in the RVM and raphe regions are sufficient to affect all of the above physiological variables.

5.2 Overview

The RVM and surrounding regions is a key relay in multiple neural pathways capable of controlling or regulating many of the essential processes of the body, including somatosensory responsiveness, respiration, thermogenesis, and cardiovascular function. The two opioid-sensitive classes of RVM neurons have long been recognized as the drivers for bimodal nociceptive modulation, but the relationship between the cell activity and other functions of the RVM has not been well studied. Here I show that changes in either ON- or OFF-cell activity can separately contribute to the same behavior (hyperalgesia), and, despite the reciprocity of firing under normal conditions, ON- and OFF-cells have independent functions. Further evidence supporting this hypothesis is the correlation between ON-cell activity and other functions of the RVM, whereas OFF-cell activity is not similarly correlated.

5.3 RVM and behavioral manipulations show separation of neuronal function

5.3.1 ON- and OFF-cells respectively facilitate acute and chronic pain

The classical hypothesis of RVM-mediated descending modulation has been that the ON- and OFF-cells represent two aspects of gain control in a single system, such that ON-cells control increases in sensitivity and OFF-cells control decreases. In such a construction, the system would modulate nociceptive sensitivity by actively balancing opposing components. This idea is based on the physiological and pharmacological parallels of ON- and OFF-cells, especially the complementary firing patterns. However, this synchrony of ON- and OFF-cells may be part of a more widespread coordination. Grahn and Heller showed that RVM neuronal activity correlates well with changes in EEG, which are often associated with varying states of arousal or attention (Grahn and Heller 1989; Klimesch 1999; Pribram and McGuinness 1975). Activity of these cells is thus potentially a reflection of larger synchrony throughout the nervous system. Indeed, ON-like and OFF-like cells are seen in other areas of the nervous system, including the mesopontine tegmentum, PAG, and parabrachial areas (Carlson et al. 2005; Haws et al. 1989; Heinricher et al. 1987). Thus while ON- and OFF-cell activity may be synchronized, the neurons may have independent modulatory functions, including their effects on nociception.

Considerable evidence links RVM neurons to hypersensitivity, including in both acute and chronic inflammation. As acute inflammation progresses towards chronicity, changes occur in the RVM that reinforce and maintain the chronic pain state. However, the transition from an acute to a chronic pain condition is not a simple extension or prolongation of the acute response to injury. Rather, the transition to chronic pain involves changes at all levels of the nervous system, such that acute and chronic pain conditions are neurophysiologically distinct although behaviorally similar. In acute inflammation, ON-cell activity and descending facilitation mediates the acute increase in sensitivity, whereas in chronic inflammation a lack of descending inhibition from OFF-cells underlies the hyperalgesia. Much previous work had gone into the hypothesis that, with respect to the RVM, chronic pain is a prolongation or extension of the response to acute pain, and that the same elements were involved in both states. The

idea that a separation of RVM neuronal elements is the distinguishing factor between acute and chronic pain is a significant break from previous ideas on the subject and warrants a more detailed discussion.

The driving observation behind the idea of ON- and OFF-cell separation of function is the similarity of hyperalgesia that can arise from changes to either ON-cell or OFF-cell firing. In naïve animals, both non-selective inhibition of RVM neurons (including OFF-cells) and a selective increase in ON-cell activity produce a behaviorally similar decrease in thermal withdrawal threshold (Kincaid et al. 2006; Martenson et al. 2009; Neubert et al. 2004; Proudfit 1980b; Proudfit and Anderson 1975; Sandkühler and Gebhart 1984b). Although in the experiments shown here lidocaine injected into the RVM of normal animals did not significantly decrease the threshold (n=5, p=0.08), the effect is more distinctly seen in experiments with greater statistical power. Indeed, although muscimol injection in the RVM blocks DMH-mediated increases in heart rate and core temperature, the behavioral effect was indistinguishable between thermal hyperalgesia driven by increases in ON-cell activity and that from decreases in OFF-cell activity. However kynurenate, which selectively blocks ON-cell activity, did attenuate the thermal hyperalgesia. (Heinricher and Roychowdhury 1997; Martenson et al. 2009).

Similarly, mechanical hyperalgesia occurs with either increased ON-cell activity or decreased OFF-cell activity. After acute CFA injection, increased ON-cell activity drives mechanical hyperalgesia, whereas in the chronic state, the novel OFF-cell sensitivity to non-noxious stimulation removes the antinociceptive influence of OFF-cells, facilitating mechanical hyperalgesia. Again, either increased ON-cell activity or decreased OFF-cell activity can manifest as hyperalgesia. Since both ON- and OFF-cells are sensitized, the difference in contributions may depend on physiological factors other than just firing rate. One possible explanation is that descending inhibition and facilitation have separate effects at the output, in the dorsal horn of the spinal cord, such that the induction of a chronic pain state brings those differences to light. Descending modulation from the PAG shows selectivity for noxious vs. non-noxious stimuli as well as for dorsal horn neurons receiving C-fiber, A-δ, or A-β inputs (Waters and Lumb 2008; Waters and Lumb 1997;

Yeomans et al. 1996). However, the possibility that descending inhibition and facilitation can separately modulate dorsal horn neurons has not yet been evaluated.

5.3.2 OFF-cell mediated antihyperalgesia in chronic nerve injury and chronic inflammation

In consideration of the mechanism underlying hyperalgesia, mechanisms of anti-hyperalgesia must also be considered. Although ON-cell mediated facilitation has been implicated in persistent pain, removing ON-cell activity does not reverse the hyperalgesia in nerve injury (Figure 22, Appendix A), and descending inhibition from the RVM has been identified as the difference that determines whether such animals will manifest with hyperalgesia (Carlson et al. 2007; De Felice et al. 2011). Likewise in chronic inflammation, removing the descending facilitation does not reverse the hyperalgesia, but removing descending inhibition worsens it. Thus, OFF-cell activity may therefore be protective against hyperalgesia, and novel sensitivity of OFF-cells to non-noxious stimulation may contribute to persistent pain. Since inhibiting ON-cell activity does not reverse the hyperalgesia, they are less likely to be involved in the maintenance of persistent pain.

The expression of hyperalgesia can be fully reversed in both the nerve injury and chronic inflammation pain models by injection of neuropeptide Y (NPY) into the RVM (Figure 23, Appendix A)(Taylor et al. 2007). Although the underlying mechanism was originally suggested to be selective ON-cell inhibition, investigation shows that the neuronal effect of NPY in the RVM is to increase spontaneous activity of all classes of RVM neurons (Figure 24, Appendix A). Rather than a selective inhibition of ON-cells, hyperalgesia from models of persistent pain can be reversed by increasing OFF-cell activity. After injection, the modest inhibition of OFF-cells that occurs during non-noxious stimulation to an injured hindpaw would be obscured by the increased spontaneous activity. Therefore the antihyperalgesic effect of NPY could be through masking the pathological inhibition of OFF-cells and thus negating the sensitization of descending inhibition. These data further separate ON-cell activity from hyperalgesia in chronic pain, as NPY injected in the RVM produces anti-hyperalgesia even while increasing ON-cell activity (Figure 24, Appendix A).

5.3.3 ON-cell activity modulates acute responses to challenges to homeostasis

The idea that ON-cells facilitate nociceptive transmission in the acute but not chronic setting coincides with observations of behavioral manifestations of acute pain. Severe pain, such as from a burn or trauma, increases respiration, heart rate, and blood pressure (Hilgard and Morgan 1975). Although the severity of the injury does not change, these physiological effects fade in the minutes to hours after the insult, as does the urgency of the pain.

Increases and decreases in ON-cell activity correlate with physiological changes as well as nociceptive facilitation. With the pharmacological increases in ON-cell activity shown here, we see concurrent increases in heart rate, respiration, and core temperature, all physiological variables associated with acute pain or stress. Conversely, pharmacological inhibition of RVM neurons decreases heart rate, respiratory rate, and core temperature. Such pharmacological decreases in ON-cell firing occur in the absence of increased OFF-cell activity, which implies that the observed effects are not secondary to pain relief. Collectively, these data show a relationship between manipulations that change ON-cell activity and nociceptive facilitation, heart rate, respiration, and thermoregulation independent of OFF-cell activity. This observation is consistent with the idea of ON-cells modulating not just pain, but acute response to injury or challenge to homeostasis.

A caveat in the interpretation of these data is the possibility that OFF-cells have secondary effects aside from pain inhibition, but that these effects go unnoticed due to ON-cell activity being a stronger influence. To illustrate, the hyperalgesic effect of increased ON-cell activity is not notable if it occurs during increased OFF-cell firing, and the inhibition of both ON- and OFF-cell activity often results in a net behavioral hyperalgesia, despite the removal of the facilitatory ON-cell influence (Martenson et al. 2009). Thus increased ON-cell activity only results in a net change in somatic sensitivity if OFF-cells do not also change firing. With respect to the physiological changes from ON-cell activity, the possibility that OFF-cells also drive some physiological changes can not be ruled out, but the effects are minor relative to those from changes in ON-cell activity. To evaluate this possibility, a pharmacological or behavioral preparation

would be needed that selectively activates OFF-cells without concurrently changing ON-cells firing. Such a preparation has not yet been identified

These results collectively show a separation of nociceptive modulation by ON- and OFF-cells that becomes clear during comparison of RVM contributions to acute and chronic pain conditions. Multiple mechanisms of nociceptive modulation may overlap within a single area, as is seen with modes of thermogenesis (McAllen et al. 2010). The differences in nociceptive modulation seen here are distinct enough to warrant the consideration of separate effects on descending inhibition and descending facilitation. Interpretation of experiments with RVM manipulation should be considered in not just how the manipulations may affect the entire descending modulatory system, but how they could affect both descending inhibition (via OFF-cells) and facilitation (via ON-cells).

5.3.4 How specificity is achieved through non-specific responses

The defining characteristics of cells within the RVM, including some cells of raphe pallidus and rostral raphe obscurus, are their responses at the withdrawal from noxious stimuli: ON-cells increase firing, OFF-cells cease firing, and NEUTRAL cells do not change firing (Fields et al. 1983). All recorded cells of the RVM can thus be classified as one of these types, albeit undefined subtypes of cells may exist (Brink and Mason 2003). The finding that manipulations that selectively affect ON- and OFF-cells drive physiological changes leads to the conclusion that at least a subset of ON- and OFF- cells also influence heart rate, respiration, and core temperature.

From this conclusion, the question arises: in an area where many of the constituent neurons respond similarly to stimulation, how are the unique inputs and outputs organized? One possibility is that pain is just the broadest of the stimuli that drive changes in neuronal firing in the RVM, and other more specific paradigms may separate out subclasses of neurons. Behavioral evidence shows that some cold stimuli are more efficacious at eliciting certain types of thermogenic responses via the raphe nuclei, and these behavioral differences are confirmed through separation of upstream neural pathways (McAllen et al.

2010). If such labeled lines exist in the RVM, testing the animal with a greater diversity of homeostatic challenges, ranging from hypercapnia to hypothermia, may reveal separation of neuronal function.

Although the organization is not well understood, we can infer that having these modulatory pathways relay in an common area would allow for greater synchrony and coordination when a response is needed. Physical proximity is a controlling variable for information flow in the nervous system, and the wide branching dendritic arborizations of RVM neurons provide ample substrate for coordinated regulation (Mason et al. 1990; Potrebic and Mason 1993). Highly synchronized regulation of interconnected systems is common in the nervous system, as seen with the hyperemia that rapidly accompanies increased neuronal activity in the cortex (Logothetis et al. 2001). Such coordination of homeostatic processes would improve the physical response to challenge. For example, an increase in heart rate and core temperature in response to injury also increases the need for oxygenated blood, and waiting to increase ventilation until blood pH is decreased would be less efficient.

5.4 Technical considerations

An important caveat in the discussion of behavior and specificity of RVM neuronal activity is the influence of anesthesia. Criticisms of the use of anesthetic in behavioral studies on nociception are not uncommon, and the possibility of anesthesia confounding or masking responses should be considered. The properties of ON-, OFF-, and NEUTRAL-cells are comparable between awake animals, lightly anesthetized animals, and decerebrate/non-anesthetized animals, and behavioral effects of pharmacological manipulations in the lightly anesthetized animal parallel those seen in awake animals (Clarke et al. 1994; Fields et al. 2006; Oliveras et al. 1990; Oliveras et al. 1989). Also, freely behaving animals have other processes that introduce confounds into the interpretation of results, especially stress, fear, and anxiety, which involve many of the same neural pathways under consideration (Cannon et al. 1983; Fanselow 1991; Helmstetter 1992; Neugebauer et al. 2004). Further, studies of physiological regulation often have to be done in anesthetized animals, due to invasive methods of measurement.

These lines of evidence collectively support the validity of the lightly anesthetized animal for understanding the role of RVM neurons in pain modulation and physiology.

If anesthesia is a confound, the likely effects would be the blunting of ON-cells responses to stimulation, an increase in OFF-cell firing, or suppression of responsiveness of NEUTRAL cells to an unidentified stimulus. The function of NEUTRAL cells and the behavioral effects of anesthesia on NEUTRAL cell firing are not well studied. However, the possibly that ON-cell and OFF-cell responses are blunted or enhanced with anesthetic is also a real possibility (Jinks et al. 2004; Leung and Mason 1995). Light anesthesia shifts the behavioral responses to noxious stimulation, such that stronger responses are required to elicit the same response in anesthetized compared to waking animals (Carlson et al. 2007). Some reports in unanaesthetized animals indicate that neurons show responses to innocuous stimulation, although these responses are often still graded with the severity of the stimulation (Saade et al. 1982; Saade et al. 1983). Regardless, a shift in ON- and OFF-cell responsiveness does not significantly change the core of RVM physiology, but only widens the range of behavioral paradigms that may involve the RVM.

5.5 Future directions

5.5.1 Physiology of ON-, OFF-, and NEUTRAL cells

One of the most significant questions raised in this work is how the different effectors and pathways overlap at the level of the RVM, and whether the responses are organized through a single group of multimodal neurons or through segregated sets of neurons with single functions. In this thesis, I have established that the RVM neurons that control respiration, heart rate, and core temperature also respond to pharmacological manipulation in a manner consistent with that of ON-cells, and so these cells may be classified as ON-cells when encountered *in vivo*. A more in-depth investigation is warranted before definitively saying that all ON-cells are also thermo- or cardiomodulatory. One experiment to address the question of multimodality and classification of RVM neurons would be to combine the nociceptive testing with other physiological perturbations, such as hypercapnia or hypothermia. With a methodical protocol, some or even all of the cell classes of the RVM may be found to contain subclasses. A subclass of ON-cells

may exist that responds primarily to changes in skin temperature, and another subclass may respond only to hypercapnia. Alternatively, if ON-cells respond to each of the stimulus types, subclasses of cells may be distinguished by the magnitude of the response.

A corollary of this investigation is the question of whether cells outside the traditional boundaries of the RVM would also respond to noxious stimuli in a manner consistent with ON- and OFF-cells. Cell responses to a change in arousal at the withdrawal from noxious stimulation may be a distinct characteristic of cells in all of the raphe nuclei or may only be seen in areas related to pain modulation. To address this hypothesis, I would test use nociceptive testing to evaluate reactions of neurons in the raphe pallidus and raphe obscurus.

5.5.2 Reversal of neuropathic pain in waking animals

In our experiments in anesthetized animals, non-selective inhibition of RVM neurons worsens hyperalgesia in rats with either nerve injury or persistent inflammation. This result contrasts to work from multiple laboratories showing that in waking animals RVM inhibition reverses or attenuates the hyperalgesia (Porreca et al. 2001; Taylor et al. 2007; Vera-Portocarrero et al. 2006b). Our results run counter to the hypothesis that ON-cell sensitization drives persistence of pain in chronic nerve injury. The obvious difference is the use of anesthesia, as either the use or lack of anesthesia can be a significant confounding factor in evaluating behavior. In awake animals, learning, anxiety, and fear all can contribute to nociceptive modulation, factors which are eliminated in the anesthetized animal. Alternatively, the differences between our results and others' may be due to the rat strains used, the experimental protocol, or an environmental cause. To address these differences, I propose implanting RVM cannula in animals with nerve injury and testing whether RVM inhibition reverses hyperalgesia. If in our hands RVM inhibition does reverse hyperalgesia in waking animals, then some function related to conscious perception of pain may be the cause. One way to get at the circuit behind this difference would be through selective lesion of candidate sites that project to the RVM, such as the DMH, MPO, or PAG, followed by repeated testing after RVM inhibition.

5.5.3 Identification of μ-opioid receptor expressing RVM neurons

A major impediment to the understanding of connections of the RVM has been the difficulty of identifying classes of RVM neurons in *ex vivo* preparations. RVM neurons are classified by their characteristic response at the withdrawal from noxious stimuli, which means that an intact nervous system is required for unambiguous identification. Although progress has been made in identifying cell types in slice based on the responses to opioids, a visual marker of the cell classes has been lacking (Sykes et al. 2007; Zhang et al. 2006). Here, I show that injection of a fluorescently labeled μ-opioid agonist (Dermorphin-Alexa488) discretely labels RVM neurons, and this labeling is attenuated by the pre-treatment with a μ-opioid antagonist. This result is promising as a potential marker for ON-cells, but further work is still needed to validate its use *in vitro*. I propose two experiments that will help histologically confirm the use of this compound as a marker for ON-cells. First is a comparison of cell labeling using Dermorphin-Alexa488 against that of another labeled agonist, CCK-Alexa555. CCK directly activates ON-cells, so I hypothesize that a significant overlap will exist between cells that label with CCK-Alexa555 and those that label with Dermorphin-Alexa488. A second experiment would be to compare the distribution of labeled RVM neurons from Dermorphin-Alexa488 with that of an immunohistochemical marker. Staining for phosphorylated-ERK (pERK), an activated MAP kinase, has been suggested as a way to identify ON-cells after acute injury. A significant overlap of the labeling from Dermorphin-Alexa488 with that of pERK would further confirm the use of both pERK and Dermorpin-Alexa488 as identifiers of ON-cells.

5.6 Summary of findings

In this thesis, I detail how multiple pathways use physiologically similar neurons within a small area of the brainstem as a coordination point for responses to homeostatic challenges. Neuronal responses to acute injury are separate from the maladaptive changes that occur during chronic pain conditions. RVM-mediated nociceptive facilitation, tachycardia, hyperthermia, and tachypnea have common factors, including the activation of ON-cells and a common upstream site for the initiation of effects (DMH). OFF-

cell activity has fewer parallels with these physiological changes, indicating that descending inhibition of nociception can be modulated separately from descending facilitation. Understanding the behavioral paradigms and neural relays involved in ON- and OFF-cell nociceptive modulation will continue to elucidate the separability of the RVM mediated functions, leading to improved treatment for acute and chronic pain with fewer side effects.

REFERENCES

Abols IA, and Basbaum AI. Afferent connections of the rostral medulla of the cat: a neural substrate for midbrain-medullary interactions in the modulation of pain. *Journal of Comparative Neurology* 201: 285-297, 1981.

Adams JE. Naloxone reversal of analgesia produced by brain stimulation in the human. *Pain* 2: 161-166, 1976.

Alhaider AA, Lei SZ, and Wilcox GL. Spinal 5-HT3 receptor-mediated antinociception: possible release of GABA. *Journal of Neuroscience* 11: 1881-1888, 1991.

Arttamangkul S, Alvarez-Maubecin V, Thomas G, Williams JT, and Grandy DK. Binding and internalization of fluorescent opioid peptide conjugates in living cells. *Molecular pharmacology* 58: 1570-1580, 2000.

Arttamangkul S, Quillinan N, Low MJ, von Zastrow M, Pintar J, and Williams JT. Differential activation and trafficking of micro-opioid receptors in brain slices. *Molecular pharmacology* 74: 972-979, 2008.

Baba H, Doubell TP, and Woolf CJ. Peripheral inflammation facilitates Abeta fiber-mediated synaptic input to the substantia gelatinosa of the adult rat spinal cord. *J Neurosci* 19: 859-867., 1999.

Bacon SJ, Zagon A, and Smith AD. Electron microscopic evidence of a monosynaptic pathway between cells in the caudal raphe nuclei and sympathetic preganglionic neurons in the rat spinal cord. *Experimental brain research Experimentelle Hirnforschung* 79: 589-602, 1990.

Bago M, Marson L, and Dean C. Serotonergic projections to the rostroventrolateral medulla from midbrain and raphe nuclei. *Brain research* 945: 249-258, 2002.

Bandler R, and Shipley MT. Columnar organization in the midbrain periaqueductal gray: modules for emotional expression? *Trends in Neurosciences* 17: 379-389, 1994.

Bar-Yishay E. Whole-body plethysmography. The human factor. *Chest* 135: 1412-1414, 2009.

Barbaro NM, Heinricher MM, and Fields HL. Putative nociceptive modulatory neurons in the rostral ventromedial medulla of the rat display highly correlated firing patterns. *Somatosensory and Motor Research* 6: 413-425, 1989.

Barbaro NM, Heinricher MM, and Fields HL. Putative pain modulating neurons in the rostral ventral medulla: reflex-related activity predicts effects of morphine. *Brain Res* 366: 203-210, 1986.

Bartolo A, Dzwonczyk RR, Roberts C, and Goldman E. Description and validation of a technique for the removal of ECG contamination from diaphragmatic EMG signal. *Medical & biological engineering & computing* 34: 76-81, 1996.

Basbaum AI, Clanton CH, and Fields HL. Opiate and stimulus-produced analgesia: functional anatomy of a medullospinal pathway. *Proceedings of the National Academy of Sciences of the United States of America* 73: 4685-4688, 1976.

Basbaum AI, Clanton CH, and Fields HL. Three bulbospinal pathways from the rostral medulla of the cat: an autoradiographic study of pain modulating systems. *Journal of Comparative Neurology* 178: 209-224, 1978.

Basbaum AI, and Fields HL. Endogenous pain control mechanisms: review and hypothesis. *Annals of Neurology* 4: 451-462, 1978.

Basbaum AI, and Fields HL. Endogenous pain control systems: brainstem spinal pathways and endorphin circuitry. *Annual review of neuroscience* 7: 309-338, 1984.

Basbaum AI, and Fields HL. The origin of descending pathways in the dorsolateral funiculus of the spinal cord of the cat and rat: further studies on the anatomy of pain modulation. *Journal of Comparative Neurology* 187: 513-531, 1979.

Bederson JB, Fields HL, and Barbaro NM. Hyperalgesia during naloxone-precipitated withdrawal from morphine is associated with increased on-cell activity in the rostral ventromedial medulla. *Somatosensory and Motor Research* 7: 185-203, 1990.

Beig MI, Baumert M, Walker FR, Day TA, and Nalivaiko E. Blockade of 5-HT2A receptors suppresses hyperthermic but not cardiovascular responses to psychosocial stress in rats. *Neuroscience* 159: 1185-1191, 2009.

Beitz AJ, Mullett MA, and Weiner LL. The periaqueductal gray projections to the rat spinal trigeminal, raphe magnus, gigantocellular pars alpha and paragigantocellular nuclei arise from separate neurons. *Brain research* 288: 307-314, 1983.

Berner NJ, Grahn DA, and Heller HC. 8-OH-DPAT-sensitive neurons in the nucleus raphe magnus modulate thermoregulatory output in rats. *Brain research* 831: 155-164., 1999.

Bhavani-Shankar K, Moseley H, Kumar AY, and Delph Y. Capnometry and anaesthesia. *Canadian journal of anaesthesia = Journal canadien d'anesthesie* 39: 617-632, 1992.

Bland JM, and Altman DG. Agreement between methods of measurement with multiple observations per individual. *Journal of biopharmaceutical statistics* 17: 571-582, 2007.

Bland JM, and Altman DG. Measuring agreement in method comparison studies. *Statistical methods in medical research* 8: 135-160, 1999.

Bland JM, and Altman DG. Statistical methods for assessing agreement between two methods of clinical measurement. *Lancet* 1: 307-310, 1986.

Blessing WW, and Nalivaiko E. Raphe magnus/pallidus neurons regulate tail but not mesenteric arterial blood flow in rats. *Neuroscience* 105: 923-929., 2001.

Borgbjerg FM, Nielsen K, and Franks J. Experimental pain stimulates respiration and attenuates morphine-induced respiratory depression: a controlled study in human volunteers. *Pain* 64: 123-128, 1996.

Brazier MAB, and Hobson JA editors. *The reticular formation revisited*. New York: Raven Press, 1980, p. 552.

Brink TS, and Mason P. Raphe magnus neurons respond to noxious colorectal distension. *Journal of neurophysiology* 89: 2506-2515, 2003.

Brink TS, Pacharinsak C, Khasabov SG, Beitz AJ, and Simone DA. Differential modulation of neurons in the rostral ventromedial medulla by neurokinin-1 receptors. *Journal of neurophysiology* 107: 1210-1221, 2012.

Burgess SE, Gardell LR, Ossipov MH, Malan TP, Jr., Vanderah TW, Lai J, and Porreca F. Time-dependent descending facilitation from the rostral ventromedial medulla maintains, but does not initiate, neuropathic pain. *Journal of Neuroscience* 22: 5129-5136, 2002.

Cameron AA, Khan IA, Westlund KN, Cliffer KD, and Willis WD. The efferent projections of the periaqueductal gray in the rat: a Phaseolus vulgaris-leucoagglutinin study. I. Ascending projections. *Journal of Comparative Neurology* 351: 568-584, 1995a.

Cameron AA, Khan IA, Westlund KN, and Willis WD. The efferent projections of the periaqueductal gray in the rat: a Phaseolus vulgaris-leucoagglutinin study. II. Descending projections. *Journal of Comparative Neurology* 351: 585-601, 1995b.

Campbell C, Weinger MB, and Quinn M. Alterations in diaphragm EMG activity during opiate-induced respiratory depression. *Respiration physiology* 100: 107-117, 1995.

Cannon JT, Lewis JW, Weinberg VE, and Liebeskind JC. Evidence for the independence of brainstem mechanisms mediating analgesia induced by morphine and two forms of stress. *Brain research* 269: 231-236, 1983.

Cao WH, Fan W, and Morrison SF. Medullary pathways mediating specific sympathetic responses to activation of dorsomedial hypothalamus. *Neuroscience* 126: 229-240, 2004.

Cao WH, and Morrison SF. Disinhibition of rostral raphe pallidus neurons increases cardiac sympathetic nerve activity and heart rate. *Brain research* 980: 1-10, 2003.

Carlson JD, Maire JJ, Martenson ME, and Heinricher MM. Sensitization of pain-modulating neurons in the rostral ventromedial medulla after peripheral nerve injury. *Journal of Neuroscience* 27: 13222-13231, 2007.

Carlson JD, Selden NR, and Heinricher MM. Nocifensive reflex-related on- and off-cells in the pedunculopontine tegmental nucleus, cuneiform nucleus, and lateral dorsal tegmental nucleus. *Brain research* 1063: 187-194, 2005.

Carrive P, Churyukanov M, and Le Bars D. A reassessment of stress-induced "analgesia" in the rat using an unbiased method. *Pain* 152: 676-686, 2011.

Carry PY, Baconnier P, Eberhard A, Cotte P, and Benchetrit G. Evaluation of respiratory inductive plethysmography: accuracy for analysis of respiratory waveforms. *Chest* 111: 910-915, 1997.

Cetas JS, Lee DR, Alkayed NJ, Wang R, Iliff JJ, and Heinricher MM. Brainstem control of cerebral blood flow and application to acute vasospasm following experimental subarachnoid hemorrhage. *Neuroscience* 163: 719-729, 2009.

Clarke RW, Morgan MM, and Heinricher MM. Identification of nocifensor reflex-related neurons in the rostroventromedial medulla of decerebrated rats. *Brain research* 636: 169-174, 1994.

Cleary DR, Neubert MJ, and Heinricher MM. Are opioid-sensitive neurons in the rostral ventromedial medulla inhibitory interneurons? *Neuroscience* 151: 564-571, 2008.

Cleary DR, Phillips RS, Wallisch M, and Heinricher MM. A novel, non-invasive method of respiratory monitoring for use with stereotactic procedures. *Journal of neuroscience methods* 209: 337-343, 2012.

Coggins CR, Duchosal F, Musy C, and Ventrone R. Measurement of respiratory patterns in rodents using whole-body plethysmography and a pneumotachograph. *Laboratory animals* 15: 137-140, 1981.

Colman Y, and Krauss B. Microstream capnograpy technology: a new approach to an old problem. *Journal of clinical monitoring and computing* 15: 403-409, 1999.

Corcoran AE, Hodges MR, Wu Y, Wang W, Wylie CJ, Deneris ES, and Richerson GB. Medullary serotonin neurons and central CO2 chemoreception. *Respiratory physiology & neurobiology* 168: 49-58, 2009.

Coutinho SV, Urban MO, and Gebhart GF. Role of glutamate receptors and nitric oxide in the rostral ventromedial medulla in visceral hyperalgesia. *Pain* 78: 59-69, 1998.

Cumming G. The body plethysmorgraph. *Postgraduate medical journal* 37: 257-258, 1961.

Da Silva LF, Desantana JM, and Sluka KA. Activation of NMDA receptors in the brainstem, rostral ventromedial medulla, and nucleus reticularis gigantocellularis mediates mechanical hyperalgesia produced by repeated intramuscular injections of acidic saline in rats. *Journal of Pain* 11: 378-387, 2010a.

Da Silva LF, Walder RY, Davidson BL, Wilson SP, and Sluka KA. Changes in expression of NMDA-NR1 receptor subunits in the rostral ventromedial medulla modulate pain behaviors. *Pain* 151: 155-161, 2010b.

Dampney RA. Functional organization of central pathways regulating the cardiovascular system. *Physiological Reviews* 74: 323-364, 1994.

De Felice M, Sanoja R, Wang R, Vera-Portocarrero L, Oyarzo J, King T, Ossipov MH, Vanderah TW, Lai J, Dussor GO, Fields HL, Price TJ, and Porreca F. Engagement of descending inhibition from the rostral ventromedial medulla protects against chronic neuropathic pain. *Pain* 2011.

Dean JB, and Nattie EE. Central CO2 chemoreception in cardiorespiratory control. *Journal of Applied Physiology* 108: 976-978, 2010.

Depuy SD, Kanbar R, Coates MB, Stornetta RL, and Guyenet PG. Control of breathing by raphe obscurus serotonergic neurons in mice. *Journal of Neuroscience* 31: 1981-1990, 2011.

Devonshire IM, Preston MJ, Dommett EJ, Murphy KL, and Greenfield SA. Design and evaluation of a low-cost respiratory monitoring device for use with anaesthetized animals. *Laboratory animals* 43: 382-389, 2009.

Di Scala G, Mana MJ, Jacobs WJ, and Phillips AG. Evidence of Pavlovian conditioned fear following electrical stimulation of the periaqueductal grey in the rat. *Physiology & behavior* 40: 55-63, 1987.

Dias MB, Li A, and Nattie E. Focal CO2 dialysis in raphe obscurus does not stimulate ventilation but enhances the response to focal CO2 dialysis in the retrotrapezoid nucleus. *Journal of Applied Physiology* 105: 83-90, 2008.

Dias MB, Nucci TB, Branco LG, and Gargaglioni LH. Opioid mu-receptors in the rostral medullary raphe modulate hypoxia-induced hyperpnea in unanesthetized rats. *Acta physiologica (Oxford, England)* 204: 435-442, 2012.

Dias MB, Nucci TB, Margatho LO, Antunes-Rodrigues J, Gargaglioni LH, and Branco LG. Raphe magnus nucleus is involved in ventilatory but not hypothermic response to CO2. *Journal of Applied Physiology* 103: 1780-1788, 2007.

DiMicco JA, Samuels BC, Zaretskaia MV, and Zaretsky DV. The dorsomedial hypothalamus and the response to stress: part renaissance, part revolution. *Pharmacology, biochemistry, and behavior* 71: 469-480, 2002.

Dreshaj IA, Haxhiu MA, and Martin RJ. Role of the medullary raphe nuclei in the respiratory response to CO2. *Respiration physiology* 111: 15-23, 1998.

Dubois AB, Botelho SY, Bedell GN, Marshall R, and Comroe JH, Jr. A rapid plethysmographic method for measuring thoracic gas volume: a comparison with a nitrogen washout method for measuring functional residual capacity in normal subjects. *The Journal of clinical investigation* 35: 322-326, 1956a.

Dubois AB, Botelho SY, and Comroe JH, Jr. A new method for measuring airway resistance in man using a body plethysmograph: values in normal subjects and in patients with respiratory disease. *The Journal of clinical investigation* 35: 327-335, 1956b.

Duggan AW, Griersmith BT, Headley PM, and Maher JB. The need to control skin temperature when using radiant heat in tests of analgesia. *Experimental neurology* 61: 471-478, 1978.

Dutschmann M, Menuet C, Stettner GM, Gestreau C, Borghgraef P, Devijver H, Gielis L, Hilaire G, and Van Leuven F. Upper airway dysfunction of Tau-P301L mice correlates with tauopathy in midbrain and ponto-medullary brainstem nuclei. *Journal of Neuroscience* 30: 1810-1821, 2010.

Enhorning G, van Schaik S, Lundgren C, and Vargas I. Whole-body plethysmography, does it measure tidal volume of small animals? *Canadian journal of physiology and pharmacology* 76: 945-951, 1998.

Fanselow MS. The midbrain periaqueductal gray as a coordinator of action in response to fear and anxiety. In: *The midbrain periaqueductal gray matter*, edited by DePaulis A, and Bandler R. New York: Plenum, 1991, p. 151-173.

Feldman JL, Mitchell GS, and Nattie EE. Breathing: rhythmicity, plasticity, chemosensitivity. *Annual review of neuroscience* 26: 239-266, 2003.

Fields H. State-dependent opioid control of pain. *Nature Reviews Neuroscience* 5: 565-575, 2004.

Fields HL. Is there a facilitating component to central pain modulation? *APS Journal* 1: 71-78, 1992.

Fields HL, Barbaro NM, and Heinricher MM. Brain stem neuronal circuitry underlying the antinociceptive action of opiates. *Progress in Brain Research* 77: 245-257, 1988.

Fields HL, and Basbaum AI. Brainstem control of spinal pain-transmission neurons. *Annual Review of Physiology* 40: 217-248, 1978.

Fields HL, Basbaum AI, Clanton CH, and Anderson SD. Nucleus raphe magnus inhibition of spinal cord dorsal horn neurons. *Brain research* 126: 441-453, 1977.

Fields HL, Basbaum AI, and Heinricher MM. Central nervous system mechanisms of pain modulation. In: *Wall and Melzack's Textbook of Pain, 5th ed*, edited by McMahon S, and Koltzenburg M. London: Elsevier, 2006, p. 125-142.

Fields HL, Bry J, Hentall I, and Zorman G. The activity of neurons in the rostral medulla of the rat during withdrawal from noxious heat. *Journal of Neuroscience* 3: 2545-2552, 1983.

Fields HL, and Heinricher MM. Anatomy and physiology of a nociceptive modulatory system. *Philos Trans of the R Soc Lond B Biol Sci* 308: 361-374, 1985.

Fields HL, Malick A, and Burstein R. Dorsal horn projection targets of ON and OFF cells in the rostral ventromedial medulla. *Journal of neurophysiology* 74: 1742-1759, 1995.

Gebhart GF, Sandkühler J, Thalhammer JG, and Zimmermann M. Inhibition of spinal nociceptive information by stimulation in midbrain of the cat is blocked by lidocaine microinjected in nucleus raphe magnus and medullary reticular formation. *Journal of neurophysiology* 50: 1446-1459, 1983.

Glaab T, Taube C, Braun A, and Mitzner W. Invasive and noninvasive methods for studying pulmonary function in mice. *Respiratory research* 8: 63, 2007.

Godal A, Belenky DA, Standaert TA, Woodrum DE, Grimsrud L, and Hodson WA. Application of the hot-wire anemometer to respiratory measurements in small animal. *Journal of Applied Physiology* 40: 275-277, 1976.

Grahn DA, and Heller HC. Activity of most rostral ventromedial medulla neurons reflect EEG/EMG pattern changes. *American journal of physiology* 257: R1496-1505, 1989.

Gray AM, Pache DM, and Sewell RD. Do alpha2-adrenoceptors play an integral role in the antinociceptive mechanism of action of antidepressant compounds? *European Journal of Pharmacology* 378: 161-168, 1999.

Gray PA, Janczewski WA, Mellen N, McCrimmon DR, and Feldman JL. Normal breathing requires preBotzinger complex neurokinin-1 receptor-expressing neurons. *Nature neuroscience* 4: 927-930, 2001.

Guan Y, Guo W, Robbins MT, Dubner R, and Ren K. Changes in AMPA receptor phosphorylation in the rostral ventromedial medulla after inflammatory hyperalgesia in rats. *Neuroscience Letters* 366: 201-205, 2004.

Guan Y, Guo W, Zou S-P, Dubner R, and Ren K. Inflammation-induced upregulation of AMPA receptor subunit expression in brain stem pain modulatory circuitry. *Pain* 104: 401-413, 2003.

Guan Y, Terayama R, Dubner R, and Ren K. Plasticity in excitatory amino acid receptor-mediated descending pain modulation after inflammation. *The Journal of pharmacology and experimental therapeutics* 300: 513-520., 2002.

Guo W, Robbins MT, Wei F, Zou S, Dubner R, and Ren K. Supraspinal brain-derived neurotrophic factor signaling: a novel mechanism for descending pain facilitation. *Journal of Neuroscience* 26: 126-137, 2006.

Guyenet PG, Stornetta RL, and Bayliss DA. Central respiratory chemoreception. *The Journal of comparative neurology* 518: 3883-3906, 2010.

Guyenet PG, Stornetta RL, and Bayliss DA. Retrotrapezoid nucleus and central chemoreception. *The Journal of physiology* 586: 2043-2048, 2008.

Hammond DL, Tyce GM, and Yaksh TL. Efflux of 5-hydroxytryptamine and noradrenaline into spinal cord superfusates during stimulation of the rat medulla. *Journal of Physiology* 359: 151-162, 1985.

Hantos Z, and Brusasco V. Assessment of respiratory mechanics in small animals: the simpler the better? *Journal of Applied Physiology* 93: 1196-1197, 2002.

Harasawa I, Fields HL, and Meng ID. Delta opioid receptor mediated actions in the rostral ventromedial medulla on tail flick latency and nociceptive modulatory neurons. *Pain* 85: 255-262, 2000.

Hassen AH, Feuerstein G, and Faden AI. Differential cardiovascular effects mediated by mu and kappa opiate receptors in hindbrain nuclei. *Peptides* 4: 621-625, 1983.

Haws CM, Williamson AM, and Fields HL. Putative nociceptive modulatory neurons in the dorsolateral pontomesencephalic reticular formation. *Brain research* 483: 272-282, 1989.

Hayashida S, Oka T, Mera T, and Tsuji S. Repeated social defeat stress induces chronic hyperthermia in rats. *Physiology & behavior* 101: 124-131, 2010.

Heinricher MM, Barbaro NM, and Fields HL. Putative nociceptive modulating neurons in the rostral ventromedial medulla of the rat: firing of on- and off-cells is related to nociceptive responsiveness. *Somatosensory and Motor Research* 6: 427-439, 1989.

Heinricher MM, Cheng ZF, and Fields HL. Evidence for two classes of nociceptive modulating neurons in the periaqueductal gray. *Journal of Neuroscience* 7: 271-278, 1987.

Heinricher MM, and Ingram SL. The brainstem and nociceptive modulation. In: *The Senses, A Comprehensive Reference, Vol 5, Pain*, edited by Bushnell MC, and Basbaum AI. San Diego: Academic Press, 2008, p. 593-626.

Heinricher MM, and Kaplan HJ. GABA-mediated inhibition in rostral ventromedial medulla: role in nociceptive modulation in the lightly anesthetized rat. *Pain* 47: 105-113, 1991.

Heinricher MM, Maire JJ, Lee D, Nalwalk JW, and Hough LB. Physiological basis for inhibition of morphine and improgan antinociception by CC12, a P450 epoxygenase inhibitor. *Journal of neurophysiology* 104: 3222-3230, 2010a.

Heinricher MM, Martenson ME, Nalwalk JW, and Hough LB. Neural basis for improgan antinociception. *Neuroscience* 169: 1414-1420, 2010b.

Heinricher MM, Martenson ME, and Neubert MJ. Prostaglandin E_2 in the midbrain periaqueductal gray produces hyperalgesia and activates pain-modulating circuitry in the rostral ventromedial medulla. *Pain* 110: 419-426, 2004.

Heinricher MM, Morgan MM, and Fields HL. Direct and indirect actions of morphine on medullary neurons that modulate nociception. *Neuroscience* 48: 533-543, 1992.

Heinricher MM, Morgan MM, Tortorici V, and Fields HL. Disinhibition of off-cells and antinociception produced by an opioid action within the rostral ventromedial medulla. *Neuroscience* 63: 279-288, 1994.

Heinricher MM, and Neubert MJ. Neural basis for the hyperalgesic action of cholecystokinin in the rostral ventromedial medulla. *Journal of neurophysiology* 92: 1982-1989, 2004.

Heinricher MM, and Roychowdhury SM. Reflex-related activation of putative pain facilitating neurons in rostral ventromedial medulla requires excitatory amino acid transmission. *Neuroscience* 78: 1159-1165, 1997.

Heinricher MM, Tavares I, Leith JL, and Lumb BM. Descending control of nociception: specificity, recruitment and plasticity. *Brain Research Reviews* 60: 214-225, 2009.

Hellman KM, Brink TS, and Mason P. Activity of Murine Raphe Magnus Cells Predicts Tachypnea and On-Going Nociceptive Responsiveness. *Journal of neurophysiology* 98: 3121-3133, 2007.

Hellman KM, Mendelson SJ, Mendez-Duarte MA, Russell JL, and Mason P. Opioid microinjection into raphe magnus modulates cardiorespiratory function in mice and rats. *American journal of physiology* 297: R1400-1408, 2009.

Helmstetter FJ. Contribution of the amygdala to learning and performance of conditional fear. *Physiology and Behavior* 51: 1271-1276, 1992.

Henry JL, and Calaresu FR. Responses of single units in the intermediolateral nucleus to stimulation of cardioregulatory medullary nuclei in the cat. *Brain Res* 77: 314-319, 1974.

Hilaire G, Voituron N, Menuet C, Ichiyama RM, Subramanian HH, and Dutschmann M. The role of serotonin in respiratory function and dysfunction. *Respiratory physiology & neurobiology* 174: 76-88, 2010.

Hilgard ER, and Morgan AH. Heart rate and blood pressure in the study of laboratory pain in man under normal conditions and as influenced by hypnosis. *Acta neurobiologiae experimentalis* 35: 741-759, 1975.

Hodges MR, Klum L, Leekley T, Brozoski DT, Bastasic J, Davis S, Wenninger JM, Feroah TR, Pan LG, and Forster HV. Effects on breathing in awake and sleeping goats of focal acidosis in the medullary raphe. *J Appl Physiol* 96: 1815-1824, 2004.

Hodges MR, and Richerson GB. Contributions of 5-HT neurons to respiratory control: neuromodulatory and trophic effects. *Respiratory physiology & neurobiology* 164: 222-232, 2008.

Hodges PW, Heijnen I, and Gandevia SC. Postural activity of the diaphragm is reduced in humans when respiratory demand increases. *The Journal of physiology* 537: 999-1008, 2001.

Hole K, and Tjolsen A. The tail-flick and formalin tests in rodents: changes in skin temperature as a confounding factor. *Pain* 53: 247-254, 1993.

Holtman JR, Jr., Anastasi NC, Norman WP, and Dretchen KL. Effect of electrical and chemical stimulation of the raphe obscurus on phrenic nerve activity in the cat. *Brain research* 362: 214-220, 1986.

Holtman JR, Jr., Norman WP, and Gillis RA. Projections from the raphe nuclei to the phrenic motor nucleus in the cat. *Neuroscience Letters* 44: 105-111, 1984.

Horn EM, and Waldrop TG. Suprapontine control of respiration. *Respiration physiology* 114: 201-211, 1998.

Hosobuchi Y, Adams JE, and Linchitz R. Pain relief by electrical stimulation of the central gray matter in humans and its reversal by naloxone. *Science (New York, NY* 197: 183-186, 1977.

Hosogai M, Matsuo S, Sibahara T, and Kawai Y. Projection of respiratory neurons in rat medullary raphe nuclei to the phrenic nucleus. *Respiration physiology* 112: 37-50., 1998.

Huckstepp RT, and Dale N. Redefining the components of central CO2 chemosensitivity--towards a better understanding of mechanism. *The Journal of physiology* 589: 5561-5579, 2011.

Hurley RW, and Hammond DL. The analgesic effects of supraspinal μ and δ opioid receptor agonists are potentiated during persistent inflammation. *Journal of Neuroscience* 20: 1249-1259, 2000.

Imbe H, Kimura A, Okamoto K, Donishi T, Aikawa F, Senba E, and Tamai Y. Activation of ERK in the rostral ventromedial medulla is involved in hyperalgesia during peripheral inflammation. *Brain research* 1187: 103-110, 2008.

Imbe H, Okamoto K, Okamura T, Kumabe S, Nakatsuka M, Aikawa F, Iwai-Liao Y, and Senba E. Effects of peripheral inflammation on activation of ERK in the rostral ventromedial medulla. *Brain research* 1063: 151-158, 2005.

Jacky JP. A plethysmograph for long-term measurements of ventilation in unrestrained animals. *J Appl Physiol* 45: 644-647, 1978.

Jacobs BL, and Fornal CA. Activity of brain serotonergic neurons in the behaving animal. *Pharmacological Reviews* 43: 563-578, 1991.

Jacobs BL, Martin-Cora FJ, and Fornal CA. Activity of medullary serotonergic neurons in freely moving animals. *Brain Research Reviews* 40: 45-52, 2002.

Jinks SL, Carstens E, and Antognini JF. Isoflurane differentially modulates medullary ON and OFF neurons while suppressing hind-limb motor withdrawals. *Anesthesiology* 100: 1224-1234, 2004.

Kamei J, Ohsawa M, Hayashi SS, and Nakanishi Y. Effect of chronic pain on morphine-induced respiratory depression in mice. *Neuroscience* 174: 224-233, 2011.

Kaplan H, and Fields HL. Hyperalgesia during acute opioid abstinence: evidence for a nociceptive facilitating function of the rostral ventromedial medulla. *Journal of Neuroscience* 11: 1433-1439, 1991.

Kerman IA. Organization of brain somatomotor-sympathetic circuits. *Experimental brain research Experimentelle Hirnforschung* 187: 1-16, 2008.

Kincaid W, Neubert MJ, Xu M, Kim CJ, and Heinricher MM. Role for medullary pain facilitating neurons in secondary thermal hyperalgesia. *Journal of neurophysiology* 95: 33-41, 2006.

Klimesch W. EEG alpha and theta oscillations reflect cognitive and memory performance: a review and analysis. *Brain research* 29: 169-195, 1999.

LaGraize SC, Guo W, Yang K, Wei F, Ren K, and Dubner R. Spinal cord mechanisms mediating behavioral hyperalgesia induced by neurokinin-1 tachykinin receptor activation in the rostral ventromedial medulla. *Neuroscience* 171: 1341-1356, 2010.

Lalley PM. Mu-opioid receptor agonist effects on medullary respiratory neurons in the cat: evidence for involvement in certain types of ventilatory disturbances. *American journal of physiology* 285: R1287-1304, 2003.

Lalley PM. Opiate slowing of feline respiratory rhythm and effects on putative medullary phase-regulating neurons. *American journal of physiology* 290: R1387-1396, 2006.

Lalley PM. Serotoninergic and non-serotoninergic responses of phrenic motoneurones to raphe stimulation in the cat. *The Journal of physiology* 380: 373-385, 1986.

Lanier WL, Iaizzo PA, Milde JH, and Sharbrough FW. The cerebral and systemic effects of movement in response to a noxious stimulus in lightly anesthetized dogs. Possible modulation of cerebral function by muscle afferents. *Anesthesiology* 80: 392-401, 1994.

LeBars D. Serotonin and pain. In: *Neuronal serotonin*, edited by Osborne NN, and Hamond M. New York: Wiley, 1988, p. 171-226.

Leung CG, and Mason P. Effects of isoflurane concentration on the activity of pontomedullary raphe and medial reticular neurons in the rat. *Brain research* 699: 71-82, 1995.

Leung CG, and Mason P. Physiological properties of raphe magnus neurons during sleep and waking. *Journal of neurophysiology* 81: 584-595, 1999.

Light AR. The spinal terminations of single, physiologically characterized axons originating in the pontomedullary raphe of the cat. *Journal of Comparative Neurology* 234: 536-548, 1985.

Light AR, Casale EJ, and Menetrey DM. The effects of focal stimulation in nucleus raphe magnus and periaqueductal gray on intracellularly recorded neurons in spinal laminae I and II. *Journal of neurophysiology* 56: 555-571, 1986.

Light AR, and Kavookjian AM. The ultrastructure and synaptic connections of the spinal terminations from single, physiologically characterized axons descending in the dorsolateral funiculus from the midline, pontomedullary region. *Journal of Comparative Neurology* 234: 549-560, 1985.

Lindsey BG, Segers LS, Morris KF, Hernandez YM, Saporta S, and Shannon R. Distributed actions and dynamic associations in respiratory-related neuronal assemblies of the ventrolateral medulla and brain stem midline: evidence from spike train analysis. *Journal of neurophysiology* 72: 1830-1851, 1994.

Loewy AD. Raphe pallidus and raphe obscurus projections to the intermediolateral cell column in the rat. *Brain Res* 222: 129-133, 1981.

Logothetis NK, Pauls J, Augath M, Trinath T, and Oeltermann A. Neurophysiological investigation of the basis of the fMRI signal. *Nature* 412: 150-157, 2001.

Lovick TA. The medullary raphe nuclei: a system for integration and gain control in autonomic and somatomotor responsiveness? *Experimental physiology* 82: 31-41, 1997.

Lundsgaard JS, Gronlund J, and Einer-Jensen N. Evaluation of a constant-temperature hot-wire anemometer for respiratory-gas-flow measurements. *Medical & biological engineering & computing* 17: 211-215, 1979.

Luukko M, Konttinen Y, Kemppinen P, and Pertovaara A. Influence of various experimental parameters on the incidence of thermal and mechanical hyperalgesia induced by a constriction mononeuropathy of the sciatic nerve in lightly anesthetized rats. *Experimental neurology* 128: 143-154, 1994.

Luukko M, and Pertovaara A. Influence of an experimental peripheral mononeuropathy on the responses of medial bulboreticular neurons to noxious skin stimulation and the modulation of the

responses by an alpha 2-adrenoceptor agonist in the rat. *Experimental neurology* 124: 390-394, 1993.

Madden CJ, and Morrison SF. Excitatory amino acid receptors in the dorsomedial hypothalamus mediate prostaglandin-evoked thermogenesis in brown adipose tissue. *American journal of physiology* 286: R320-325, 2004.

Madden CJ, and Morrison SF. Hypoxic activation of arterial chemoreceptors inhibits sympathetic outflow to brown adipose tissue in rats. *Journal of Physiology* 566: 559-573, 2005.

Manzke T, Guenther U, Ponimaskin EG, Haller M, Dutschmann M, Schwarzacher S, and Richter DW. 5-HT4(a) receptors avert opioid-induced breathing depression without loss of analgesia. *Science (New York, NY* 301: 226-229, 2003.

Marcinkiewcz CA, Green MK, Devine DP, Duarte P, Vierck CJ, and Yezierski RP. Social defeat stress potentiates thermal sensitivity in operant models of pain processing. *Brain research* 1251: 112-120, 2009.

Martenson M, Houts J, Heinricher M, and Ogden B. A simple device for humidification of inspired gases during volatile anesthesia in rats. *Contemporary topics in laboratory animal science / American Association for Laboratory Animal Science* 44: 46-48, 2005.

Martenson ME, Cetas JS, and Heinricher MM. A possible neural basis for stress-induced hyperalgesia. *Pain* 142: 236-244, 2009.

Mason P. From descending pain modulation to obesity via the medullary raphe. *Pain* 152: S20-24, 2011.

Mason P. Physiological identification of pontomedullary serotonergic neurons in the rat. *Journal of neurophysiology* 77: 1087-1098, 1997.

Mason P, Floeter MK, and Fields HL. Somatodendritic morphology of on- and off-cells in the rostral ventromedial medulla. *Journal of Comparative Neurology* 301: 23-43, 1990.

Mason P, Gao K, and Genzen JR. Serotonergic Raphe Magnus Cell Discharge Reflects Ongoing Autonomic and Respiratory Activities. *Journal of neurophysiology* 98: 1919-1927, 2007.

Mayer DJ, and Liebeskind JC. Pain reduction by focal electrical stimulation of the brain: an anatomical and behavioral analysis. *Brain research* 68: 73-93., 1974.

McAllen RM, Tanaka M, Ootsuka Y, and McKinley MJ. Multiple thermoregulatory effectors with independent central controls. *European journal of applied physiology* 109: 27-33, 2010.

McDowall LM, Horiuchi J, and Dampney RA. Effects of disinhibition of neurons in the dorsomedial hypothalamus on central respiratory drive. *American journal of physiology* 293: R1728-1735, 2007.

McGaraughty S, Reinis S, and Tsoukatos J. Investigating the role of anaesthetics on the rostral ventromedial medulla: implications for a GABAergic link between ON and OFF cells. *Neuroscience Letters* 149: 119-122, 1993a.

McGaraughty S, Reinis S, and Tsoukatos J. Two distinct unit activity responses to morphine in the rostral ventromedial medulla of awake rats. *Brain research* 604: 331-333, 1993b.

McMullan S, Simpson DAA, and Lumb BM. A reliable method for the preferential activation of C- or A-fibre heat nociceptors. *Journal of neuroscience methods* 138: 133-139, 2004.

McQuay HJ. Potential problems of using both opioids and local anaesthetic. *British journal of anaesthesia* 61: 121, 1988.

Menuet C, Borghgraef P, Matarazzo V, Gielis L, Lajard AM, Voituron N, Gestreau C, Dutschmann M, Van Leuven F, and Hilaire G. Raphe tauopathy alters serotonin metabolism and breathing activity in

terminal Tau.P301L mice: possible implications for tauopathies and Alzheimer's disease. *Respiratory physiology & neurobiology* 178: 290-303, 2011.

Miki K, Zhou QQ, Guo W, Guan Y, Terayama R, Dubner R, and Ren K. Changes in gene expression and neuronal phenotype in brain stem pain modulatory circuitry after inflammation. *Journal of neurophysiology* 87: 750-760, 2002.

Millhorn DE. Stimulation of raphe (obscurus) nucleus causes long-term potentiation of phrenic nerve activity in cat. *The Journal of physiology* 381: 169-179, 1986.

Miyawaki T, Goodchild AK, and Pilowsky PM. Activation of mu-opioid receptors in rat ventrolateral medulla selectively blocks baroreceptor reflexes while activation of delta opioid receptors blocks somato-sympathetic reflexes. *Neuroscience* 109: 133-144, 2002.

Mokha SS, McMillan JA, and Iggo A. Pathways mediating descending control of spinal nociceptive transmission from the nuclei locus coeruleus (LC) and raphe magnus (NRM) in the cat. *Experimental brain research Experimentelle Hirnforschung* 61: 597-606, 1986.

Montagne-Clavel J, and Oliveras JL. Are ventromedial medulla neuronal properties modified by chronic peripheral inflammation? A single-unit study in the awake, freely moving polyarthritic rat. *Brain research* 657: 92-104, 1994.

Montandon G, Qin W, Liu H, Ren J, Greer JJ, and Horner RL. PreBotzinger complex neurokinin-1 receptor-expressing neurons mediate opioid-induced respiratory depression. *J Neurosci* 31: 1292-1301, 2011a.

Montandon G, Qin W, Liu H, Ren J, Greer JJ, and Horner RL. PreBotzinger complex neurokinin-1 receptor-expressing neurons mediate opioid-induced respiratory depression. *Journal of Neuroscience* 31: 1292-1301, 2011b.

Morel A, Rouiller E, de Ribaupierre Y, and de Ribaupierre F. Tonotopic organization in the medial geniculate body (MGB) of lightly anesthetized cats. *Experimental brain research Experimentelle Hirnforschung* 69: 24-42, 1987.

Morrison S. Central neural pathways for thermoregulatory cold defense. *Journal of Applied Physiology* 110: 1137-1149, 2011.

Morrison SF. Central pathways controlling brown adipose tissue thermogenesis. *News Physiol Sci* 19: 67-74, 2004.

Morrison SF. Raphe pallidus excites a unique class of sympathetic preganglionic neurons. *American journal of physiology* 265: R82-89., 1993.

Morrison SF. Raphe pallidus neurons mediate prostaglandin E2-evoked increases in brown adipose tissue thermogenesis. *Neuroscience* 121: 17-24, 2003.

Morrison SF, and Nakamura K. Central neural pathways for thermoregulation. *Frontiers in Biosciences* 16: 74-104, 2011.

Mulkey DK, Rosin DL, West G, Takakura AC, Moreira TS, Bayliss DA, and Guyenet PG. Serotonergic Neurons Activate Chemosensitive Retrotrapezoid Nucleus Neurons by a pH-Independent Mechanism. *Journal of Neuroscience* 27: 14128-14138, 2007.

Mustapic S, Radocaj T, Sanchez A, Dogas Z, Stucke AG, Hopp FA, Stuth EA, and Zuperku EJ. Clinically relevant infusion rates of mu-opioid agonist remifentanil cause bradypnea in decerebrate dogs but not via direct effects in the pre-Botzinger complex region. *Journal of neurophysiology* 103: 409-418, 2010.

Nakamura K, Matsumura K, Hubschle T, Nakamura Y, Hioki H, Fujiyama F, Boldogkoi Z, Konig M, Thiel HJ, Gerstberger R, Kobayashi S, and Kaneko T. Identification of sympathetic premotor neurons

in medullary raphe regions mediating fever and other thermoregulatory functions. *Journal of Neuroscience* 24: 5370-5380, 2004.

Nakamura K, and Morrison SF. Central efferent pathways mediating skin cooling-evoked sympathetic thermogenesis in brown adipose tissue. *American journal of physiology* 292: R127-136, 2007.

Nalwalk JW, Svokos K, Taraschenko O, Leurs R, Timmerman H, and Hough LB. Activation of brain stem nuclei by improgan, a non-opioid analgesic. *Brain research* 1021: 248-255, 2004.

Nason MW, Jr., and Mason P. Medullary Raphe Neurons Facilitate Brown Adipose Tissue Activation. *Journal of Neuroscience* 26: 1190-1198, 2006.

Nattie E. Julius H. Comroe, Jr., distinguished lecture: central chemoreception: then ... and now. *Journal of Applied Physiology* 110: 1-8, 2011.

Nattie E, and Li A. Central chemoreception is a complex system function that involves multiple brain stem sites. *Journal of Applied Physiology* 106: 1464-1466, 2009.

Nattie E, and Li A. CO2 dialysis in the medullary raphe of the rat increases ventilation in sleep. *Journal of Applied Physiology* 90: 1247-1257., 2001.

Nettleton RT, Wallisch M, and Olsen GD. Respiratory effects of chronic in utero methadone or morphine exposure in the neonatal guinea pig. *Neurotoxicology and teratology* 30: 448-454, 2008.

Neubert MJ, Kincaid W, and Heinricher MM. Nociceptive facilitating neurons in the rostral ventromedial medulla. *Pain* 110: 158-165, 2004.

Neugebauer V, Li W, Bird GC, and Han JS. The amygdala and persistent pain. *Neuroscientist* 10: 221-234, 2004.

Nickerson JW, and Attaran A. The inadequate treatment of pain: collateral damage from the war on drugs. *PLoS Med* 9: e1001153, 2012.

O'Neil JJ, and Raub JA. Pulmonary function testing in small laboratory mammals. *Environmental health perspectives* 56: 11-22, 1984.

Okun A, DeFelice M, Eyde N, Ren J, Mercado R, King T, and Porreca F. Transient inflammation-induced ongoing pain is driven by TRPV1 sensitive afferents. *Molecular pain* 7: 4, 2011.

Oliveras JL, Guilbaud G, and Besson JM. A map of serotoninergic structures involved in stimulation producing analgesia in unrestrained freely moving cats. *Brain research* 164: 317-322, 1979.

Oliveras JL, Martin G, Montagne J, and Vos B. Single unit activity at ventromedial medulla level in the awake, freely moving rat: effects of noxious heat and light tactile stimuli onto convergent neurons. *Brain research* 506: 19-30, 1990.

Oliveras JL, Vos B, Martin G, and Montagne J. Electrophysiological properties of ventromedial medulla neurons in response to noxious and non-noxious stimuli in the awake, freely moving rat: a single-unit study. *Brain research* 486: 1-14, 1989.

Ootsuka Y, and Blessing WW. Inhibition of medullary raphe/parapyramidal neurons prevents cutaneous vasoconstriction elicited by alerting stimuli and by cold exposure in conscious rabbits. *Brain Res* 2005.

Orem J, and Trotter RH. Medullary respiratory neuronal activity during augmented breaths in intact unanesthetized cats. *Journal of Applied Physiology* 74: 761-769, 1993.

Palecek F. Measurement of ventilatory mechanics in the rat. *Journal of Applied Physiology* 27: 149-156, 1969.

Pan ZZ, Williams JT, and Osborne PB. Opioid actions on single nucleus raphe magnus neurons from rat and guinea-pig *in vitro*. *Journal of Physiology* 427: 519-532, 1990.

Pattinson KT, Governo RJ, MacIntosh BJ, Russell EC, Corfield DR, Tracey I, and Wise RG. Opioids depress cortical centers responsible for the volitional control of respiration. *Journal of Neuroscience* 29: 8177-8186, 2009.

Paxinos G, and Watson C. *The Rat Brain in Stereotaxic Coordinates*. Sydney: Academic Press, 1997.

Pertovaara A, Keski-vakkuri U, Kalmari J, Wei H, and Panula P. Response properties of neurons in the rostroventromedial medulla of neuropathic rats: attempted modulation of responses by [1DMe]NPYF, a neuropeptide FF analogue. *Neuroscience* 2001: 457-468, 2001.

Pertovaara A, Wei H, and Hamalainen MM. Lidocaine in the rostroventromedial medulla and the periaqueductal gray attenuates allodynia in neuropathic rats. *Neuroscience Letters* 218: 127-130, 1996.

Pilowsky PM, Miyawaki T, Minson JB, Sun QJ, Arnolda LF, Llewellyn-Smith IJ, and Chalmers JP. Bulbospinal sympatho-excitatory neurons in the rat caudal raphe. *Journal of hypertension* 13: 1618-1623, 1995.

Porreca F, Burgess SE, Gardell LR, Vanderah TW, Malan TP, Jr., Ossipov MH, Lappi DA, and Lai J. Inhibition of neuropathic pain by selective ablation of brainstem medullary cells expressing the μ-opioid receptor. *Journal of Neuroscience* 21: 5281-5288, 2001.

Porreca F, Ossipov MH, and Gebhart GF. Chronic pain and medullary descending facilitation. *Trends in Neuroscience* 25: 319-325, 2002.

Potrebic SB, Fields HL, and Mason P. Serotonin immunoreactivity is contained in one physiological cell class in the rat rostral ventromedial medulla. *Journal of Neuroscience* 14: 1655-1665, 1994.

Potrebic SB, and Mason P. Three-dimensional analysis of the dendritic domains of on- and off-cells in the rostral ventromedial medulla. *The Journal of comparative neurology* 337: 83-93, 1993.

Pribram KH, and McGuinness D. Arousal, activation, and effort in the control of attention. *Psychological review* 82: 116-149, 1975.

Proudfit HK. Effects of raphe magnus and raphe pallidus lesions on morphine-induced analgesia and spinal cord monoamines. *Pharmacology, Biochemistry and Behavior* 13: 705-714, 1980a.

Proudfit HK. Reversible inactivation of raphe magnus neurons: effects on nociceptive threshold and morphine-induced analgesia. *Brain research* 201: 459-464, 1980b.

Proudfit HK, and Anderson EG. Morphine analgesia: blockade by raphe magnus lesions. *Brain research* 98: 612-618, 1975.

Ramirez F, and Vanegas H. Tooth pulp stimulation advances both medullary off-cell pause and tail flick. *Neuroscience Letters* 100: 153-156, 1989.

Randich A, Mebane H, Deberry JJ, and Ness TJ. Rostral Ventral Medulla Modulation of the Visceromotor Reflex Evoked by Urinary Bladder Distension in Female Rats. *Journal of Pain* 2008.

Rathner JA, Madden CJ, and Morrison SF. Central pathway for spontaneous and prostaglandin E2-evoked cutaneous vasoconstriction. *American journal of physiology* 295: R343-354, 2008.

Rathner JA, Owens NC, and McAllen RM. Cold-activated raphe-spinal neurons in rats. *Journal of Physiology* 535: 841-854, 2001.

Reed JL, Pouget P, Qi HX, Zhou Z, Bernard MR, Burish MJ, Haitas J, Bonds AB, and Kaas JH. Widespread spatial integration in primary somatosensory cortex. *Proc Natl Acad Sci U S A* 105: 10233-10237, 2008.

Ren K, and Dubner R. Descending modulation in persistent pain: an update. *Pain* 100: 1-6, 2002.

Ren K, and Dubner R. Enhanced descending modulation of nociception in rats with persistent hindpaw inflammation. *Journal of neurophysiology* 76: 3025-3037, 1996.

Ren K, and Dubner R. NMDA receptor antagonists attenuate mechanical hyperalgesia in rats with unilateral inflammation of the hindpaw. *Neuroscience Letters* 163: 22-26, 1993.

Ren K, Hylden JL, Williams GM, Ruda MA, and Dubner R. The effects of a non-competitive NMDA receptor antagonist, MK-801, on behavioral hyperalgesia and dorsal horn neuronal activity in rats with unilateral inflammation. *Pain* 50: 331-344., 1992.

Reynolds DV. Surgery in the rat during electrical analgesia induced by focal brain stimulation. *Science (New York, NY* 164: 444-445, 1969.

Rice CD, Lois JH, Kerman IA, and Yates BJ. Localization of serotoninergic neurons that participate in regulating diaphragm activity in the cat. *Brain research* 1279: 71-81, 2009.

Richardson DE, and Akil H. Pain reduction by electrical brain stimulation in man. Part 1: Acute administration in periaqueductal and periventricular sites. *Journal of Neurosurgery* 47: 178-183, 1977.

Roberts J, Ossipov MH, and Porreca F. Glial activation in the rostroventromedial medulla promotes descending facilitation to mediate inflammatory hypersensitivity. *The European journal of neuroscience* 30: 229-241, 2009.

Saadé NE, and Jabbur SJ. Nociceptive behavior in animal models for peripheral neuropathy: Spinal and supraspinal mechanisms. *Progress in neurobiology* 86: 22-47, 2008.

Saade NE, Jundi AS, Jabbur SJ, and Banna NR. Dorsal column input to inferior raphe centralis neurons. *Brain research* 250: 345-348, 1982.

Saade NE, Salibi NA, Banna NR, Towe AL, and Jabbur SJ. Spinal input pathways affecting the medullary gigantocellular reticular nucleus. *Experimental neurology* 80: 582-600, 1983.

Samuels BC, Zaretsky DV, and DiMicco JA. Dorsomedial hypothalamic sites where disinhibition evokes tachycardia correlate with location of raphe-projecting neurons. *American journal of physiology* 287: R472-478, 2004.

Samuels BC, Zaretsky DV, and DiMicco JA. Tachycardia evoked by disinhibition of the dorsomedial hypothalamus in rats is mediated through medullary raphe. *The Journal of physiology* 538: 941-946, 2002.

Sandkuhler J. The organization and function of endogenous antinociceptive systems. *Progress in neurobiology* 50: 49-81, 1996.

Sandkuhler J, Fu QG, and Zimmermann M. Spinal pathways mediating tonic or stimulation-produced descending inhibition from the periaqueductal gray or nucleus raphe magnus are separate in the cat. *Journal of neurophysiology* 58: 327-341, 1987.

Sandkühler J, and Gebhart GF. Characterization of inhibition of a spinal nociceptive reflex by stimulation medially and laterally in the midbrain and medulla in the pentobarbital-anesthetized rat. *Brain research* 305: 67-76, 1984a.

Sandkühler J, and Gebhart GF. Relative contributions of the nucleus raphe magnus and adjacent medullary reticular formation to the inhibition by stimulation in the periaqueductal gray of a spinal nociceptive reflex in the pentobarbital-anesthetized rat. *Brain research* 305: 77-87, 1984b.

Sanoja R, Tortorici V, Fernandez C, Price TJ, and Cervero F. Role of RVM neurons in capsaicin-evoked visceral nociception and referred hyperalgesia. *European journal of pain (London, England)* 14: 120 e121-129, 2010.

Sanoja R, Vanegas H, and Tortorici V. Critical Role of the Rostral Ventromedial Medulla in Early Spinal Events Leading to Chronic Constriction Injury Neuropathy in Rats. *Journal of Pain* 2008.

Schepers RJ, Mahoney JL, and Shippenberg TS. Inflammation-induced changes in rostral ventromedial medulla mu and kappa opioid receptor mediated antinociception. *Pain* 136: 320-330, 2008.

Sorkin LS, McAdoo DJ, and Willis WD. Raphe magnus stimulation-induced antinociception in the cat is associated with release of amino acids as well as serotonin in the lumbar dorsal horn. *Brain research* 618: 95-108, 1993.

Spoelstra EN, Ince C, Koeman A, Emons VM, Brouwer LA, van Luyn MJ, Westerink BH, and Remie R. A novel and simple method for endotracheal intubation of mice. *Laboratory animals* 41: 128-135, 2007.

Steffey MA, Brosnan RJ, and Steffey EP. Assessment of halothane and sevoflurane anesthesia in spontaneously breathing rats. *American journal of veterinary research* 64: 470-474, 2003.

Stein C, Millan MJ, and Herz A. Unilateral inflammation of the hindpaw in rats as a model of prolonged noxious stimulation: alterations in behavior and nociceptive thresholds. *Pharmacology, biochemistry, and behavior* 31: 455-451, 1988.

Strack AM, Sawyer WB, Platt KB, and Loewy AD. CNS cell groups regulating the sympathetic outflow to adrenal gland as revealed by transneuronal cell body labeling with pseudorabies virus. *Brain research* 491: 274-296, 1989.

Stromberg NO, Dahlback GO, and Gustafsson PM. Evaluation of various models for respiratory inductance plethysmography calibration. *Journal of Applied Physiology* 74: 1206-1211, 1993.

Stucke AG, Zuperku EJ, Sanchez A, Tonkovic-Capin M, Tonkovic-Capin V, Mustapic S, and Stuth EA. Opioid receptors on bulbospinal respiratory neurons are not activated during neuronal depression by clinically relevant opioid concentrations. *Journal of neurophysiology* 100: 2878-2888, 2008.

Subramanian HH, and Holstege G. Midbrain and medullary control of postinspiratory activity of the crural and costal diaphragm in vivo. *Journal of neurophysiology* 105: 2852-2862, 2011.

Sugiyo S, Takemura M, Dubner R, and Ren K. Trigeminal transition zone/rostral ventromedial medulla connections and facilitation of orofacial hyperalgesia after masseter inflammation in rats. *The Journal of comparative neurology* 493: 510-523, 2005.

Sykes KT, White SR, Hurley RW, Mizoguchi H, Tseng LF, and Hammond DL. Mechanisms responsible for the enhanced antinociceptive effects of mu-opioid receptor agonists in the rostral ventromedial medulla of male rats with persistent inflammatory pain. *The Journal of pharmacology and experimental therapeutics* 322: 813-821, 2007.

Taylor BK, Abhyankar SS, Vo N-TT, Kriedt CL, Churi SB, and Urban JH. Neuropeptide Y acts at Y1 receptors in the rostral ventral medulla to inhibit neuropathic pain. *Pain* 131: 83-95, 2007.

Taylor NC, Li A, and Nattie EE. Ventilatory effects of muscimol microdialysis into the rostral medullary raphe region of conscious rats. *Respiratory physiology & neurobiology* 153: 203-216, 2006.

Terayama R, Guan Y, Dubner R, and Ren K. Activity-induced plasticity in brain stem pain modulatory circuitry after inflammation. *Neuroreport* 11: 1915-1919, 2000.

Torsney C. Inflammatory pain unmasks heterosynaptic facilitation in lamina I neurokinin 1 receptor-expressing neurons in rat spinal cord. *Journal of Neuroscience* 31: 5158-5168, 2011.

Urban MO, Coutinho SV, and Gebhart GF. Involvement of excitatory amino acid receptors and nitric oxide in the rostral ventromedial medulla in modulating secondary hyperalgesia produced by mustard oil. *Pain* 81: 45-55, 1999a.

Urban MO, Zahn PK, and Gebhart GF. Descending facilitatory influences from the rostral medial medulla mediate secondary, but not primary hyperalgesia in the rat. *Neuroscience* 90: 349-352, 1999b.

Vanegas H, Barbaro NM, and Fields HL. Tail-flick related activity in medullospinal neurons. *Brain research* 321: 135-141, 1984.

Vanegas H, and Schaible H-G. Descending control of persistent pain: inhibitory or facilitatory? *Brain Research Reviews* 46: 295-309, 2004.

Vaughan CW, McGregor IS, and Christie MJ. Cannabinoid receptor activation inhibits GABAergic neurotransmission in rostral ventromedial medulla neurons *in vitro*. *British Journal of Pharmacology* 127: 935-940., 1999.

Veasey SC, Fornal CA, Metzler CW, and Jacobs BL. Response of serotonergic caudal raphe neurons in relation to specific motor activities in freely moving cats. *Journal of Neuroscience* 15: 5346-5359, 1995.

Vera-Portocarrero LP, Xie JY, Kowal J, Ossipov MH, King T, and Porreca F. Descending facilitation from the rostral ventromedial medulla maintains visceral pain in rats with experimental pancreatitis. *Gastroenterology* 130: 2155-2164, 2006a.

Vera-Portocarrero LP, Zhang ET, Ossipov MH, Xie JY, King T, Lai J, and Porreca F. Descending facilitation from the rostral ventromedial medulla maintains nerve injury-induced central sensitization. *Neuroscience* 140: 1311, 2006b.

Verner TA, Goodchild AK, and Pilowsky PM. A mapping study of cardiorespiratory responses to chemical stimulation of the midline medulla oblongata in ventilated and freely breathing rats. *American journal of physiology* 287: R411-421, 2004.

Viemari JC, and Tryba AK. Bioaminergic neuromodulation of respiratory rhythm in vitro. *Respiratory physiology & neurobiology* 168: 69-75, 2009.

Wallisch M, Subban CV, Nettleton RT, and Olsen GD. Chronic in utero buprenorphine exposure causes prolonged respiratory effects in the guinea pig neonate. *Neurotoxicology and teratology* 32: 398-405, 2011.

Waters AJ, and Lumb BM. Descending control of spinal nociception from the periaqueductal grey distinguishes between neurons with and without C-fibre inputs. *Pain* 134: 32-40, 2008.

Waters AJ, and Lumb BM. Inhibitory effects evoked from both the lateral and ventrolateral periaqueductal grey are selective for the nociceptive responses of rat dorsal horn neurones. *Brain research* 752: 239-249, 1997.

Watkins LR, Griffin G, Leichnetz GR, and Mayer DJ. The somatotopic organization of the nucleus raphe magnus and surrounding brain stem structures as revealed by HRP slow-release gels. *Brain research* 181: 1-15, 1980.

Webster LR, Cochella S, Dasgupta N, Fakata KL, Fine PG, Fishman SM, Grey T, Johnson EM, Lee LK, Passik SD, Peppin J, Porucznik CA, Ray A, Schnoll SH, Stieg RL, and Wakeland W. An analysis of the root

causes for opioid-related overdose deaths in the United States. *Pain Med* 12 Suppl 2: S26-35, 2011.

Wei F, Dubner R, and Ren K. Nucleus reticularis gigantocellularis and nucleus raphe magnus in the brain stem exert opposite effects on behavioral hyperalgesia and spinal Fos protein expression after peripheral inflammation. *Pain* 80: 127-141, 1999.

Wei F, Dubner R, Zou S, Ren K, Bai G, Wei D, and Guo W. Molecular depletion of descending serotonin unmasks its novel facilitatory role in the development of persistent pain. *Journal of Neuroscience* 30: 8624-8636, 2010.

Weksler B, Ng B, Lenert J, and Burt M. A simplified method for endotracheal intubation in the rat. *Journal of Applied Physiology* 76: 1823-1825, 1994.

Winkler CW, Hermes SM, Chavkin CI, Drake CT, Morrison SF, and Aicher SA. Kappa opioid receptor (KOR) and GAD67 immunoreactivity are found in OFF and NEUTRAL cells in the rostral ventromedial medulla. *Journal of neurophysiology* 96: 3465-3473, 2006.

Woolf CJ, Shortland P, and Sivilotti LG. Sensitization of high mechanothreshold superficial dorsal horn and flexor motor neurones following chemosensitive primary afferent activation. *Pain* 58: 141-155, 1994.

Xie JY, Herman DS, Stiller CO, Gardell LR, Ossipov MH, Lai J, Porreca F, and Vanderah TW. Cholecystokinin in the rostral ventromedial medulla mediates opioid-induced hyperalgesia and antinociceptive tolerance. *Journal of Neuroscience* 25: 409-416, 2005.

Xu M, Kim CJ, Neubert MJ, and Heinricher MM. NMDA receptor-mediated activation of medullary pro-nociceptive neurons is required for secondary thermal hyperalgesia. *Pain* 127: 253-262, 2007.

Yasaki S, and Dyck PJ. A simple method for rat endotracheal intubation. *Laboratory animal science* 41: 620-622, 1991.

Yeomans DC, Pirec V, and Proudfit HK. Nociceptive responses to high and low rates of noxious cutaneous heating are mediated by different nociceptors in the rat: behavioral evidence. *Pain* 68: 133-140, 1996.

Yoshiya I, Shimada Y, and Tanaka K. Evaluation of a hot-wire respiratory flowmeter for clinical applicability. *Journal of Applied Physiology* 47: 1131-1135, 1979.

Zaretskaia MV, Zaretsky DV, and DiMicco JA. Role of the dorsomedial hypothalamus in thermogenesis and tachycardia caused by microinjection of prostaglandin E2 into the preoptic area in anesthetized rats. *Neuroscience Letters* 340: 1-4, 2003.

Zaretsky DV, Zaretskaia MV, and DiMicco JA. Stimulation and blockade of GABA(A) receptors in the raphe pallidus: effects on body temperature, heart rate, and blood pressure in conscious rats. *American journal of physiology* 285: R110-116, 2003.

Zhang ET, Ossipov MH, Zhang DQ, Lai J, and Porreca F. Nerve injury-induced tactile allodynia is present in the absence of FOS labeling in retrogradely labeled post-synaptic dorsal column neurons. *Pain* 129: 143-154, 2007a.

Zhang L, Sykes KT, Buhler AV, and Hammond DL. Electrophysiological heterogeneity of spinally-projecting serotonergic and non-serotonergic neurons in the rostral ventromedial medulla. *Journal of neurophysiology* 95: 1853-1863, 2006.

Zhang Z, Xu F, Zhang C, and Liang X. Activation of opioid micro-receptors in medullary raphe depresses sighs. *American journal of physiology* 296: R1528-1537, 2009.

Zhang Z, Xu F, Zhang C, and Liang X. Activation of opioid mu receptors in caudal medullary raphe region inhibits the ventilatory response to hypercapnia in anesthetized rats. *Anesthesiology* 107: 288-297, 2007b.

Zhuo M, and Gebhart GF. Biphasic modulation of spinal nociceptive transmission from the medullary raphe nuclei in the rat. *Journal of neurophysiology* 78: 746-758, 1997.

Zhuo M, and Gebhart GF. Characterization of descending facilitation and inhibition of spinal nociceptive transmission from the nuclei reticularis gigantocellularis and gigantocellularis pars alpha in the rat. *Journal of neurophysiology* 67: 1599-1614, 1992.

Zimmermann M. Ethical guidelines for investigations of experimental pain in conscious animals. *Pain* 16: 109-110, 1983.

Zorman G, Hentall ID, Adams JE, and Fields HL. Naloxone-reversible analgesia produced by microstimulation in the rat medulla. *Brain research* 219: 137-148, 1981.

APPENDIX A

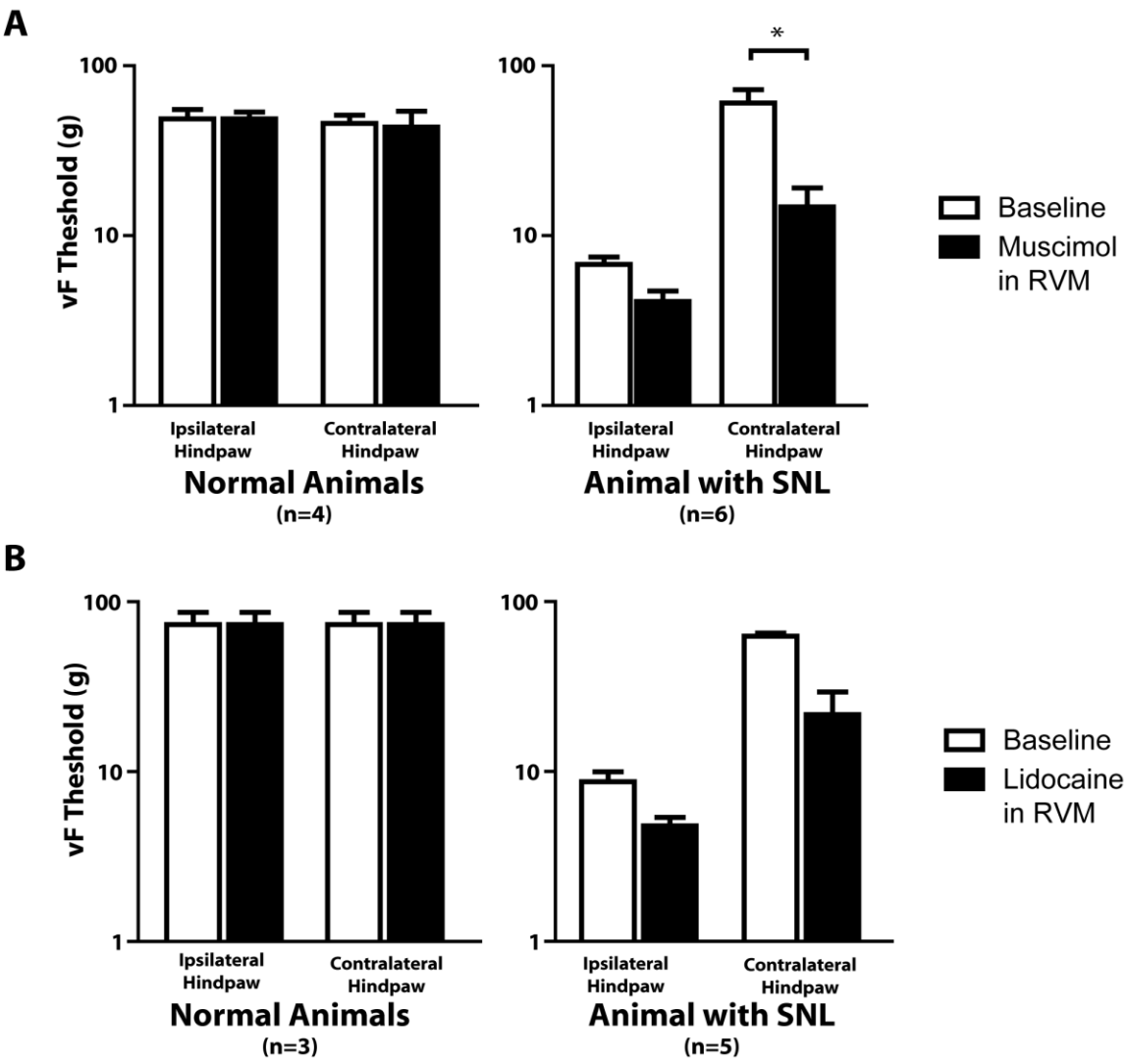
A
100
10
1
vF Theshold (g)
*
Ipsilateral Hindpaw
Contralateral Hindpaw
Normal Animals
(n=4)
Animal with SNL
(n=6)
Baseline
Muscimol in RVM
B
Lidocaine in RVM

Figure 22: Inhibition of RVM does reverse hyperalgesia in animals with nerve injury.

Either muscimol (A) or lidocaine (B) was injected into the RVM of naïve animals (left) or animals with prior spinal nerve ligation surgery (right). Inhibition of RVM neurons did not reverse the mechanical hyperalgesia in naïve animals. * $p < 0.05$, Wilcoxon rank-sum test. (Carlson et al, unpublished).

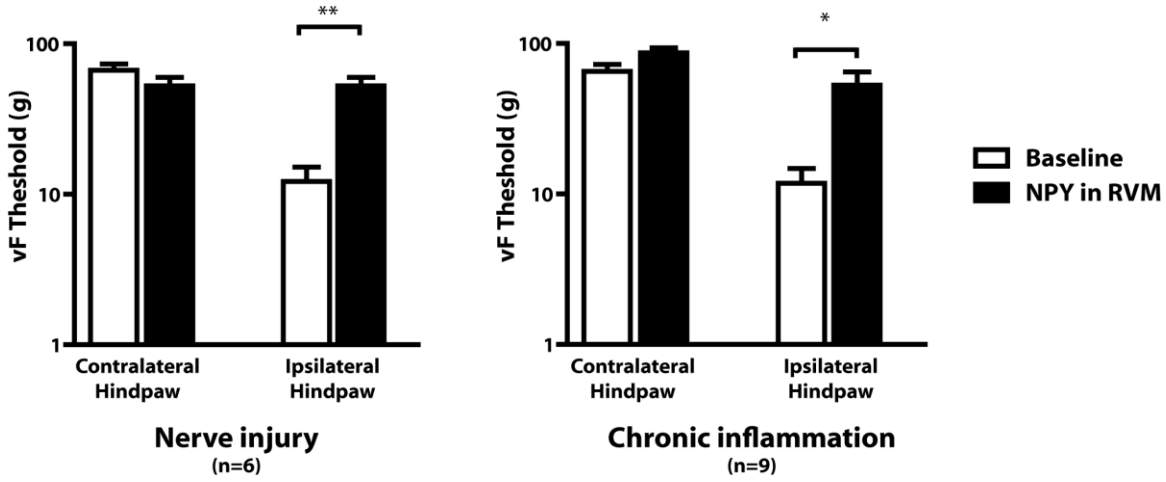
**
100
10
1
vF Theshold (g)
Contralateral Hindpaw
Ipsilateral Hindpaw
Nerve injury
(n=6)
*
100
10
1
vF Theshold (g)
Contralateral Hindpaw
Ipsilateral Hindpaw
Chronic inflammation
(n=9)
Baseline
NPY in RVM

Figure 23: NPY reverses mechanical hyperalgesia in both models of chronic inflammation and nerve injury. Injection of 1-10ug NPY in 200nl of aCSF reversed mechanical hyperalgesia in the ipsilateral (injured) hindpaw without changing the withdrawal threshold in the contralateral paw. (Cleary et al., unpublished)

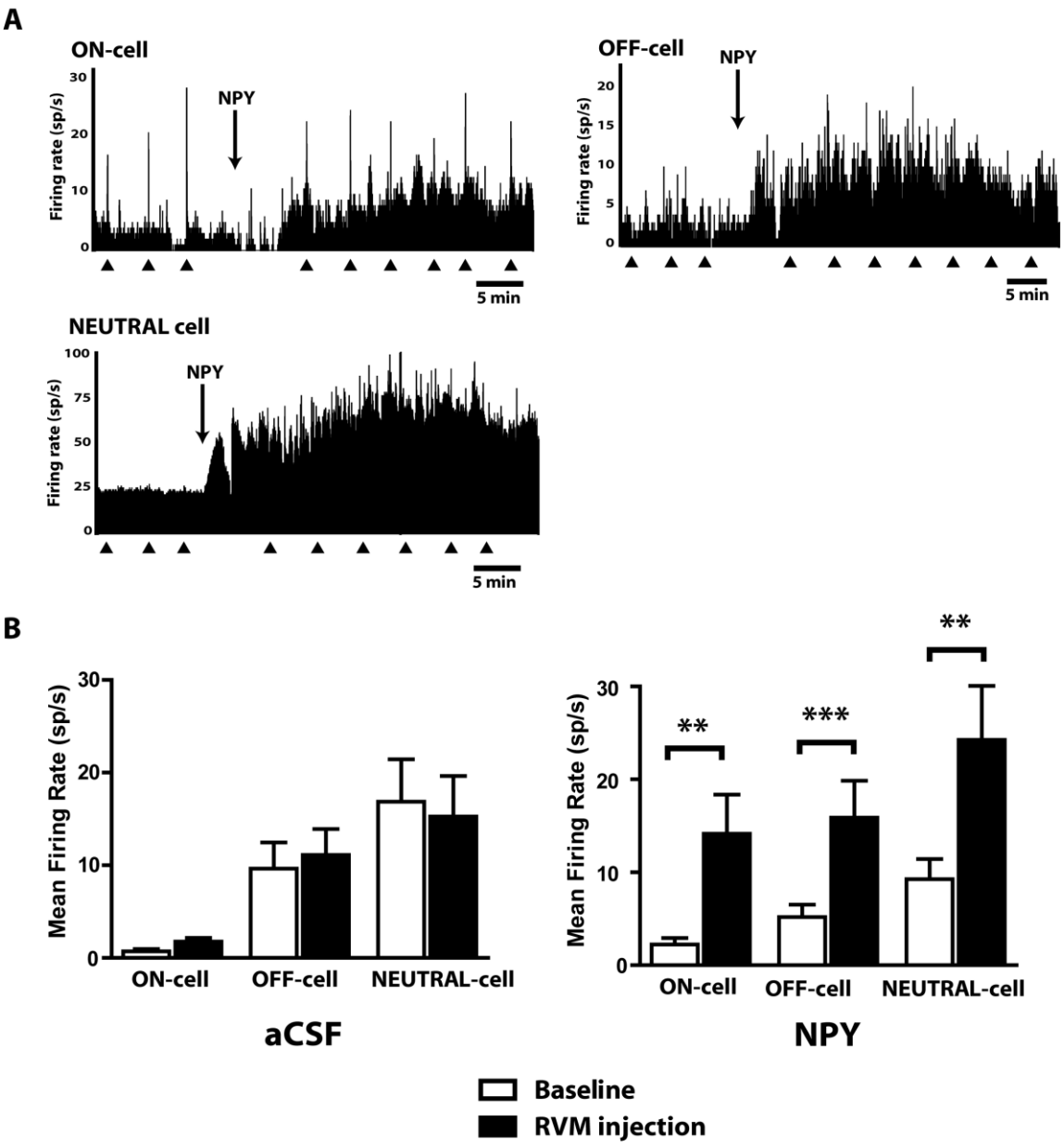
A
ON-cell
NPY
Firing rate (sp/s)
30
20
10
0
5 min
OFF-cell
NPY
Firing rate (sp/s)
20
15
10
5
0
5 min
NEUTRAL cell
NPY
Firing rate (sp/s)
100
75
50
25
0
5 min
B
Mean Firing Rate (sp/s)
30
20
10
0
ON-cell
OFF-cell
NEUTRAL-cell
aCSF
**
***
**
Mean Firing Rate (sp/s)
30
20
10
0
ON-cell
OFF-cell
NEUTRAL-cell
NPY
Baseline
RVM injection

Figure 24: NPY non-selectively increased neuronal activity.

A) Ratemeters showing the effects on cell firing of injection of 1ug NPY in 200nl aCSF into the RVM. All cells tested, including ON-, OFF-, and NEUTRAL cells, showed increased spontaneous activity.

B) Quantification of spontaneous cell activity after either aCSF (left) or NPY (right) injection into the RVM. NPY injection significantly increased the firing of all cell classes. ** $p < 0.01$, ** $p < 0.001$, Wilcoxon rank-sum test. n=5 to 11 for each group. (Cleary et al., unpublished)